

# UC Santa Barbara

## UC Santa Barbara Electronic Theses and Dissertations

### Title

Mechanism and Activation of the Iron(II) Dependent Alcohol Dehydrogenases Using gamma-hydroxybutyrate Dehydrogenase as a Model

### Permalink

<https://escholarship.org/uc/item/6618c8z2>

### Author

Taxon, Esther

### Publication Date

2018

Peer reviewed|Thesis/dissertation

UNIVERSITY OF CALIFORNIA

Santa Barbara

Mechanism and Activation of the Iron(II) Dependent Alcohol Dehydrogenases Using  
*gamma*-hydroxybutyrate Dehydrogenase as a Model

A dissertation submitted in partial satisfaction of the  
requirements for the degree Doctor of Philosophy  
in Biochemistry and Molecular Biology

by

Esther Sara Taxon

Committee in charge:

Professor Stanley Parsons, Chair

Professor David Low

Professor Dennis Clegg

December 2018

The dissertation of Esther Sara Taxon is approved.

---

David Low

---

Dennis Clegg

---

Stanley Parsons, Committee Chair

December 2018

Mechanism and Activation of the Iron(II) Dependent Alcohol Dehydrogenases Using  
*gamma*-hydroxybutyrate Dehydrogenase as a Model

Copyright © 2018

by

Esther Sara Taxon

## ACKNOWLEDGEMENTS

My graduate work has been a long and difficult path for me, in which I suffered nearly as many setbacks as successes. I would like to thank my professor, Stan Parsons, for his steadfast support, encyclopedic knowledge of biochemical fundamentals, and unwavering ability to ask the right questions. I must also thank him for being willing to take on a weird, shy student in his last years at UC Santa Barbara and help me grow, both as a scientist and as a person.

Second, I must thank Dr. John Lew, who decided I was one of his protégés whether I was in his lab or not. He then went from a professor I who was honestly intimidating when we first met, to my go-to resource for help when both Dr. Parsons and I were stumped. Dr. Lew helped push me outside my comfort zone where necessary, and always had a smile and a plan.

My undergraduate assistant, Lila Halbers, also deserves a huge thank-you. She helped collect most of the data in this dissertation, and without her work, the experiments could not have been completed in a reasonable timeframe. Likewise, she helped me to grow as a mentor in my capacity as her direct supervisor; and I hope that, to some extent, I was able to help her grow as a scientist.

I would be remiss if I did not thank Stella Hahn, whose official title as program manager of BMSE does not do justice to a woman who gave her students a cell phone number so she could be contacted whenever the need arose. She has always gone above and beyond, and deserved recognition.

Finally, I must thank my friends and family. To those of you who listened whenever I was freaking out; who were willing to put up with constant phone calls and emails; and who, on rare but notable occasion, allowed me to simply park myself on your couch for several hours while I worked. You know who you are. From the bottom of my heart, thank you.

CURRICULUM VITA OF ESTHER SARA TAXON  
December 2018

EDUCATION

Bachelor of Science in Biochemistry, Kettering University, 2010 (summa cum laude)  
Doctor of Philosophy in Biomolecular Science, University of California, Santa Barbara,  
September 2018

PROFESSIONAL EMPLOYMENT

2006-2010: Cooperative Employment Student, General Motors  
Summer 2011: Intern, Transonic Combustion  
2011-2018: Teaching Assistant, Department of Molecular, Cell, and Developmental  
Biology, University of California, Santa Barbara

AWARDS

Block Grant Award, Department of Biomolecular Science and Engineering, University of  
California, Santa Barbara, 2014

Excellence in Teaching Award, Graduate Student Association, University of California,  
Santa Barbara, 2018

## ABSTRACT

Mechanism and Activation of the Iron(II) Dependent Alcohol Dehydrogenases Using  
*gamma*-hydroxybutyrate Dehydrogenase as a Model

by

Esther Sara Taxon

The Group III Iron(II) Dependent Alcohol Dehydrogenases represent an understudied family of dehydrogenase enzymes. Although multiple members of the family have been cloned, expressed, and even crystallized and three-dimensional structure determined, very little work has gone into their chemical or kinetic mechanisms. Furthermore, it has been shown that certain members of the nudix hydrolase (**n**ucleoside **d**iphosphates linked to **x**) family of enzymes are capable of activating Group III dehydrogenases by two to tenfold. The method by which the nudix hydrolases cause activation is unknown. Using initial-rate and product inhibition studies in both non-activated and activated systems, the kinetic mechanism of one Group III Iron(II) Dependent Alcohol Dehydrogenase, *gamma*-hydroxybutyrate dehydrogenase (GHBDH) has been elucidated. Using mutational studies, the chemical mechanism of (GHBDH) was also studied. In GHBDH, the kinetic mechanism does not change upon activation by Nudix hydrolase; a proposed catalytic histidine does not appear to be necessary for the action of GHBDH. Finally, I have shown that *in vitro* studies of Group III ADHs may be missing a layer of metabolic control present in live cells.



## TABLE OF CONTENTS

I.	Introduction.....	1
	A. Group III Iron(II)-dependent Alcohol Dehydrogenases .....	1
	B. Nudix hydrolase enzymes and activation .....	6
	C. gamma-Hydroxybutyrate Dehydrogenase as a Model .....	7
II.	GHBDH Homology Model.....	9
	A. Motivation.....	9
	B. Results and Discussion .....	9
	C. Materials and Methods .....	11
III.	Kinetics of GHBDH .....	13
	A. Motivation.....	13
	B. Theoretical basis of experiments .....	14
	1. Ternary Reaction Mechanisms .....	14
	2. Product Inhibition Equations .....	22
	3. Determining Kinetic Mechanism by Experimentation .....	29
	C. Results and Discussion .....	31
	D. Materials and Methods .....	38
	1. Purification of GHBDH.....	38
	2. GHBDH Assays.....	39
	3. Dead-end Inhibition Assays.....	40
	4. GHBDH Product Inhibition Assays.....	40
	5. Data Processing .....	40

IV.	Activator Assays .....	42
	A. Motivation.....	42
	B. Results and Discussion .....	43
	C. Materials and Methods .....	50
	1. Purification of Activator Protein (ACT).....	50
	2. Assays of ACT nudix hydrolysis activity .....	51
	3. ACT Titration Assays (with pre-incubation).....	52
	4. ACT Titration Assays (without pre-incubation).....	52
	5. GHBDH Assays with AMP and NMN <sup>+</sup> .....	53
	6. Data Processing .....	53
V.	Activated Kinetics of GHBDH .....	54
	A. Motivation.....	54
	B. Results and Discussion .....	55
	C. Materials and Methods .....	63
	1. GHBDH Activation Assay in the Reduction of Aldehyde .....	63
	2. GHBDH pH Rate Profiles .....	64
	3. Activated GHBDH Product Inhibition Assays .....	64
	4. Data Processing .....	64
VI.	GHBDH Mutations .....	65
	A. Motivation.....	65
	B. Results and Discussion .....	67
	C. Materials and Methods .....	70
	1. Mutagenesis .....	70

	2.	Mutant Protein Expression and Purification.....	72
	3.	ApoGHBDH Expression and Purification.....	72
	4.	Wild-type and Mutant GHBDH Assays .....	73
	5.	Data Processing .....	73
VII.		Conclusions.....	74
	A.	GHBDH Homology Model.....	74
	B.	GHBDH Product Inhibition Assays.....	74
	C.	Activator Assays .....	74
	D.	Activated GHBDH Product Inhibition Assays .....	75
	E.	GHBDH Mutations .....	75
	F.	Final Remarks .....	76
VIII.		Bibliography .....	78
IX.		Appendix.....	87
	A.	Derivation of Mono-Iso Theorell-Chance Inhibition Equations: ....	87
	B.	Sample Mathematica Fitting Script .....	91

## LIST OF FIGURES

- Figure 1. Sequence alignment of selected Group III ADHs. The sequences were aligned using Clustal Omega (Sievers, et al., 2014). The proteins are:  $\gamma$ -hydrobutyrate dehydrogenase (GHBDH) from *Cupriavidus necator* (UniProt Q0KBD6); methanol dehydrogenase (MDH) from *Bacillus methanolicus* (UniProt P31005); lactaldehyde reductase (FucO) from *Escherisia coli* (UniProt P08971); alcohol dehydrogenase II (ADH2) from *Zymomonas mobilis* (UniProt P0DJA2); and alcohol dehydrogenase IV (ADH4) from *Saccharomyces cerevisia* (UniProt P10127). The Group III cofactor binding site GGSXXD is marked “=”. The four iron-coordinating residues are marked “☞”. The histidine that was proposed to be catalytic is marked “⚡”. Residues that are identical in all sequences are shaded dark grey. Residues that have conservative substitutions are shaded medium grey. Residues that have only semi-conservative substitutions are shaded light grey. “-” indicates no corresponding amino acid. ..2
- Figure 2. Homology model of GHBDH, with the  $\text{Fe}^{2+}$  (sphere in orange) held in place by its four chelator residues. The surface is outlined, the N-terminus is blue, the C-terminus is red, and the cleft through the protein is visible. .... 10
- Figure 3.  $\text{NAD}^+$  (cyan and heteroatoms) and GHB (pink and heteroatoms) positioned inside the active site of GHBDH, next to the  $\text{Fe}^{2+}$  (orange sphere). Note the van der Waals overlap between the GHB and the nicotinamide ring, indicating that in this orientation the two molecules are close enough for hydride transfer. .... 10
- Figure 4. A close-up of GHBDH C257 and C359 highlighted (in neon green) and with their sidechains explicitly drawn..... 11
- Figure 5. Cleland notation for a Random Sequential Bi Bi Mechanism. Image reproduced from (36)..... 15
- Figure 6. Cleland notation for an Ordered Sequential Bi Bi Mechanism. Note that the  $k$ 's here specifically refer to *rates*. Thus,  $k_2$  is related to  $K_{ia}$ ,  $k_4$  to  $K_{ib}$ , and so on, but  $K_{ia}$  etc. refer to the equilibrium dissociation constants, while the rates will vary according to how close the system is to those equilibria.  $K_a$  etc. are Michaelis constants, each of which is related to multiple rates. Image reproduced from (36)..... 16
- Figure 7. Cleland notation for a Theorell-Chance Mechanism. Image reproduced from (36)..... 17
- Figure 8. Cleland notation for an Ordered-On/Random-Off Bi Bi Mechanism. Image reproduced from (36)..... 17
- Figure 9. Cleland notation for a Ping-Pong Mechanism. Image reproduced from (36).18
- Figure 10. Cleland notation for a Di-Iso Theorell-Chance Mechanism. Image reproduced from (36)..... 19

Figure 11. Cleland notation for a Mono-Iso Ordered Sequential Bi Bi Mechanism. Image adapted from (36). .....	19
Figure 12. Cleland notation for an Ordered Sequential Bi Bi Mechanism with abortive complex formation. Image reproduced from (36). .....	21
Figure 13. Lineweaver-Burke plot of GHBDH inhibition by ADPR with NAD <sup>+</sup> as the variable substrate. Error bars are not shown where they would be smaller than the height of the symbol. ● 0 mM ADPR; ■ 0.04 mM ADPR; ▲ 0.12 mM ADPR; ▼ 0.4 mM ADPR. ....	32
Figure 14. Lineweaver-Burke plot of GHBDH inhibition by NADH with NAD <sup>+</sup> as the variable substrate. Error bars are not shown where they would be smaller than the diameter of the symbol. ● 0 mM NADH; ■ 0.0126 mM NADH; ▲ 0.04 mM NADH; ▼ 0.1 mM NADH. ....	34
Figure 15. Lineweaver-Burke plot of GHBDH inhibition by SSA with NAD <sup>+</sup> as the variable substrate. Error bars are not shown where they would be smaller than the diameter of the symbol. ● 0 mM SSA; ■ 0.1 mM SSA; ▲ 0.3 mM SSA. ....	35
Figure 16. Lineweaver-Burke plot of GHBDH inhibition by NADH with GHB as the variable substrate. Error bars are not shown where they would be smaller than the diameter of the symbol. ● 0 mM NADH; ■ 0.0126 mM NADH; ▲ 0.04 mM NADH. ....	35
Figure 17. Lineweaver-Burke plot of GHBDH inhibition by SSA with GHB as the variable substrate. Error bars are not shown where they would be smaller than the height of the symbol. ● 0 mM SSA; ■ 0.01 mM SSA; ▲ 0.1 mM SSA. ....	36
Figure 18. Titration of GHBDH activation against ACT added. Velocity has been normalized to maximum activity when activated. ....	44
Figure 19. Titration of GHBDH activation against ACT added without a pre-incubation. Velocity has been normalized to maximum activity when activated. ....	45
Figure 20. The inhibition of GHBDH by AMP. Error bars are not shown where they would be smaller than the height of the symbol. ● 0 mM AMP; ■ 1 mM AMP; ▲ 5 mM AMP. ....	46
Figure 21. The lack of inhibition of GHBDH by NMN <sup>+</sup> . Error bars are not shown where they would be smaller than the height of the symbol. ● 0 mM NMN <sup>+</sup> ; ■ 1 mM NMN <sup>+</sup> ; ▲ 5 mM NMN <sup>+</sup> . ....	47
Figure 22. Reverse-direction reaction. Even under conditions which should be saturating in the reverse direction (0.15 mM NADH, 0.1 mM SSA), the reverse direction does not become activated (23). ....	55

- Figure 23. GHBDH pH Rate profiles in the absence (▲) and presence (■) of ACT.57
- Figure 24. Lineweaver-Burke plot of activated GHBDH inhibition by NADH with NAD<sup>+</sup> as the variable substrate. Error bars are not shown where they would be smaller than the height of the symbol. ● 0 mM NADH; ■ 0.04 mM NADH; ▲ 0.125 mM NADH. 58
- Figure 25. Lineweaver-Burke plot of activated GHBDH inhibition by SSA with NAD<sup>+</sup> as the variable substrate. Error bars are not shown where they would be smaller than the height of the symbol. ● 0 mM SSA; ■ 0.1 mM SSA; ▲ 0.3 mM SSA; ▼ 1 mM SSA. ....59
- Figure 26. Lineweaver-Burke plot of activated GHBDH inhibition by NADH with GHB as the variable substrate. Error bars are not shown where they would be smaller than the height of the symbol. ● 0 mM NADH; ■ 0.01 mM NADH; ▲ 0.04 mM NADH. 59
- Figure 27. Lineweaver-Burke plot of activated GHBDH inhibition by SSA with GHB as the variable substrate. Error bars are not shown where they would be smaller than the height of the symbol. ● 0 mM SSA; ■ 0.1 mM SSA; ▲ 0.3 mM SSA.....60
- Figure 28. Energy schematic of the oxidation of GHB by GHBDH when unactivated (blue) and activated (orange).....61
- Figure 29. Partial sequence alignment of selected Group III ADHs and hydroxyacid-oxoacid transhydrogenases (HOTs). The sequences were aligned using Clustal Omega (Sievers, et al., 2014). The proteins are:  $\gamma$ -hydroxybutyrate dehydrogenase from *Cupriavidus necator* (UniProt Q0KBD6); methanol dehydrogenase from *Bacillus methanolicus* (UniProt P31005); lactaldehyde reductase from *Escherisia coli* (UniProt P08971); alcohol dehydrogenase II from *Zymomonas mobilis* (UniProt P0DJA2); alcohol dehydrogenase IV from *Saccharomyces cerevisia* (UniProt P10127); hydroxyacid-oxoacid transhydrogenase from *Drosophila melanogaster* (UniProt Q9W265); hydroxyacid-oxoacid transhydrogenase from *Xenopus laevis* (UniProt Q08B39); hydroxyacid-oxoacid transhydrogenase from *Homo spaiens* (UniProt Q8IWW8); and hydroxyacid-oxoacid transhydrogenase from *Rattus norvegicus* (UniProt Q4QQW3). The four iron-coordinating residues are marked “⚡”. The histidine that was proposed to be catalytic, as well as the tyrosine residue that replaces it in higher organisms, is marked “†”. Residues that are identical in all sequences are shaded dark grey. Residues that have conservative substitutions are shaded medium grey. Residues that have only semi-conservative substitutions are shaded light grey. “-” indicates no corresponding amino acid.....66
- Figure 30. pH rate profiles of GHBDH chelator mutants. Wild type is not shown due to scaling issues. ● H280A; ■ D193A; ▲ H197A; ▼ H261A.....68
- Figure 31. pH rate profiles of GHBDH H265 mutants. ● Wild-type; ■ H265A; ▲ H265C; ▼ H265D; ◆ H265Y.....69

## **I. Introduction**

Alcohol dehydrogenases (ADHs) comprise a huge and diverse group of enzymes. Broadly speaking, they are used biologically in reactions interconverting alcohols to aldehydes or ketones, and electron carriers from oxidized to reduced state. In many microbes, the formation of alcohols is vital to regeneration of cofactors necessary for anaerobic metabolism. In obligate aerobes, the generation of reduced cofactors is necessary to provide electrons to feed the electron transport chain.

There are three evolutionary families of nicotinamide adenine utilizing ADHs. Group I ADHs are medium/long chain protein that have a requisite zinc cofactor. This group includes horse liver ADH, and has been well-studied. Group II ADHs are short-chain protein that contain no metal cofactor. Group III are called the “Fe<sup>2+</sup>-dependent” ADHs (1). This is the least studied of the three ADH families.

### ***A. Group III Iron(II)-dependent Alcohol Dehydrogenases***

Group III Fe<sup>2+</sup>-dependent ADHs were first identified as a third family of ADHs in 1987, based on sequence similarity. Subsequent crystal structure work has shown that the tertiary structures of Group III ADHs are more conserved than sequence, which is general tends to be on the order of ~20% identity. Conserved sequence elements include three histidines and one aspartate that are required for metal binding, a histidine that was proposed to be catalytic, and an unusual GGGS motif that is used in the cofactor binding fold. In members of the family which utilize NAD(H), this motif is extended to GGGSXXD, with the aspartate providing steric and electrostatic discrimination against the extra phosphate of NADP(H).

```

C. necator GBHDH      ---MAFIYYLTHIHLDFGAVSLLKSECERIGIRRPLLVTDKGVVAAGVAQRAIDAM--QG
B. methanolicus MDH  ---MTNFFI PPASVIGRGAVKEVGRTRKQIGAKKALIVTDAFLHSTGLSEEVAKNIREAG
E. coli FUCO         --MANRMILNETAWFGRGAVGALTDEVKRRGYQKALIVTDKTLVQCGVVAKVTDKMDAAG
Z. mobilis ADH2      -MASSTFYIPFVNEMGEGSLEKAIKDLNGSGFKNALIVSDAFMNKSGVVKQVADLLKAQG
S. cerevisiae ADH4   MSSVTGFYI PPI SFFGEGALEETADYIKNKDYKKALIVTDPGIAAIGLSGRVQKMLEERD

C. necator GBHDH      LQVAVFDETPSNPTEAMVRKAAAQYREAGCDGLVAVGGGSSIDLAKGIAILATHE--GEL
B. methanolicus MDH  LDVAIFPKAQDPADTQVHEGVDFVKQENCALVSI GGGSSHD TAKAIGLVAANG--GRI
E. coli FUCO         LAWAIYDGVVNPNTITVVKELGVFQNSGADYLI AIGGGSPQDTCKAIGIISNNPEFADV
Z. mobilis ADH2      INSAVYDGVMPNPTVTAVLEGLKILKDNNSDFV I SLGGGSPHDCAKAIALVATNG--GEV
S. cerevisiae ADH4   LNVAIYDKTQPNENIANVTAGLKVLEQNSEI VVSIGGSAHDNKAIAIALATNG--GEI

C. Necator GBHDH     TTYATIEGGSARITDKAAPLIAVPTTSGTGSEVARGAII I LDD-GRKLG FHSWHL LPKSA
B. Methanolicus MDH NDYQGVN----SVEKPVV PVVAITTTAGTGSETTSLAVITDSARKVKMPVIDEKITPTVA
E. Coli FUCO         RSLEGLS----PTNKPSVPI LAIPTTAGTAAEVTINYVITDEEKRRKFVVCVDPHDIPQVA
Z. Mobilis ADH2     KDYEGID----KSKKPALPLMSINTTAGTASEMTRFCII TDEVVRHVKMAIVDRHVTMVS
S. cerevisiae ADH4  GDYEGVN----QSKKAALPLFAINTTAGTASEMTRFTII SNEEKKIKMAIIDNNVTPAVA

C. Necator GBHDH     VCDPELTLGLEPAGLTAATGMDAIAHCIETFLAPAFNPPADGIALDGLERGWGHI ERATR D
B. Methanolicus MDH IVDPELMVKKPAGLTIATGMDALSHAIEAYVAKGATPVTD AFAIQAMKLINEYLPKAVAN
E. Coli FUCO         FIDADMMDGMPALKAATGVDALTHAIEGYITRGAWALTDALHIKAIEI IAGALRGSVAG
Z. Mobilis ADH2     VNDP LLMVGM PKGLTAATGMDALTHAFEAYSSTAATPI TDACALKAASMI AKNLKTACDN
S. cerevisiae ADH4  VNDPSTMFG LPPALTAATGLDALTHCIEAYVSTASNPITD ACALKGIDLINESLVAAAYKD

C. Necator GBHDH     GQDRDARLNMSASMQGAMAFQ-KGLGCVHSLSHPLGGLKIDGRTGLHHGTLNNAVVM PAV
B. Methanolicus MDH GEDIEAREAMAYA QYMAGVAFNNGGLGLVHSISHQVGGVY----K LQHIGICNSVNM P HV
E. Coli FUCO         --DKDAGEEMALGQYVAGMGFSNVGLGLVHGM AHP LGA FY----NTPHGVCNAI L LPHV
Z. Mobilis ADH2     GKDM PAREAMAYA QFLAGMAFNNASLGYVHAMAHQLGGY Y----NLPHGVCNAV L LPHV
S. cerevisiae ADH4  GKDKKARTDMCYAEYLAGMAFNNASLGYVHALAHQLGGFY----H LPHGVCNAV L LPHV

C. Necator GBHDH     LRFNADAPT VVRDDRYARLRAMHL-----PDGADIAQAVHDMTVRLGLPTGLRQMG
B. Methanolicus MDH CAFNLI AK----TERFAHIAELLGENVSGLSTAAA AERAIVALERYNKNF GIPSGYAEMG
E. Coli FUCO         MRYNADFT----GEKYRDIARVMGVKVEGMSLEEARNAAVEAVFALNRDVGI PPHLRDVG
Z. Mobilis ADH2     LAYNASVVAG----RLKDVGVAMGLDIANLGDKEGAEATIQA VRDLAASIGI PANLTELG
S. cerevisiae ADH4  QEANMQCPKA--KKRLGEIALHFG-----ASQEDPEETIKALHVLNRTMNI PRNLKELG

C. Necator GBHDH     VTEDMFDKVIAGALVDHCHKTNPK EASAADYRRMLEQSM--
B. Methanolicus MDH VKEEDI ELLAKNAFEDVCTQSNPRVATVQDIAQI IKNAL--
E. Coli FUCO         VRKEDI PALAQAALDDVCTGGNPREATLEDIVELYHTAW--
Z. Mobilis ADH2     AKKEDVPLLADHALKDACALTNPRQGDQKEVEELFLSAF--
S. cerevisiae ADH4  VKTEDFEILAEHAMHDACHLTNPFVQFTKEQVVAI IKKAYEY

```

**Figure 1.** Sequence alignment of selected Group III ADHs. The sequences were aligned using Clustal Omega (Sievers, et al., 2014). The proteins are:  $\gamma$ -hydrobutyrate dehydrogenase (GHBDH) from *Cupriavidus necator* (UniProt Q0KBD6); methanol dehydrogenase (MDH) from *Bacillus methanolicus* (UniProt P31005); lactaldehyde reductase (FucO) from *Escherisia coli* (UniProt P08971); alcohol dehydrogenase II (ADH2) from *Zymomonas mobilis* (UniProt PODJA2); and alcohol dehydrogenase IV (ADH4) from *Saccharomyces cerevisia* (UniProt P10127). The Group III cofactor binding site GGGSSXD is marked “=”. The four iron-coordinating residues are marked “⌘”. The histidine that was proposed to be catalytic is marked “†”. Residues that are identical in all sequences are shaded dark grey. Residues that have conservative substitutions are shaded medium grey. Residues that have only semi-conservative substitutions are shaded light grey. “-” indicates no corresponding amino acid.



The identity of the metal cofactor has presented some problems. Despite the name, Fe<sup>2+</sup>-dependent ADHs do not appear to be strictly limited to Fe<sup>2+</sup>. A number of proteins, including *Bacillus stearothermophilus* glycerol dehydrogenase (2) and *Saccharomyces cerevisiae* alcohol dehydrogenase IV (3), appear to naturally utilize Zn<sup>2+</sup>. However, in other family members, addition of Zn<sup>2+</sup> acts as an inhibitor (4), (5), (6), presumably by replacing Fe<sup>2+</sup> in the metal-ion site without supporting activity. It has been suggested (6) that the switch from Fe<sup>2+</sup> to Zn<sup>2+</sup> might be an evolutionary response to the development of an oxidizing atmosphere. Certainly, a number of proteins which definitely contain Fe<sup>2+</sup> are anaerobic and quickly lose activity in an oxygen atmosphere (7). A recent paper showed that one such protein, ADH from *Pyrococcus horikoshii*, can be somewhat rescued by addition of Ni<sup>2+</sup> to the bacterial growth medium (8), which then replaces Fe<sup>2+</sup> in the metal-binding site and supports aerobic activity. Thus, it is reasonable to posit that this group is dependent on divalent cations, but the specific ion requirement has diverged evolutionarily on the basis of metal ion stability and availability.

Like other protein families, Group III ADHs have a wide range of substrates, both across the family and with regards to individual enzymes. For example, a few homologues from *Bacillus methanolicus* have been annotated as methanol dehydrogenases (MDHs) because they have been identified as enzymes which are necessary for growth with methanol as the sole carbon source. However, when tested against a panel of different substrates, it was found that these enzymes have a much better activity against ethanol, followed by 1-propanol and 1-butanol and only then methanol (9). While most of the Group III ADHs act on short 3- or 4-carbon alcohols, one of them is capable of good activity even against n-octanol (8). With that said, due to the reaction site geometry, all Group III ADHs work on

primary alcohols, converting them to aldehydes. Some of the substrates, such as glycerol, 1,2-propanediol, and 1,3-propanediol, have more than one alcohol, but it is always the terminal alcohol that becomes oxidized. There seems to be no mechanistic difference between diols and primary alcohols, and indeed many Group III ADHs can oxidize ethanol in addition to diol substrates. Even with this flexibility, most Group III ADHs do tend to show a preference for one specific substrate, even if it isn't the substrate for which they have been named.

In general, Group III ADHs have two distinct pH optima, depending on the direction of the reaction (5), (9), (10), (11), (12), (13), (14), (15). In the direction of reducing an aldehyde substrate to an alcohol, the pH optimum is 6-7. In the direction of oxidizing an alcohol substrate to an aldehyde, the pH optimum is much higher, 8.5-10. This is to be expected considering that the oxidation is a proton-forming reaction and the reduction is a proton-utilizing one. Thus, in biological systems, the reduction is typically favored, especially when NAD(P)H is in excess. Conversely, when energy charge<sup>1</sup> is low but alcohol substrate concentration is high, the oxidation is favored.

This last point is important, not in terms of the bacteria themselves, but in terms of the potential useful applications. It has long been known that the obligate anaerobe *Clostridium acetobutylicum* can produce acetone, butanol, and ethanol from starch in a process known as ABE fermentation. Prior to WWII, this was a major source of industrial solvent. As petroleum extraction became less expensive, this became unprofitable. However, the push for renewables has led to a resurgence of interest in biological production of basic

---

<sup>1</sup> Defined as  $\frac{[ATP]+1/2[ADP]}{[ATP]+[ADP]+[AMP]}$

chemicals. The enzymes responsible for butanal reduction to butanol in *C. acetobutylicum* turn out to be a pair of Group III ADHs (16).

Several Group III ADHs have been crystallized (17). These crystal structures have revealed the geometry of the active site and the binding pockets. The  $\text{Fe}^{2+}$  is held by the four residues in a nearly octahedral arrangement. The other two sites are filled by water in substrate-free enzyme. One of the waters is replaced by the alcohol/aldehyde substrate, and the nicotinamide ring of the NAD(P)(H) cofactor displaces the other. The two binding pockets are well-defined and non-overlapping, and form a deep cleft that runs entirely through the protein. Although no crystal has been generated with both NAD(P) and substrate present, superposition of crystals shows that the closest approach between the substrate and cofactor occurs between the terminal carbon of the substrate and C4 of the nicotinamide ring, at a distance of  $\sim 3\text{\AA}$ . (The structures do not have fine enough resolution to see the individual hydrogen atoms, but based on C-H bond length, it is probable that nicotinamide C4 is  $\sim 2\text{\AA}$  from the hydride it accepts.) It is worthwhile to note that multiple research groups observed low electron densities for the nicotinamide ring itself, which indicates that the ring has positional flexibility and might reasonably be even closer to the substrate during the reaction cycle.

The crystals all demonstrate some degree of oligomerization. This is in accordance with prior gel-filtration studies (5), (3), (2) which indicate either dimers or tetramers. Two of the crystals, those of *B. stearothermophilus* glycerol dehydrogenase (18) and *Klebsiella pneumoniae* (19), show radial multimerization of dimers into an octamer and a decamer, respectively. It is likely that all Group III ADHs dimerize natively; these dimers may then further self-associate. The *K. pneumoniae* enzyme activity shows slight cooperativity,

implying that multimers of dimers not only form natively, but also that the subunits affect one another.

### ***B. Nudix hydrolase enzymes and activation***

Nudix hydrolases, a second large family of enzymes, catalyze the hydrolysis of nucleoside diphosphates linked to X. The X moiety is highly diverse. As an example, *E. coli* 8-oxo-dGTP pyrophosphohydrolase (MutT) cleaves a pyrophosphate from 8-oxo-dGTP, a mutagenic nucleotide triphosphate that occurs when guanidine oxidizes, and thus prevents it from being incorporated into DNA (20). In eukaryotes, the enzyme responsible for removing 7-methylguanylate 5' RNA caps, thus signaling for degradation of RNA and nucleotide recycling, is a nudix hydrolase (21). There are many more examples from both prokaryotes and eukaryotes. Given the importance of nudix hydrolase enzymes, they are ubiquitous in all cell types.

Mechanistically, most nudix hydrolases work by coordinating a nucleophilic attack by water on a phosphorous. A divalent cation is used to balance charge and coordinate the pyrophosphate target in the correct orientation. In order to acidify the water molecule and generate a good nucleophile, a second divalent cation is often used. A third metal ion has been detected by X-ray crystallography. Experimental results suggest that the third metal ion is necessary for some enzymes, but may be an artifact of the crystallization in others. Regardless, all nudix hydrolases display an absolute requirement for physiological concentrations of divalent cation. This is most commonly  $Mg^{2+}$ , but  $Mn^{2+}$  has also been shown to support activity in some nudix hydrolases (20). Unlike Group III ADHs, the divalent cation(s) of nudix hydrolases are not strongly bound, and removing them is usually a matter of buffer exchange.

A number of nudix hydrolase enzymes have been shown to be capable of activating Group III ADHs by 2-7-fold (9). This activation is strictly dependent on the hydrolysis activity of the nudix hydrolase; in experiments that omit  $Mg^{2+}$  from the buffer, there is no activation or hydrolysis even when nudix hydrolase enzyme is present in excess. In an *in vitro* experiment, there is typically only one molecule that can be a target of a nudix hydrolase: the NAD(H). It was therefore suggested that the activation was a result of the nudix hydrolase interacting directly with the Group III ADH and cleaving a bound  $NAD^+$ , releasing an  $NMN^+$  but leaving an AMP bound to the ADH. This AMP was then supposed to be responsible for the activation (22). However, the activation is extremely odd in that it occurs in one direction only, the oxidation of alcohol substrate to aldehyde. Although this seems mechanistically impossible, this is the result found by Krog et. al. (23) and confirmed by this lab. The activation thus merits further study to understand how evolution managed such a feat.

Also unknown is whether activation changes the kinetic mechanism of the reaction. Clearly at least one of the microscopic steps must change. At the same time, the proposal that activation changes the ADH kinetics from a ping-pong reaction to a ternary complex reaction is difficult to believe, if for no other reason than Group III ADHs, like all other ADHs, probably do not operate by a ping-pong reaction.

### ***C. gamma-Hydroxybutyrate Dehydrogenase as a Model***

*Gamma*-Hydroxybutyrate Dehydrogenase (GHBDH) is a Group III ADH that interconverts *gamma*-hydroxybutyrate (GHB) and succinic semialdehyde (SSA) and uses

NAD(H) as the electron carrier. The gene was originally isolated from *Cupriavidus necator*<sup>2</sup> (24). This soil bacterium, a gram-negative facultative anaerobe (25), copolymerizes *gamma*-hydroxybutyrate (GHB) with other hydroxybutyrates as a form of carbon and energy storage (26). In fact much work on “green” polyhydroxyalkanoate plastics focus on *C. necator* precisely for this copolymerization ability, since varying the feedstock and metabolic conditions of the cell results in fine control over the incorporated monomers and therefore the properties of the plastic that is made (27).

GHBDH contains all the standard features of a Group III ADH: the Rossmann-fold-like GGGSSXXD binding motif for NAD<sup>+</sup>, the conserved amino acids necessary for Fe<sup>2+</sup> chelation, and the conserved proposed catalytic histidine. This laboratory had previously cloned a fusion protein of GHBDH with glutathione-S-transferase, an expression tag which allows binding to an affinity column presenting covalently bound glutathione, and this expression system produces upwards of 15 mg recoverable GHBDH fusion protein per liter of growth.

---

<sup>2</sup> *C. necator* has undergone many changes of name over the course of its history. This species has been variously known as *Hydrogenomonas eutrophus*, *Alcaligenes eutropha*, *Ralstonia eutropha*, and *Wautersia eutropha* (66).

## II. GHBDH Homology Model

### A. Motivation

GHBDH has not been crystallized, but many Group III ADHs have. Using the crystal structure data from related enzymes, it was therefore possible to build a homology model for the GHBDH fusion protein. Although such a model cannot capture the complex ensemble of 3D structures that are found in solution, it gives an estimate of the tertiary fold of the GHBDH molecule and provides a platform for prediction of surface and molecular features of GHBDH. Additionally, it allows limited modelling of NAD<sup>+</sup> and GHB positions in the binding pocket, and some prediction of substrates which would *not* have fit in the binding site.

### B. Results and Discussion

The homology model shows that GHBDH likely conforms to the primary fold of other Group III ADHs, with an N-terminal domain that contains  $\alpha$ -helices and  $\beta$ -sheets, and a C-terminal domain that is mostly  $\alpha$ -helical. The four Fe<sup>2+</sup> chelating residues are oriented about the Fe<sup>2+</sup> as expected. The deep cleft that passes entirely through the protein comprises the binding pocket of both GHB and NAD<sup>+</sup>. When NAD<sup>+</sup> is bound, it physically blocks that part of the cleft and prevents water diffusion. GHB is smaller, so it is possible that the active site still has access to bulk solution in that direction.

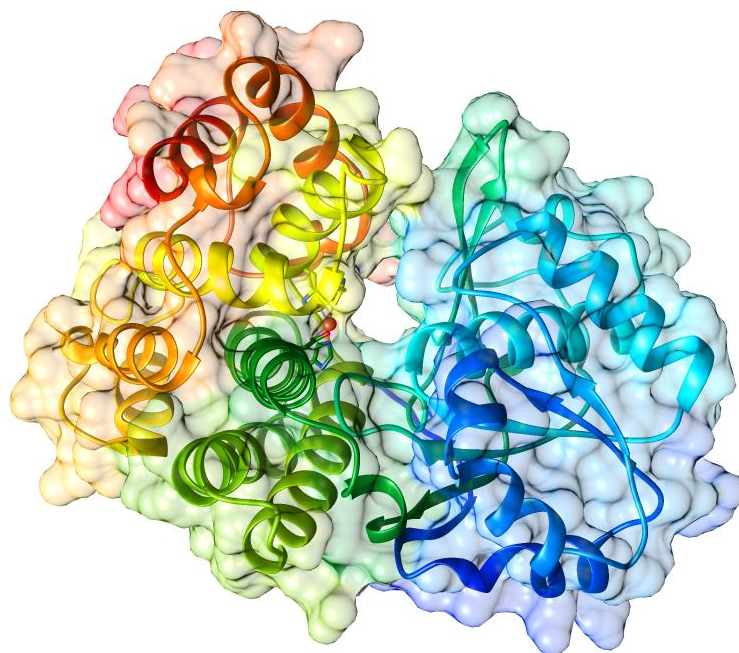


**Figure 2.** Homology model of GHBDH, with the Fe<sup>2+</sup> (sphere in orange) held in place by its four chelator residues. The surface is outlined, the N-terminus is blue, the C-terminus is red, and the cleft through the protein is visible.

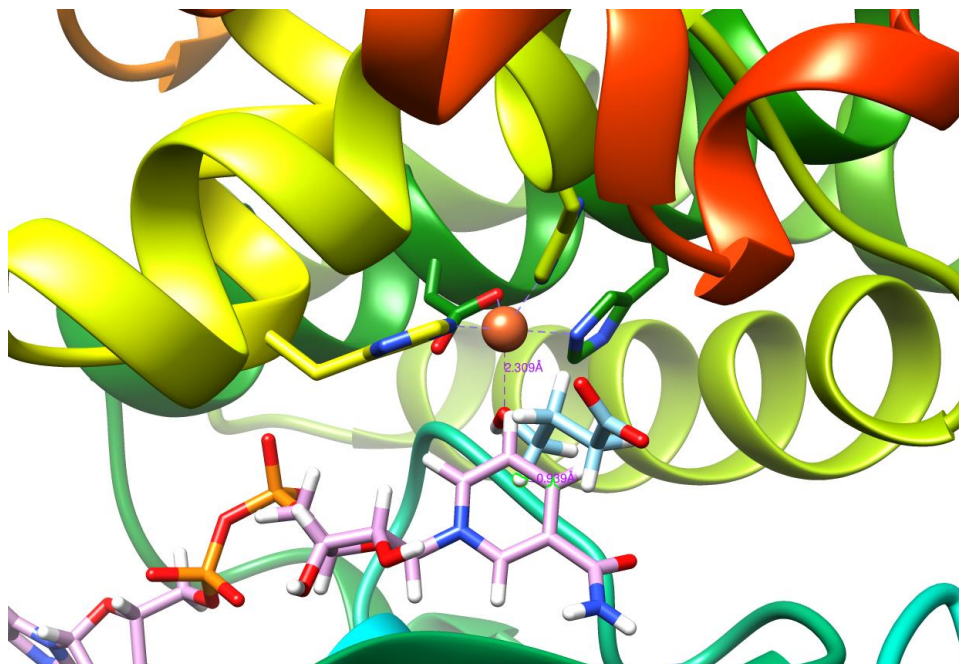


**Figure 3.** NAD<sup>+</sup> (cyan and heteroatoms) and GHB (pink and heteroatoms) positioned inside the active site of GHBDH, next to the Fe<sup>2+</sup> (orange sphere). Note the van der Waals overlap between the GHB and the nicotinamide ring, indicating that in this orientation the two molecules are close enough for hydride transfer.



There was one particularly interesting feature that was observed from the homology model and might explain some later experimental results. Although another Group III ADH could be protected by DTT in solution (11), GHBDH loses activity in solution with any added thiols like 1,4-dithiothreitol. The homology model shows that two cysteine residues, C257 and C359, are positioned closely together. It is possible that these two cysteines natively form a disulfide bond which helps hold the structure together. However, it should be noted that other Group III ADHs which do not have two cysteines at that position are still capable of folding properly and of turning over, so if they are necessary, this is unique to GHBDH.

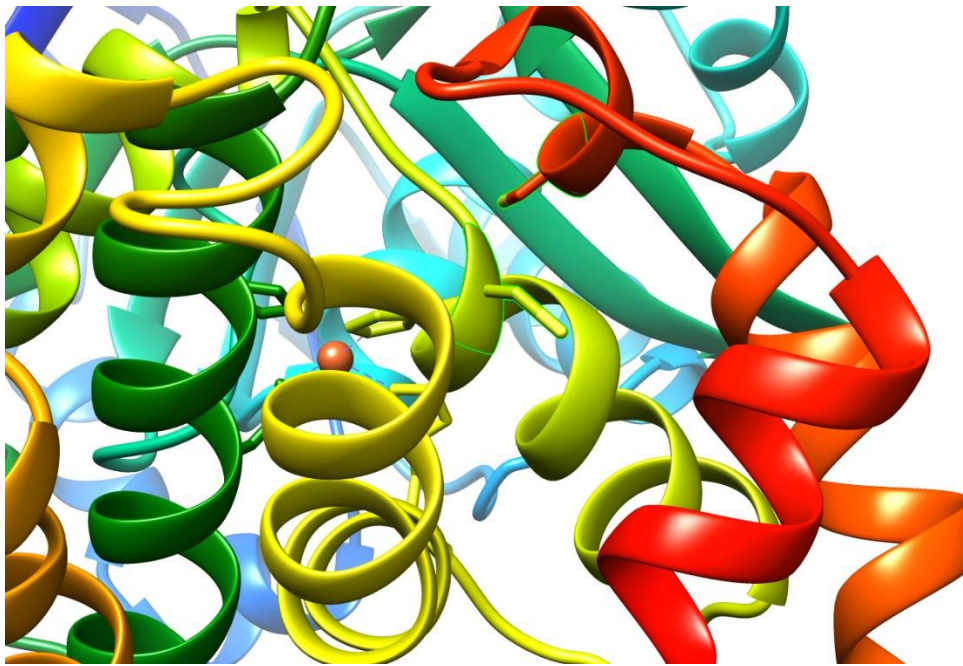


**Figure 4.** A close-up of GHBDH C257 and C359 highlighted (in neon green) and with their sidechains explicitly drawn.

### ***C. Materials and Methods***

The structures of *E. coli* lactaldehyde reductase (pdb 1RRM) and *K. pneumoniae* 1,3-propanediol dehydrogenase (pdb 3BFJ) were used as templates. Homology modelling was

accomplished using the MODELLER 9.16 (28) extension to UCSF Chimera (29). The best model was selected based on the lowest Discrete Optimized Protein Energy (DOPE) model score (30). The modelled structure was then manually modified by addition of an  $\text{Fe}^{2+}$  pseudobonded to the chelator residues at appropriate distances.

The homology model was prepared for docking using UCSF Chimera's DockPrep tool. Ligands were downloaded from the ZINC database (31). The surface of GHBDH was generated from the homology model by Chimera. The binding cleft was generated by DOCK's INSPH command (32) and then manually whittled down to two binding pockets, which roughly corresponded to  $\text{NAD}^+$  and GHB. Docking was calculated using DOCK 6.8 (33), a flexible anchor-and-chain method, and output limited to a maximum of 500 structures.  $\text{NAD}^+$  structures were manually evaluated based on the  $\text{NAD}^+$ 's orientation (nicotinamide in, AMP occupying the probable AMP binding site) and GHB structures were manually evaluated based on their orientation and distance of the hydroxyl oxygen from the  $\text{Fe}^{2+}$  and the  $\gamma$ -carbon from the nicotinamide ring. These were not necessarily the lowest-energy conformers, but it is impossible for the hydride transfer to occur when the  $\gamma$ -carbon and nicotinamide ring are not in close proximity, so these are the most realistic.

### III. Kinetics of GHBDH

#### A. Motivation

Despite the work that has gone into characterizing and crystallizing Group III ADHs, there has been almost no kinetics work done on any member of this family. The exceptions are two studies: an incomplete kinetics experiment done on butanol dehydrogenase (BDH) from *C. acetobutylicum* (16), and one paper on the *E. coli* 1,2-propanediol dehydrogenase (FucO) (34). The former paper partially tested the reaction in the reductive direction, as the reduction of butanal to butanol is the important one with regards to industrial solvent generation. The experiments in which butanol was used as a product inhibitor of butaldehyde reduction do not show competitive inhibition, and thus suggest an Ordered Sequential Bi Bi kinetic mechanism. However, instead of using  $\text{NAD}^+$  as a product inhibitor of NADH, the authors chose to use a non-oxidizable NADH analogue, S-NADH, wherein the nitrogen of the nicotinamide ring is replaced with a sulfur. Although this very definitely competed with NADH, it did not prove that  $\text{NAD}^+$  would also compete. From these experiments, the authors concluded that NADH binds first, then butanal, followed by hydride transfer and product release.

The latter paper studied primarily the stereospecificity of *E. coli* FucO, but also looked at the viscosity and kinetic isotope effects when the hydride being transferred is deuterated. The conclusion was that the hydride transfer is a slow step, but that there are other partially-rate-limiting steps associated with reagent binding, product release, and/or an isomerization, which are kinetically important and partially mask the hydride transfer step. Although this

conclusion is not wrong *per se*, such measurements do not give any information on the order in which those steps occur. Thus no information is available on the kinetics of FucO.

From these two papers no very clear picture of the kinetic mechanism of any Group III ADH can be drawn. In order to fill in this gap in scientific knowledge, then, a series of experiments was performed to understand the basic kinetic mechanism of GHBDH, and more broadly the Group III ADHs as a whole.

### ***B. Theoretical basis of experiments***

There are, for the sake of distinguishing kinetic models, three types of inhibition: competitive, uncompetitive, and mixed type. This section will review the meaning of 'kinetic mechanism', and several types of kinetic mechanism will be examined. Then types of inhibition as applied to determining the kinetic mechanism of a two-substrate enzyme, using product inhibition studies, will be explained. Finally, the experiments on GHBDH will be presented.

#### 1. Ternary Reaction Mechanisms

A ternary reaction refers to any enzymatic reaction in which a central ternary complex exists. For example, in a cleavage reaction, enzyme E first binds substrate A to form E·A complex. E then cleaves A to form products P and Q in E·P·Q complex. P and Q must then dissociate before E can bind A again. In a condensation, the reverse reaction occurs. Additionally, many two-substrate two-product enzymatic reactions employ ternary reactions in which central complexes can interconvert between E·A·B and E·P·Q.

In such a system, there are, at least in theory, multiple pathways in which A, B, and E can combine to form the ternary complex E·A·B, and then the ternary complex E·P·Q

may release products P and Q. It is extremely unlikely that A and B can bind simultaneously; all three molecules are assumed to be tumbling freely in solution, and the chances of all three encountering each other at exactly the same instant, and in exactly the correct orientation, are so small as to be functionally nonexistent. Thus, work over the last several decades has always focused on the sequence of additions of A and B to E and the sequence of release of P and Q from E. The sequences of binding and release events is known as the kinetic mechanism of the reaction, although in reality it is largely independent of the individual rate constants which are more usually associated with the word 'kinetics.' There are many types of ternary reaction; this section will give a review of the most common, and a few of the more unusual, types of ternary reaction kinetic mechanisms.

*Random Sequential Bi Bi Mechanism*

Firstly, there is the Random Sequential Bi Bi Mechanism, in which A and B bind in random order and P and Q are released in random order. In the notation of Cleland (35) this is described by:

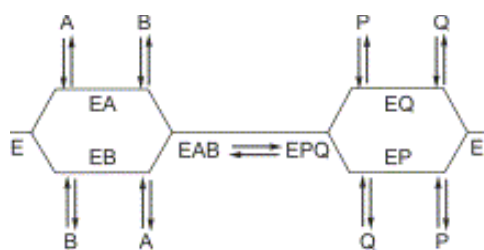


**Figure 5.** Cleland notation for a Random Sequential Bi Bi Mechanism. Image reproduced from (36).

In this reaction, enzyme E binds to A or B to make either the E·A or E·B complex. E·A then binds to B or E·B binds to A to make E·A·B complex. E·A·B reacts covalently to form E·P·Q. One of the products, P or Q, dissociates to form E·Q or E·P complex; these

complexes then dissociate further, releasing the second product and leaving E free to perform another reaction. Such an enzyme has eighteen microscopic rate constants. As such, the system is extremely complex. It can be simplified by the rapid equilibrium assumption, which states that the E·A·B to E·P·Q reaction is slow, and all the other equilibria are fast in comparison. The system can then be described with a series of Michaelis constants and equilibrium dissociation constants.  $K_a$  and  $K_b$  describe the respective Michaelis-Menten constants of A and B in the forward directions, while  $K_p$  and  $K_q$  are the Michaelis-Menten constants of P and Q in the reverse direction.  $K_{ia}$  and  $K_{ib}$ , meanwhile, describe the equilibrium dissociation constants of substrates A and B, and  $K_{ip}$  and  $K_{iq}$  are the equilibrium dissociation constants for the products P and Q.  $V_{max}$  describes the theoretical maximum velocity in the forward direction when all substrates are saturating, and is related to the  $k_{cat}$ , which is the previously-mentioned slow reaction rate.

#### *Ordered Sequential Bi Bi Mechanism*

By contrast, in an Ordered Sequential Bi Bi Mechanism, A must bind before B, and P must be released before Q:

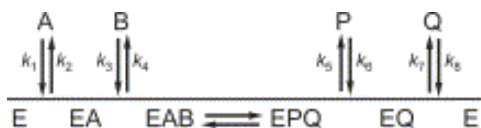


**Figure 6.** Cleland notation for an Ordered Sequential Bi Bi Mechanism. Note that the  $k$ 's here specifically refer to *rates*. Thus,  $k_2$  is related to  $K_{ia}$ ,  $k_4$  to  $K_{ib}$ , and so on, but  $K_{ia}$  etc. refer to the equilibrium dissociation constants, while the rates will vary according to how close the system is to those equilibria.  $K_a$  etc. are Michaelis constants, each of which is related to multiple rates. Image reproduced from (36).

As with the Random Sequential Bi Bi Mechanism, this reaction has a  $K_m$  and  $K_i$  for each species, as well as a  $V_{max}$ .

### *Theorell-Chance Mechanism*

A special case of an Ordered Sequential Bi Bi Mechanism is called the Theorell-Chance Mechanism after its originators Hugo Theorell and Britton Chance (37). In such a mechanism, the  $E \cdot A \cdot B$  to  $E \cdot P \cdot Q$  reaction and first product release rates are so high that the ternary complex  $E \cdot A \cdot B / E \cdot P \cdot Q$  is not ordinarily detectable<sup>3</sup>, and P appears to be released as soon as B binds followed by a slower equilibrium dissociation of Q:

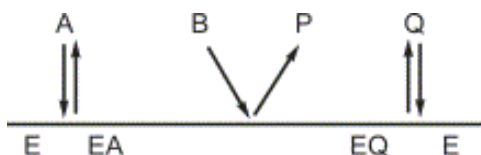


**Figure 7.** Cleland notation for a Theorell-Chance Mechanism. Image reproduced from (36).

### *Combination Random/Ordered Mechanism*

Combinations of Ordered and Random Sequential Bi Bi Mechanisms also exist. In the Ordered-On/Random-Off Bi Bi Mechanism, binding of A must precede binding of B, but dissociation of P and Q may occur in either order:

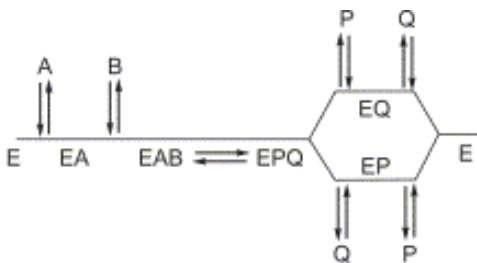


**Figure 8.** Cleland notation for an Ordered-On/Random-Off Bi Bi Mechanism. Image reproduced from (36).

---

<sup>3</sup> At least by watching product formation or substrate depletion rates. Transition state analogues, which can ‘freeze out’ the enzyme in the middle of the reaction, and associated crystal structure work, can and have identified ternary complexes of Theorell-Chance enzymes (36).

In the reverse direction, such a reaction is termed a Random-On/Ordered-Off Bi Bi Mechanism. Such enzymes, while rare, have been experimentally shown; examples include sulfate adenylyltransferase from *Penicillium chrysogenum* (38) and adenine phosphoribosyltransferase from *Giardia lamblia* (39). The equations describing the kinetics of such an enzyme are extremely complex and will not be discussed.

### *Ping-Pong Mechanism*

For comparison's sake, the Ping-Pong type of reaction can be considered. In this type of reaction, there is no central ternary complex in the reaction. Rather, A binds to E to form E·A. This reacts to form F·P; the modified enzyme F then releases P. B then binds to F to produce F·B, and reacts to form E·Q. Once Q dissociates, E is ready to begin another reaction. The Ping-Pong reaction takes its name from the way the enzyme “bounces” between two possible covalent states during the full reaction cycle. Ping-pong enzymes are capable of single turnover events with either substrate in the absence of the other, provided the enzyme was in the right form, but they do not reach steady-state without both substrates present:

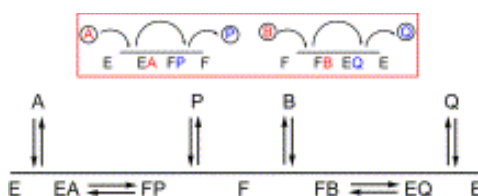


**Figure 9.** Cleland notation for a Ping-Pong Mechanism. Image reproduced from (36).

### *Iso Mechanisms*

Finally, some discussion of the more unusual types of kinetic mechanism is necessary. In Iso Mechanisms, there is at least one slow isomerization of the enzyme somewhere in the reaction cycle. If the isomerization were fast in comparison to the



slowest step, it would not be detectable; the term Iso is used *only* when there are indications of a kinetically significant population of isomerized enzyme. In other words, the enzyme may have two slow steps, one of which is the isomerization, and both steps contribute to limiting the overall rate of the reaction.

There are two types of Iso mechanisms: Di-Iso and Mono-Iso. In a Di-Iso mechanism, the enzyme (possibly while in a complex) isomerizes to another form; later, but still during the overall reaction, the enzyme isomerizes back. As an example, the Di-Iso Theorell-Chance Mechanism is written:



**Figure 10.** Cleland notation for a Di-Iso Theorell-Chance Mechanism. Image reproduced from (36).

Symmetric isomerizations, like the one shown above, do not affect the associated rate equations, and, consequently, the observed experiments in Ordered Sequential Bi Bi or Theorell-Chance Mechanisms (36). However, they will greatly affect a Ping-Pong reaction, completely removing the uncompetitive inhibition which is otherwise the hallmark of that type of kinetic mechanism.

Mono-Iso mechanisms are somewhat different. Sometime during the reaction cycle, the enzyme isomerizes. Then, after the release of the final product, but before the next substrate can bind, the enzyme must undergo an isomerization back to the original form:

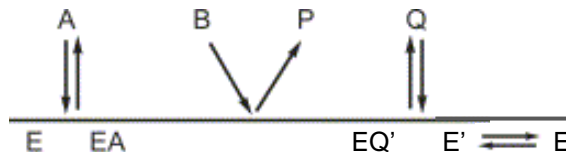


**Figure 11.** Cleland notation for a Mono-Iso Ordered Sequential Bi Bi Mechanism. Image adapted from (36).

Unlike a Di-Iso mechanism, a Mono-Iso mechanism does change the final form of the associated initial velocity equations. In general, terms accounting for the propensity of A to bind to E', and Q to bind to E, must be added. These terms are called *isoinhibition* constants, and are denoted  $K_{ii}$ , e.g.,  $K_{iia}$ ,  $K_{iiq}$ , etc. Iso mechanisms in general are few, but they can sometimes explain experimental oddities.

Given the wide variety of possible ternary reaction mechanisms, when faced with a new enzyme or enzyme family, it is customary to do some research to determine which of these possible mechanisms the enzyme follows. There are a few ways to do this. Most convenient are use of the complete competitive or “dead end” inhibitors. Competitive inhibitors are usually molecular analogues of either substrate A or B, denoted  $I_A$  and  $I_B$ .  $I_A$  will always be a competitive inhibitor with respect to A, and  $I_B$  will always be a competitive inhibitor with respect to B. However, as  $I_A$  binds in the binding pocket of A, its presence often cannot prevent the binding of B.  $I_A$  is still an inhibitor; its presence will lower the initial velocity of the reaction. Therefore, while  $I_A$  is competitive *with respect to A*, it will be uncompetitive or mixed-type *with respect to B*. When either  $I_A$  is applied to E while varying [B], or when  $I_B$  is applied to E while varying [A], the difference in observed inhibitory behavior depends on which kinetic mechanism is followed. This method of kinetic determination was the first to be attempted, and the results will be shown. However, in the end, this method failed because it would require a good competitive inhibitor of GHBDH with respect to GHB, and none of the tested substrate analogs could fill this role.

If good dead-end inhibitors are not available for both substrates, it is often still possible to determine the kinetic mechanism using a product as the inhibitor. In the

simplest case, product inhibitors effectively cause the reaction to begin closer to the equilibrium, and therefore the forward reaction proceeds more slowly in their presence. However, often product inhibitors have a second effect as well. Because products are structurally very similar to the reagents, they will bind to enzymes in the middle of the reaction cycle. As an example, take an enzyme conforming to an Ordered Sequential Bi Bi Mechanism, which converts A to Q and B to P. In this reaction, E first binds A to form E·A complex. To progress, the enzyme must then bind B; but it may be possible for product P to bind, leading to non-productive E·A·P complex. Likewise, it's possible for substrate B to bind E·Q complex after the dissociation of P but before the dissociation of Q, leading to non-productive E·B·Q complex:

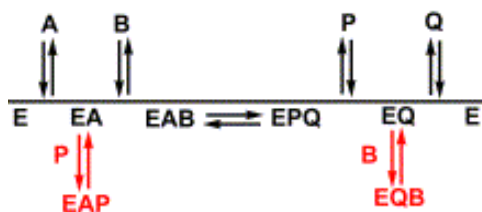


**Figure 12.** Cleland notation for an Ordered Sequential Bi Bi Mechanism with abortive complex formation. Image reproduced from (36).

These non-productive complexes are termed “abortive complexes.” In them, P and Q, in addition to changing how far the system initially is from equilibrium, also act as *dead-end* competitive inhibitors. Whether or not an abortive complex is possible is limited to some degree by binding pocket and active site geometry, and by the flexibility of the enzyme in question. In some cases, only one abortive complex is possible. When product inhibitors form abortive complexes, another pair of constants becomes necessary. In the above example,  $K_{ib}$  and  $K_{ip}$  refer to the dissociation constants of B and P from abortive complexes;  $K_{ib}$  and  $K_{ip}$  retain their original meanings.

## 2. Product Inhibition Equations

As previously mentioned, all of the above reactions can be described with equations in terms of the  $V_{max}$ ,  $K_m$ ,  $K_i$ ,  $K_I$ , and  $K_{ii}$  values. The derivation of such equations begins by writing the reaction in terms of the many microscopic rate constants ( $k$ ), but eventually simplifies to macroscopic constants. In some cases, especially when dealing with dead-end inhibitors, the macroscopic constant is the equilibrium dissociation, e.g., the  $k_{off}/k_{on}$  for a particular species. In other cases, however, the macroscopic constant is a complex combination of many individual rate constants. This section will give an overview of the equations describing the kinetic mechanisms already introduced and show how the equations are manipulated to predict the patterns of inhibition that reveal the underlying kinetic mechanism.

For enzymes which follow a Random Sequential Bi Bi Mechanism, an Ordered Sequential Bi Bi Mechanism, or a Theorell-Chance Bi Bi Mechanism, the initial rate of product formation in the absence of any product inhibitor is:

$$\frac{1}{v} = \frac{1}{V_{max}} + \frac{K_a}{V_{max}[A]} + \frac{K_b}{V_{max}[B]} + \frac{K_{ia}K_b}{V_{max}[A][B]}$$

When products are added into this initial-velocity equation, however, the resulting equations are different depending on the kinetic mechanism. This allows determination of the kinetic mechanism through a series of experiments in which [A] and [B] are independently varied, and different [P] or [Q] (but not both) applied to the reaction.

### Random Sequential Bi Bi Mechanism

In a Random Sequential Bi Bi Mechanism<sup>4</sup>, the addition of Q to the reaction yields the reciprocal initial-velocity equation:

$$\frac{1}{v} = \frac{1}{V_{max}} + \frac{K_a}{V_{max}[A]} + \frac{K_b}{V_{max}[B]} + \frac{K_{ia}K_b}{V_{max}[A][B]} \left[ 1 + \frac{[Q]}{K_{iq}} \right]$$

This can be rewritten to isolate  $\frac{1}{[A]}$ :

$$\frac{1}{v} = \frac{1}{V_{max}} + \frac{K_b}{V_{max}[B]} + \frac{1}{[A]} \left( \frac{K_a}{V_{max}} + \frac{K_{ia}K_b}{V_{max}[B]} \left[ 1 + \frac{[Q]}{K_{iq}} \right] \right)$$

The equation is now of the form  $y = mx + b$ . The  $\frac{1}{V_{max}} + \frac{K_b}{V_{max}[B]}$  term serves as the y-intercept, since [B] is constant in any experiment where [A] is the independent variable.

The  $\left( \frac{K_a}{V_{max}} + \frac{K_{ia}K_b}{V_{max}[B]} \left[ 1 + \frac{[Q]}{K_{iq}} \right] \right)$  term becomes the slope, which should vary with [Q].

Because the y-intercept is not affected by [Q] but the slope is, the apparent inhibition pattern is competitive. Using the same type of manipulation to isolate  $\frac{1}{[B]}$ , it can be shown that Q gives competitive inhibition with regards to both substrates. Of course, Q can only be a molecular analogue of one; but by initial velocity alone, it would appear to be competitive with both.

Likewise, in the same Random Sequential Bi Bi Mechanism, the addition of P to the reaction yields the initial-velocity equation:

$$\frac{1}{v} = \frac{1}{V_{max}} + \frac{K_a}{V_{max}[A]} + \frac{K_b}{V_{max}[B]} + \frac{K_{ia}K_b}{V_{max}[A][B]} \left[ 1 + \frac{[P]}{K_{ip}} \right]$$

---

<sup>4</sup> To which the rapid-equilibrium assumption has been applied.

Using the same manipulations as previously, it can thus be shown that P will *also* appear to be a competitive inhibitor of both A and B.

### *Ordered Sequential Bi Bi Mechanism*

In enzymes which follow an Ordered Sequential Bi Bi Mechanism, the product inhibition equations are different. When inhibited with product Q, the initial velocity equation is:

$$\frac{1}{v} = \frac{1}{V_{max}} + \frac{K_a}{V_{max}[A]} \left[ 1 + \frac{[Q]}{K_{iq}} \right] + \frac{K_b}{V_{max}[B]} + \frac{K_{ia}K_b}{V_{max}[A][B]} \left[ 1 + \frac{[Q]}{K_{iq}} \right]$$

Rewritten to isolate  $\frac{1}{[A]}$ , this equation becomes:

$$\frac{1}{v} = \frac{1}{V_{max}} + \frac{K_b}{V_{max}[B]} + \frac{1}{[A]} \left( \frac{K_a}{V_{max}} + \frac{K_{ia}K_b}{V_{max}[B]} \right) \left[ 1 + \frac{[Q]}{K_{iq}} \right]$$

The y-intercept is described by  $\frac{1}{V_{max}} + \frac{K_b}{V_{max}[B]}$ , and is a constant as long as [B] is invariant. The slope is described by  $\left( \frac{K_a}{V_{max}} + \frac{K_{ia}K_b}{V_{max}[B]} \right) \left[ 1 + \frac{[Q]}{K_{iq}} \right]$  and varies with [Q]. Thus, inhibition by Q when A is the independent variable will display competitive inhibition.

When this equation is written to specifically isolate  $\frac{1}{[B]}$ , it becomes:

$$\frac{1}{v} = \frac{1}{V_{max}} + \frac{K_a}{V_{max}[A]} \left[ 1 + \frac{[Q]}{K_{iq}} \right] + \frac{1}{[B]} \left( \frac{K_b}{V_{max}} + \frac{K_{ia}K_b}{V_{max}[A]} \left[ 1 + \frac{[Q]}{K_{iq}} \right] \right)$$

It is apparent that both the y-intercept and the slope vary with [Q]. Therefore, inhibition with Q when B is the independent variable will display *noncompetitive* inhibition.

When inhibited with product P, the initial velocity equation is:

$$\frac{1}{v} = \frac{1}{V_{max}} \left[ 1 + \frac{[P]}{K_{ip}} \right] + \frac{K_a}{V_{max}[A]} + \frac{K_b}{V_{max}[B]} \left[ 1 + \frac{K_q[P]}{K_{ip}K_{iq}} \right] + \frac{K_{ia}K_b}{V_{max}[A][B]} \left[ 1 + \frac{K_q[P]}{K_{ip}K_{iq}} \right]$$

Rewritten to isolate  $\frac{1}{[A]}$ , this becomes:

$$\frac{1}{v} = \frac{1}{V_{max}} \left[ 1 + \frac{[P]}{K_{ip}} \right] + \frac{K_b}{V_{max}[B]} \left[ 1 + \frac{K_q[P]}{K_{ip}K_{iq}} \right] + \frac{1}{[A]} \left( \frac{K_a}{V_{max}} + \frac{K_{ia}K_b}{V_{max}[B]} \left[ 1 + \frac{K_q[P]}{K_{ip}K_{iq}} \right] \right)$$

Both the y-intercept and the slope of this equation are functions of [P]. When A is the independent variable and P is added, the inhibition pattern will be noncompetitive.

When the same equation is written to isolate  $\frac{1}{[B]}$ , it becomes:

$$\frac{1}{v} = \frac{1}{V_{max}} \left[ 1 + \frac{[P]}{K_{ip}} \right] + \frac{K_a}{V_{max}[A]} + \frac{1}{[B]} \left( \frac{K_b}{V_{max}} \left[ 1 + \frac{K_q[P]}{K_{ip}K_{iq}} \right] + \frac{K_{ia}K_b}{V_{max}[A]} \left[ 1 + \frac{K_q[P]}{K_{ip}K_{iq}} \right] \right)$$

Again, since both the slope and the y-intercept are functions of [P], the inhibition pattern will be noncompetitive.

#### *Theorell-Chance Mechanism*

In an enzyme operating by Theorell-Chance kinetics, the initial velocity equation for inhibition by [Q] is:

$$\frac{1}{v} = \frac{1}{V_{max}} + \frac{K_a}{V_{max}[A]} \left[ 1 + \frac{[Q]}{K_{iq}} \right] + \frac{K_b}{V_{max}[B]} + \frac{K_{ia}K_b}{V_{max}[A][B]} \left[ 1 + \frac{[Q]}{K_{iq}} \right]$$

Note that this is the same as the equation for an Ordered Sequential Bi Bi Mechanism that is inhibited by Q. The mathematical manipulations result in the same predictions: when A is the independent variable, Q will display a competitive inhibition pattern; while when B is the independent variable, Q will display a noncompetitive inhibition pattern.

In an enzyme operating by Theorell-Chance kinetics, the initial velocity equation for inhibition by [P] is:

$$\frac{1}{v} = \frac{1}{V_{max}} + \frac{K_a}{V_{max}[A]} + \frac{K_b}{V_{max}[B]} \left[ 1 + \frac{[P]}{K_{ip}} \right] + \frac{K_{ia}K_b}{V_{max}[A][B]} \left[ 1 + \frac{[P]}{K_{ip}} \right]$$

This is *not* the same as the equation describing the inhibition of an Ordered Sequential Bi Bi Mechanism enzyme by P. It is, however, essentially identical to the Theorell-Chance inhibition by Q, except that as Q is the counterpart of A, B is the counterpart of P. Therefore, when B is the independent variable there is a competitive inhibition pattern, whereas A displays a noncompetitive inhibition pattern.

### *Ping-Pong Inhibition*

A Ping-Pong reaction mechanism is somewhat simpler, because there is no central ternary complex. Even in the absence of any product inhibitor, it follows:

$$\frac{1}{v} = \frac{1}{V_{max}} + \frac{K_a}{V_{max}[A]} + \frac{K_b}{V_{max}[B]}$$

Rearranging to isolate  $\frac{1}{[A]}$  gives:

$$\frac{1}{v} = \frac{1}{V_{max}} + \frac{K_b}{V_{max}[B]} + \frac{1}{[A]} \left( \frac{K_a}{V_{max}} \right)$$

It should be apparent that the slope is dependent solely on the constants  $K_a$  and the  $V_{max}$ , and is independent of the concentration of any of the species in solution. If this experiment is done by varying  $[A]$ , and repeated at several different  $[B]$ , a series of parallel lines is generated. Because the equation is symmetrical, varying  $[B]$  at several different  $[A]$  will *also* give parallel lines. Therefore, a Ping-Pong mechanism can be easily observed even without product inhibition.

However, it's perfectly possible to determine a Ping-Pong mechanism by product inhibition. When inhibiting with Q, the equation is:



$$\frac{1}{v} = \frac{1}{V_{max}} + \frac{K_a}{V_{max}[A]} \left[ 1 + \frac{[Q]}{K_{iq}} \right] + \frac{K_b}{V_{max}[B]}$$

It is immediately obvious that Q then displays a competitive inhibition pattern against [A]. Less obviously is the fact that, with respect to B, the slope is independent of [Q] but the y-intercept is not. With respect to B, inhibition by Q will display the parallel lines characteristic of uncompetitive inhibition.

The equation for inhibition of a Ping-Pong enzyme by P is:

$$\frac{1}{v} = \frac{1}{V_{max}} + \frac{K_a}{V_{max}[A]} + \frac{K_b}{V_{max}[B]} \left[ 1 + \frac{[P]}{K_{ip}} \right]$$

This is the exact counterpart of inhibition by Q. P then gives competitive inhibition when B is the independent variable, but uncompetitive inhibition when A is the independent variable. Bisubstrate enzymes operating by a Ping-Pong mechanism are the only ones to display uncompetitive inhibition and can be easily identified.

### *Iso Inhibition*

As mentioned, Di-Iso mechanisms do not change the form of Ordered Sequential Bi Bi or Theorell-Chance Mechanisms. However, in a Ping-Pong reaction, additional terms for AQ, BP, ABP, ABQ, APQ, and BPQ species must be added to the rate equation. Of course, many of these terms are physically impossible: if Q is the product of A, then it is likely to be a molecular analogue of A and the two will not physically be able to inhabit the same enzyme molecule at the same time. Mathematically, these extra terms represent the propensity of various substrate and product species to associate with the “wrong” isomeric enzyme form.

Mono-Iso mechanisms, by contrast, always change the associated rate equation, because terms accounting for the post-reaction isomerization must be appended. As an example, the equation for a Mono-Iso Theorell-Chance Mechanism when inhibited by Q is:

$$\frac{1}{v} = \frac{1}{V_{max}} \left[ 1 + \frac{[Q]}{K_{iiq}} \right] + \frac{K_a}{V_{max}[A]} \left[ 1 + \frac{[Q]}{K_{iq}} \right] + \frac{K_b}{V_{max}[B]} + \frac{K_{ia}K_b}{V_{max}[A][B]} \left[ 1 + \frac{[Q]}{K_{iq}} \right]$$

Note the addition of the  $K_{iiq}$  term, which is the isoinhibition necessary to account for the propensity of Q to bind to E. When rewritten to isolate  $\frac{1}{[A]}$ , this equation becomes:

$$\frac{1}{v} = \frac{1}{V_{max}} \left[ 1 + \frac{[Q]}{K_{iiq}} \right] + \frac{K_b}{V_{max}[B]} + \frac{1}{[A]} \left( \frac{K_a}{V_{max}} \left[ 1 + \frac{[Q]}{K_{iq}} \right] + \frac{K_{ia}K_b}{V_{max}[B]} \left[ 1 + \frac{[Q]}{K_{iq}} \right] \right)$$

Since there is a Q term in both the slope and the intercept, inhibition by Q when A is the variable substrate will result in *noncompetitive* inhibition, rather than the competitive inhibition seen for a non-iso Theorell-Chance mechanism. Likewise, when rewritten to isolate  $\frac{1}{[B]}$ , the equation is:

$$\frac{1}{v} = \frac{1}{V_{max}} \left[ 1 + \frac{[Q]}{K_{iiq}} \right] + \frac{K_a}{V_{max}[A]} \left[ 1 + \frac{[Q]}{K_{iq}} \right] + \frac{1}{[B]} \left( \frac{K_b}{V_{max}} + \frac{K_{ia}K_b}{V_{max}[A]} \left[ 1 + \frac{[Q]}{K_{iq}} \right] \right)$$

Again, Q appears in both the slope and intercept terms, and will again display noncompetitive inhibition.

The equation for a Mono-Iso Theorell-Chance Mechanism when inhibited by P is:

$$\frac{1}{v} = \frac{1}{V_{max}} + \frac{K_a}{V_{max}[A]} + \frac{K_b}{V_{max}[B]} \left[ 1 + \frac{P}{K_{ip}} \right] + \frac{K_{ia}K_b}{V_{max}[A][B]} \left[ 1 + \frac{[P]}{K_{ip}} \right]$$

Rewritten to isolate  $\frac{1}{[A]}$ , this becomes:

$$\frac{1}{v} = \frac{1}{V_{max}} + \frac{K_b}{V_{max}[B]} \left[ 1 + \frac{P}{K_{ip}} \right] + \frac{1}{[A]} \left( \frac{K_a}{V_{max}} + \frac{K_{ia}K_b}{V_{max}[B]} \left[ 1 + \frac{[P]}{K_{ip}} \right] \right)$$

This leads to noncompetitive inhibition by P with respect to A. Finally, rewritten to isolate  $\frac{1}{[B]}$ , the equation is:

$$\frac{1}{v} = \frac{1}{V_{max}} + \frac{K_a}{V_{max}[A]} + \frac{1}{[B]} \left( \frac{K_b}{V_{max}} \left[ 1 + \frac{P}{K_{ip}} \right] + \frac{K_{ia}K_b}{V_{max}[A][B]} \left[ 1 + \frac{[P]}{K_{ip}} \right] \right)$$

This leads to competitive inhibition by P with respect to B. Thus, a Mono-Iso mechanism can be differentiated from a Di-Iso mechanism; but a Di-Iso mechanism, except in the case of Ping-Pong, cannot be differentiated from a non-iso mechanism.

It should be noted that the inhibition patterns produced by iso mechanisms are often the same as those produced by a different mechanism. Above, the inhibition pattern predicted for Mono-Iso Theorell-Chance Mechanism is the same as the inhibition pattern predicted for an Ordered Sequential Bi Bi Mechanism, with the identities of A and B switched, and of P and Q switched. Without other available information the simple solution is preferred. Therefore, a series of inhibition experiments in which there are three noncompetitive substrate/inhibition pairs and one competitive substrate/inhibition pair would be evaluated as an Ordered Sequential Bi Bi Mechanism. Iso mechanisms should only be invoked when the product inhibition patterns are abnormal, or when there is other evidence to suggest that the simpler solution is incorrect.

### 3. Determining Kinetic Mechanism by Experimentation

The series of experiments necessary to determine which of these kinetic mechanisms any given enzyme follows is straightforward. For ease of understanding, there are two substrates, S and T, and two products, X and Y; these correspond to A, B, P, and Q, but

which is which is not known *a priori*. First, holding the concentration of S constant, the concentration of T is varied at different constant concentrations of X. Second, still holding S constant, the concentration of T is varied at different concentrations of Y. Third, now holding T constant, the concentration of S is varied while at different concentrations of X. Fourth, again holding T constant, the concentration of S is varied while at different concentrations of Y. Note that in all cases, the concentration of the nonvariable substrate must be held at sub-saturating levels. Saturating with the nonvaried substrate will sometimes cause that substrate to “outcompete” the inhibitor, and thus no inhibition will be observed. Finally, use nonlinear fitting to determine which type of inhibition is observed and plot the data. Lineweaver-Burke plotting is a much easier way to visualize which *type* of inhibition any particular inhibitor displays, but the nonlinear fitting has smaller error in determining the parameter values.

Theoretically, competition of all products with all substrates indicates a Random Sequential Bi Bi Kinetic Mechanism, in which case A and B, and P and Q, are arbitrary (36). Competition of only one pair indicates both an Ordered Sequential Bi Bi Mechanism, and that the competing substrate-product pair can be assigned as A and Q, respectively. Competition of two pairs indicates a Theorell-Chance Mechanism; in this case the identities of A and B, and Q and P, can't be assigned based on this experimental evidence alone. Other experiments, for example a binding study, are needed to definitively determine which substrate binds first and is therefore A. Finally, any uncompetitive inhibition indicates a Ping-Pong mechanism. Again, the identities of A and P, and B and Q, can't be assigned based on the experimental evidence alone because at steady-state the enzyme is bouncing between two states E and F. Only if there's some

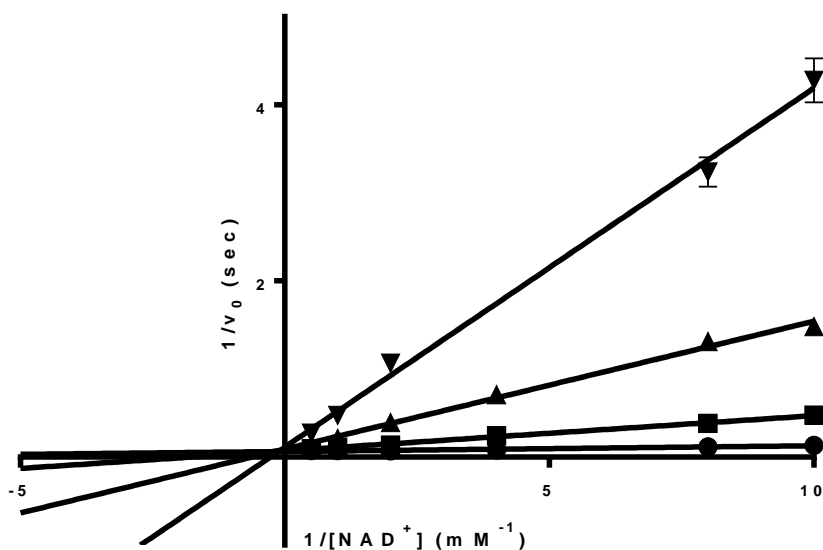
other knowledge about what form the enzyme was synthesized in, and which of the two products must bind “first,” can A and B be confidently assigned.

### ***C. Results and Discussion***

The first experiment was a simple substrate-saturation curve, holding one substrate at saturation while varying the other in order to determine  $K_m$  and  $V_{max}$ . Table 1 shows the results of this experiment:

<b>Table 1.</b> Substrate selectivity of GHBDH			
Variable substrate	$k_{cat}$ ( $\text{sec}^{-1}$ )	$K_m$ (mM)	$k_{cat}/K_m$ ( $\text{mM}^{-1} \text{sec}^{-1}$ )
NAD <sup>+</sup>	$8.9 \pm 0.2$	$0.064 \pm 0.0063$	$139 \pm 14$
GHB	$8.4 \pm 0.3$	$0.98 \pm 0.11$	$8.6 \pm 1$

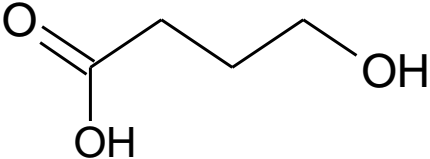
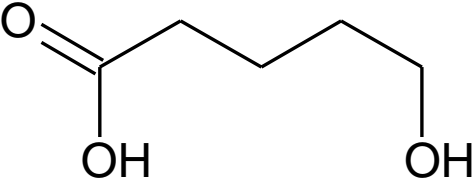
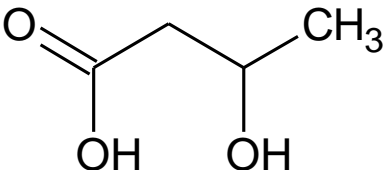
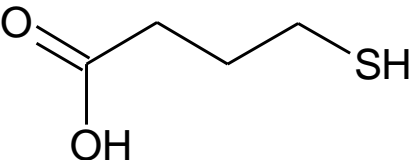
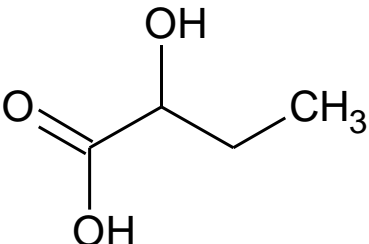
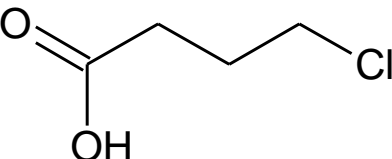
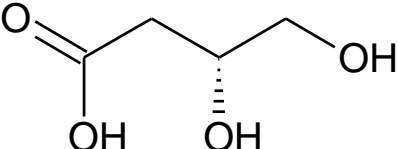
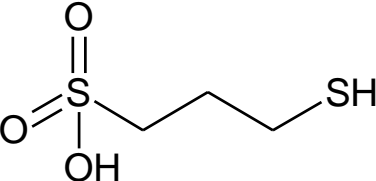
The next set of experiments was an attempt to use dead-end inhibition to determine the kinetic mechanism. The two substrates of GHBDH are NAD<sup>+</sup> and GHB. Therefore, the prospective inhibitors were chosen rationally based on structural similarity to these two substrates. The compound chosen as an inhibitor of NAD<sup>+</sup> was adenosine-5'-diphospho-ribose (ADPR). This chemical is essentially an NAD<sup>+</sup> molecule which is missing the terminal nicotinamide ring. It is thus unable to be oxidized or reduced. ADPR is an excellent competitive inhibitor of NAD<sup>+</sup>, having a  $K_i$  of only 5.6  $\mu\text{M}$ .



**Figure 13.** Lineweaver-Burke plot of GHBDH inhibition by ADPR with  $NAD^+$  as the variable substrate. Error bars are not shown where they would be smaller than the height of the symbol. ● 0 mM ADPR; ■ 0.04 mM ADPR; ▲ 0.12 mM ADPR; ▼ 0.4 mM ADPR.

Then a good competitive inhibitor of GHB was necessary. The compounds in Table 2 were tested for their ability to inhibit GHBDH as competitive inhibitors with respect to GHB. Although all of them, except for 4-chlorobutyrate, were inhibitors of GHBDH, they were all mixed-type inhibitors. Without a good competitive inhibitor to establish kinetics, product inhibition assays were instead chosen for kinetic analysis.

**Table 2.** Compounds assessed as potential competitive inhibitors of GHBDH with respect to GHB.

 <p><i>gamma</i>-hydroxybutyric acid</p>	 <p>5-hydroxypentanoic acid</p>
 <p><i>beta</i>-hydroxybutyric acid</p>	 <p>4-mercaptobutyric acid</p>
 <p><i>alpha</i>-hydroxybutyric acid</p>	 <p>4-chlorobutyric acid</p>
 <p>R-2,4-dihydroxybutyric acid</p>	 <p>1-mercapto-3-propanesulfonic acid</p>

When  $\text{NAD}^+$  is the independent variable, NADH displays noncompetitive inhibition (Fig. 10). This immediately rules out an Ordered Sequential Bi Bi Mechanism with  $\text{NAD}^+$  binding first; NADH should compete with  $\text{NAD}^+$  in this case. This is peculiar, because most ADHs bind  $\text{NAD}^+$  first followed by the alcohol/aldehyde substrate. The data, however, are unambiguous:

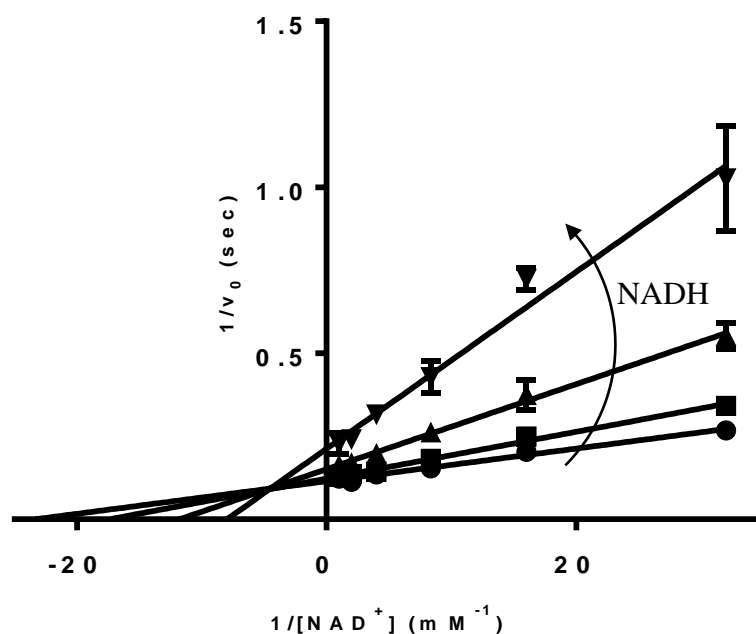


**Figure 14.** Lineweaver-Burke plot of GHBDH inhibition by NADH with  $NAD^+$  as the variable substrate. Error bars are not shown where they would be smaller than the diameter of the symbol. ● 0 mM NADH; ■ 0.0126 mM NADH; ▲ 0.04 mM NADH; ▼ 0.1 mM NADH.

When  $NAD^+$  is the independent variable, SSA displays noncompetitive inhibition (Figure 15). Crystal structures of various Group III ADHs have shown that the  $NAD(P)(H)$  binding site and the alcohol/aldehyde binding site are separate and for the most part non-overlapping. Therefore,  $NAD^+/SSA$  and  $GHB/NADH$  pairs are not expected to occupy any part of each other's binding sites and compete with each other:



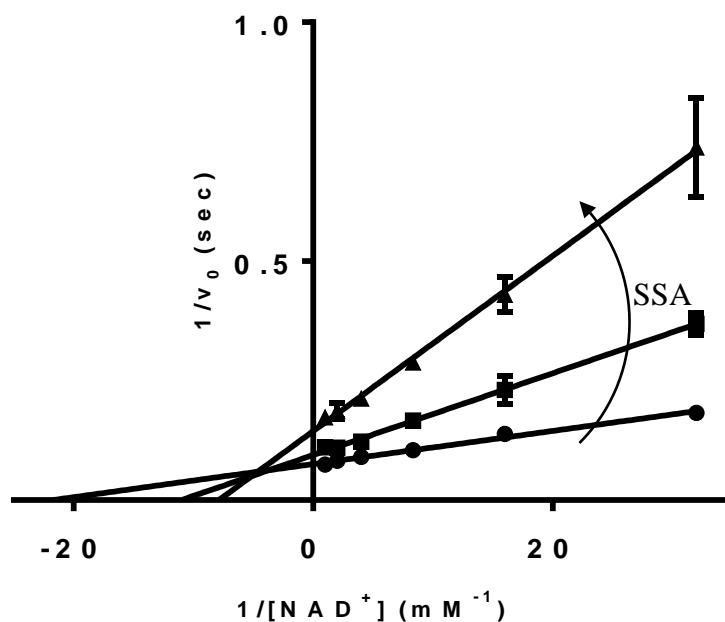


**Figure 15.** Lineweaver-Burke plot of GHBDH inhibition by SSA with  $\text{NAD}^+$  as the variable substrate. Error bars are not shown where they would be smaller than the diameter of the symbol. ● 0 mM SSA; ■ 0.1 mM SSA; ▲ 0.3 mM SSA.

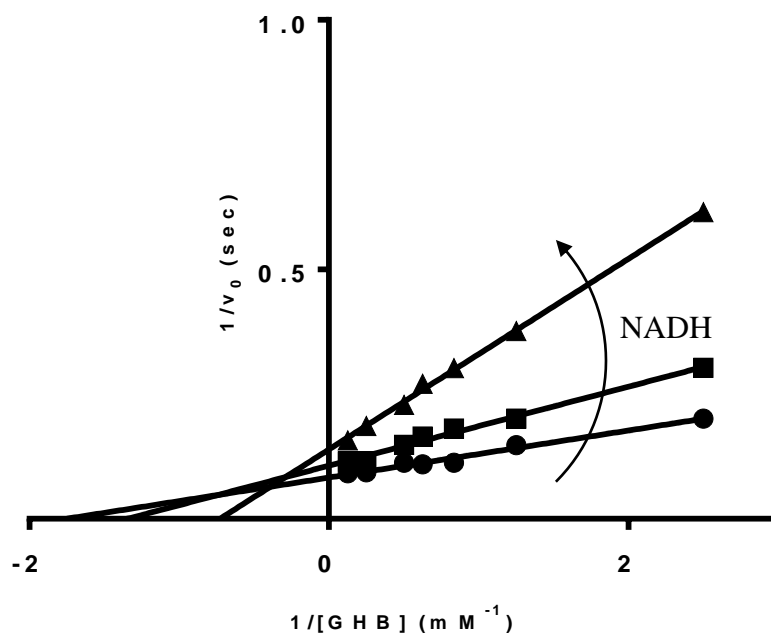


**Figure 16.** Lineweaver-Burke plot of GHBDH inhibition by NADH with GHB as the variable substrate. Error bars are not shown where they would be smaller than the diameter of the symbol. ● 0 mM NADH; ■ 0.0126 mM NADH; ▲ 0.04 mM NADH.

When GHB is the independent variable, NADH displays noncompetitive inhibition.

When GHB is the independent variable, SSA displays competitive inhibition:

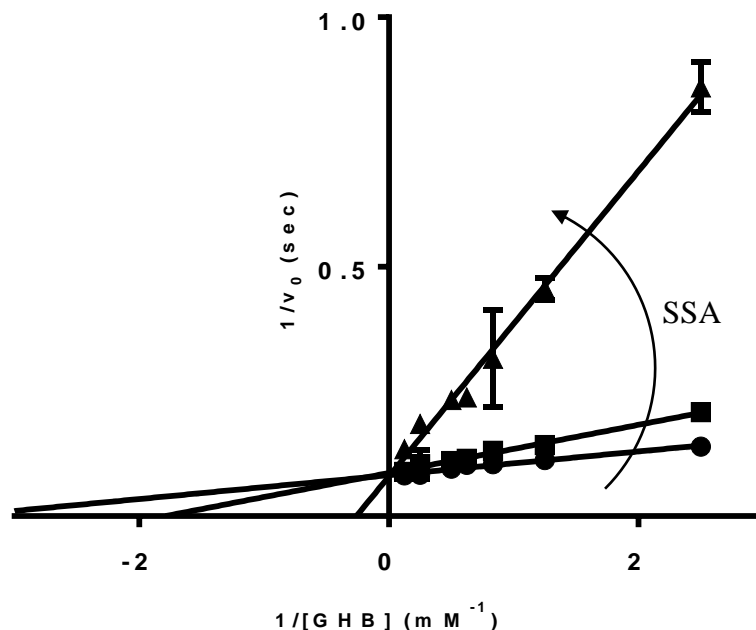


**Figure 17.** Lineweaver-Burke plot of GHBDH inhibition by SSA with GHB as the variable substrate. Error bars are not shown where they would be smaller than the height of the symbol. ● 0 mM SSA; ■ 0.01 mM SSA; ▲ 0.1 mM SSA.

The kinetics of GHBDH thus conform either to an Ordered Sequential Bi Bi Mechanism, or to a Mono-Iso Theorell-Chance Mechanism (36). Of the two, the Ordered Sequential Bi Bi Mechanism is considered less likely, for two reasons. First, the Ordered Sequential Mechanism would require that GHB binds to enzyme first, and SSA leaves last. In contrast, the vast majority of alcohol dehydrogenases in any family bind cofactor (NAD(P)(H)) before binding substrate (1). From an evolutionary perspective, it is much easier to diversify when the cofactor binding pocket remains the same but the substrate binding pocket changes, than having to completely rearrange both binding pockets. While there are dehydrogenase enzymes which follow substrate-then-cofactor binding order (40), (41), there

is evidence that this is not the case with Group III ADHs and, consequently, GHBDH: eight separate groups have reported cocrystals of a Group III ADH with NAD(P) (17). This is probably not an artefact of the crystallization, and instead represents real cofactor binding to enzyme in the absence of substrate. Therefore, the Mono-Iso Theorell-Chance Mechanism is favored.

A second piece of evidence comes from the study of the Group III ADH *FucO*, from *E. coli* by Blikstad and Widersten (34). The study focused primarily on the stereospecificity of the hydride transfer, but the kinetic isotope effect (KIE) and the effect of solvent viscosity on the catalytic rate were also studied. From the discrepancy of the effect of solvent viscosity on the rate when a favored and unfavored substrate were used, and the KIE results, Blikstad and Widersten concluded that there is at least one slow step which partially masks the rate-limiting slow step of the hydride transfer. They then attributed this slow step to two isomerization events, proposing a Di-Iso Ordered Sequential Bi Bi Mechanism. In such a mechanism, there are two internal isomerizations during the reaction cycle. They gave no further evidence for a Di-Iso mechanism, however, and a Mono-Iso mechanism would really be the minimum requirement for a second slow step that is partially rate-limiting.

Based on this evidence, it seems more likely that GHBDH operates by a Mono-Iso Theorell-Chance kinetic mechanism. In this reaction, NAD<sup>+</sup> binds first followed by GHB, then hydride transfer occurs, and finally the products SSA and NADH are released in that order. Finally, there must be an isomerization step from some isomerized form of enzyme back to free enzyme E. This mechanism explains why NADH and NAD<sup>+</sup> do not compete as they would in an ordinary Ordered Sequential Bi Bi Mechanism: they do not bind to the same form of enzyme and are thus not competitive. The enzyme responsible for the transfer

of a methyl group to vitexin 2"-O-rhamnoside to produce the oat plant flavonoid 7-0-methylvitexin 2"-O-rhamnoside also functions by a Mono-Iso Theorell-Chance mechanism (42).

#### ***D. Materials and Methods***

##### **1. Purification of GHBDH**

*E. coli* cells harboring the pGEX-2T/GHB-DH plasmid were grown in 1 L LB broth supplemented with 50 µg/mL ampicillin. When the culture had reached an OD<sub>600</sub> of ~1, GHBDH was induced by addition of 0.1 mM of isopropyl β-D-thiogalactoside (IPTG) and the temperature lowered to 19°C. After 18-22 hours of further shaking, 1 mM each of benzamidine and phenylmethylsulfonyl fluoride (PMSF) were added directly to the culture medium to inhibit proteases. Cells were then harvested by centrifugation at 4,412 g for 30 minutes. The supernatant was decanted, and the cells resuspended in ice-cold GHBDH Resuspension Buffer (30 mM MOPS, pH 7.4, 50 mM NaCl) which had also been supplemented with 1 mM PMSF, 1.5 mM benzamidine, and 0.6 µM aprotinin. The cell suspension was transferred to a JA-20 microcentrifuge rotor and ~5 mg lysozyme (a heaping spatula) was added. The tube was then closed and submerged in liquid nitrogen until frozen. The tube was placed in water to thaw, then opened and supplemented with ~5 mg DNase I (a heaping spatula). The tube was closed and again frozen and thawed. Cell debris were pelleted by centrifugation at 14600 g for 30 minutes. All steps after this were performed at 4°C. The supernatant was passed through a 0.45 µm filter to remove any remaining debris. The clarified supernatant was then flowed onto a column of ~30 mL GSH-agarose which had been previously equilibrated with GHBDH Resuspension

Buffer until the clarified crude extract had all entered the bed volume. Then the column was capped and the fusion protein allowed to adsorb to the column for 20 minutes. Next, 20 mL of GHBDH Wash Buffer #1 (30 mM MOPS, pH 7.4, 500 mM NaCl, 0.1% Tween-20) was used to wash the column of any nonspecifically bound protein. A second wash, comprising 20 mL of GHBDH Wash Buffer #2 (30 mM MOPS, pH 7.4) was used to wash any remaining Tween from the column prior to elution. Finally, 10 mL of GHBDH Elution Buffer (30 mM MOPS, pH 7, 5 mM S-hexylglutathione) was applied to the column. The column was again capped and allowed to rest for 1 hour while the protein dissociated off the column. A further 40 mL of GHBDH Elution Buffer was slowly flowed through the column, and eluent was collected in 5 mL fractions. Fractions were then immediately assayed for enzymatic activity. The fractions with the most activity were pooled (typically about 15 mL), aliquoted in 0.4 mL fractions into cryostorage tubes, frozen in liquid nitrogen, and stored at -80°C.

## 2. GHBDH Assays

The assay mixture comprised GHB,  $\text{NAD}^+$ , either SSA or NADH, the enzyme fraction, and enough GHBDH Assay Buffer to bring to a total volume of 1 mL. GHBDH Assay Buffer was 0.1 M each of MES, HEPES, and AMPSO, adjusted to pH 9 with NaOH, and supplemented with 5 mM  $\text{MgSO}_4$ . When GHB was the variable substrate, the concentration of  $\text{NAD}^+$  was held constant at 1 mM. When  $\text{NAD}^+$  was the variable substrate, the concentration of GHB was held constant at 16 mM. To start the reaction, 5  $\mu\text{L}$  of enzyme was added. After quickly mixing by inversion, the absorbance at 340 nm was measured continuously for 60 s. Each assay was performed in triplicate, and one of the replicates used to confirm pH. Background activity was measured by adding buffer

instead of enzyme fraction, or by omitting one of the substrates (GHB or NAD<sup>+</sup>).

Background activity was negligible in all cases.

### 3. Dead-end Inhibition Assays

The assay was performed as described above. Inhibitors were dissolved in GHBDH Assay Buffer, and this was added to the assay mixture first and allowed to equilibrate for a minimum of 5 minutes before starting the reaction.

### 4. GHBDH Product Inhibition Assays

The assay was performed as described above. When GHB was the variable substrate, the concentration of NAD<sup>+</sup> was held constant at 0.1 mM. When NAD<sup>+</sup> was the variable substrate, the concentration of GHB was held constant at 6 mM. Due to their propensity toward oxidation, SSA and NADH solutions were prepared shortly before the experiment. The substrates and product inhibitors (when present) were mixed into buffer first, and 5  $\mu$ L of enzyme added last to initiate the reaction.

### 5. Data Processing

The data were first transformed from A<sub>340</sub> to concentration of NADH, and from there to number of turnovers per molecule of enzyme. These were then fit using Mathematica® either to a line (in the case of controls and low activity samples) or to a hyperbola of the type:

$$v = ae^{-kt} + C$$

The first derivative at time 0 was then taken to approximate the initial velocity. If Mathematica® was unable to confidently assign a  $k$  ( $p < 0.05$ ), or the rate was negative, that datum was omitted from further analyses.

Once initial velocities had been generated, they were input into GraphPad PRISM® data processing software. PRISM® software has nonlinear regression capable of determining type of inhibition, as well as making appropriate graphics. Initial velocity data were fitted against all four types of inhibition. Mixed-type inhibition invariably had the lowest  $R^2$ , simply because the program had a larger number of parameters to adjust ( $K_i'$  and  $K_i$  vs  $K_i$  only). The pair with the best competitive inhibition fit (as measured by lowest absolute sum of squares) was GHB/SSA; the pair with the *worst* competitive fit was NAD/NADH. Therefore, while surprising, GHB and SSA were assigned to competitive inhibition. Additionally, the Lineweaver-Burke transform was applied to all data, and the transformed data used to generate plots for displaying the data. In Lineweaver-Burke plots, SSA is a clear competitive inhibitor with respect to GHB, while NADH is clearly a mixed-type inhibitor with respect to  $\text{NAD}^+$ .

## IV. Activator Assays

### A. Motivation

Activator proteins must activate in one of two ways: either there is a direct protein-protein interaction, or the activator protein (which is itself an enzyme) is producing some other species, which interacts directly with the Group III ADH and activates it. However, there are a few facts about the activation that suggest it is *not* a direct protein-protein interaction.

First and most importantly, activator proteins work cross-species (9). If the activation were dependent on a specific protein-protein interaction, then the activation should to some extent be dependent on the “goodness” of the interaction; the activator of one species would not be expected to have a tight interaction with the Group III ADH of another species. When a panel of nudix hydrolases and Group III ADHs from several species were tested against each other by other workers, almost all of the nudix hydrolases activated all of the Group III ADHs. (The one exception was NudE, an *E. coli* nudix hydrolase, which didn’t activate anything.) Either all species’ nudix hydrolases interact well with all Group III ADHs, or a direct interaction is not necessary. This was true of the activation assays done here on GHBDH; the activator protein (ACT) is a *B. methanolicus* nudix hydrolase, but it was able to activate GHBDH from *C. necator*.

Second, the activation is strictly dependent on the presence of  $Mg^{2+}$ , to the point that addition of ACT in  $Mg^{2+}$ -free buffer was one of the controls. Although that does not prove that the activator is something that ACT produces, it does show that the activation is not a simple change caused by ACT binding to GHBDH. ACT must be able to function



enzymatically, or there is not activation. Thus, assays were undertaken to determine ACT protein is necessary for activation, or if there is some other small molecule that ACT was producing that was the activator.

### ***B. Results and Discussion***

The ACT preparation was shown to be highly active using ADPR and somewhat active using  $\text{NAD}^+$  as substrate, in agreement with prior work. In general, ACT required both more  $\text{NAD}^+$  and time to give a similar amount of phosphate product as it had when ADPR was used as substrate. This is not surprising, however, if ACT is an ADPR pyrophosphatase (ADPRase) that only incidentally cleaves  $\text{NAD}^+$ . NudF, the *E. coli* ADPRase, is a homologous ADPRase which has been better-studied. Although the sequence identity with ACT is only ~25%, there are another ~25% of amino acids with conservative substitutions, for an overall similarity of >50%. Thus, NudF probably is a good model for explaining features of ACT. Crystal structures of NudF are available, alone and in complex with  $\text{Mg}^{2+}$  ions and a non-hydrolysable ADPR analogue (43). In these crystals, the ADPR analogue is bent into a horseshoe shape, with both the adenosine moiety and the terminal ribose in binding pockets. The hydrolysis of the pyrophosphate bond occurs at the surface of the molecule and involves the binding of  $\text{Mg}^{2+}$  ions to coordinate a nucleophilic attack by water. The mismatch between the size of a binding pocket sized for ribose and the extra nicotinamide ring probably accounts for low activity against  $\text{NAD}^+$ .

Once ACT protein had been purified, the attempt was made to titrate GHBDH activation with activator protein. This produced the frankly unbelievable result that ~90% of activation could be achieved by adding ACT at a ratio of only 2% of the GHBDH concentration, in

moles, and complete activation could be achieved by adding 10%. Whatever the activator is, clearly it is very potent.

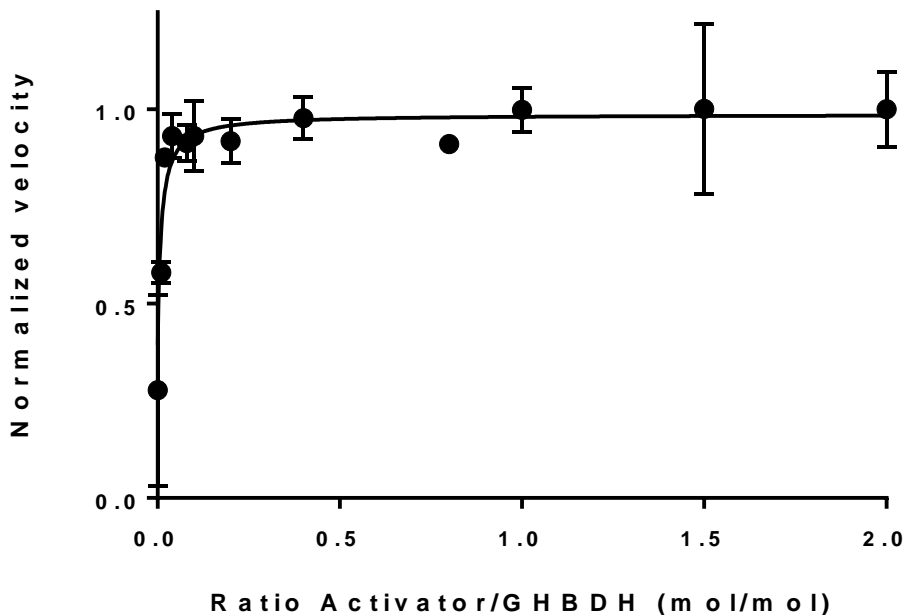


**Figure 18.** Titration of GHBDH activation against ACT added. Velocity has been normalized to maximum activity when activated.

Like all Group III ADHs, GHBDH forms dimers. No information is known about the native oligomerization state beyond dimerization. As mentioned in the introduction, two crystal structures, *B. stearothermophilus* glycerol dehydrogenase (18) and *Klebsiella pneumoniae* 1,3-propanediol dehydrogenase (19), show association of dimers. To get a ratio of 2% activator:GHBDH, GHBDH would have to be associating into 50-mers, which would then each be completely activated by a single subunit of ACT. This is plainly unrealistic, and it made even less realistic by the fact that nudix hydrolases are *also* known to exist natively as dimers, so really the result corresponds to one activator dimer activating fifty GHBDH dimers.

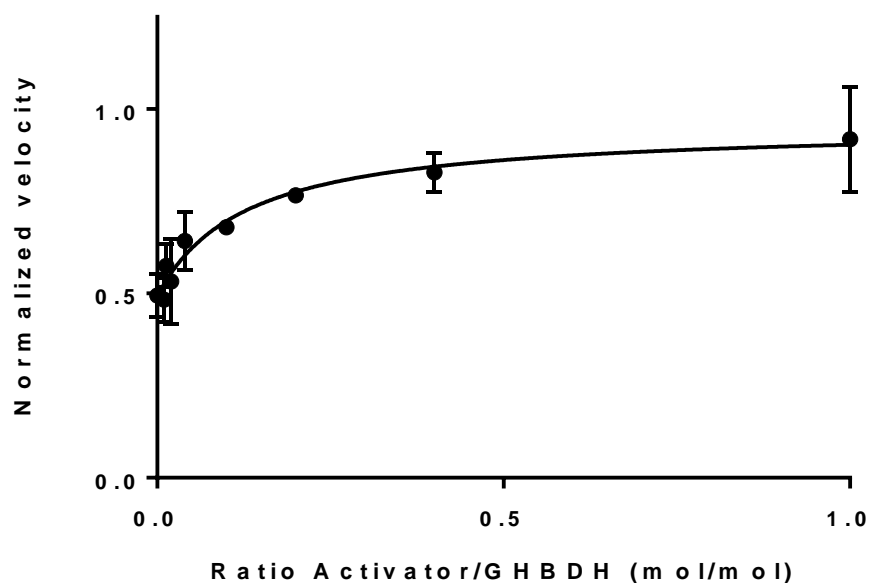


**Figure 19.** Titration of GHBDH activation against ACT added without a pre-incubation. Velocity has been normalized to maximum activity when activated.

To reconcile these results, a different approach was taken: in addition to just titrating *amounts* of GHBDH and ACT, a second factor, time, was considered. When ACT was added to solution just prior to GHBDH addition, the results were much more reasonable: complete activation required one mol of ACT per mol GHBDH. This discrepancy between the results when ACT is allowed 5 minutes in GHBDH assay mixture prior to the assay, and ACT added seconds before GHBDH, is further evidence that the true activator is not ACT, but some potent product that ACT is producing. For all future assays, a ratio of ~0.3 mols ACT to 1 mol GHBDH was used, but a minimum of five minutes of pre-incubation ensured that ACT had time to produce enough of the true activator to achieve complete activation.

The next logical question was: what is the activator, if it is not ACT protein itself but rather something that ACT protein makes? ACT is a nudix hydrolase, which means it cleaves in or around pyrophosphates. The natural substrate seems to be ADPR; when

cleaved, the products are adenosine 5'-monophosphate (AMP) and nicotinamide riboside (NR). The species in GHBDH assay solution which contained a pyrophosphate was  $\text{NAD}^+$ ; the analogous cleavage products of  $\text{NAD}^+$  are AMP and nicotinamide mononucleotide ( $\text{NMN}^+$ ). Accordingly, AMP and  $\text{NMN}^+$  were added to GHBDH assays in the absence of any ACT to test this possibility.

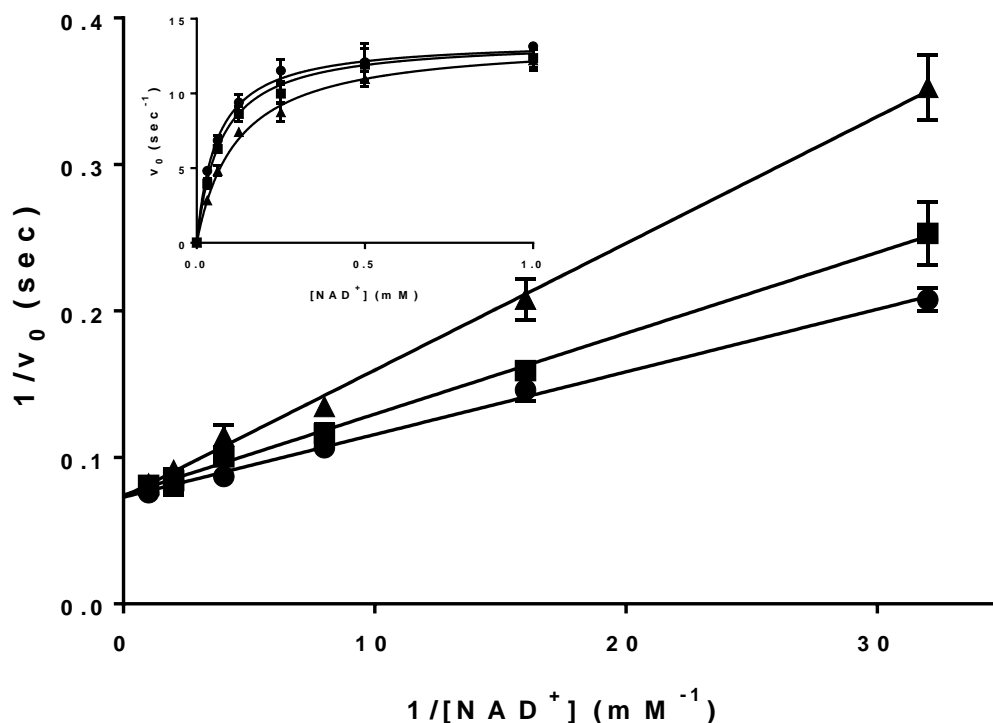


**Figure 20.** The inhibition of GHBDH by AMP. Error bars are not shown where they would be smaller than the height of the symbol. ● 0 mM AMP; ■ 1 mM AMP; ▲ 5 mM AMP.

The results show that AMP is an *inhibitor* of GHBDH, albeit a poor one; it has a  $K_i$  of 4.9 mM. The cellular AMP concentration in *E. coli* is  $\sim 151 \mu\text{M}$  (44), so 4.9 mM represents a concentration more than an order of magnitude higher than would ever be expected in a live bacterial cell. The inhibition is unexceptionable, as AMP (or any adenosine-containing moiety) can occupy the adenosine site of the  $\text{NAD}^+$  binding pocket and thus compete with

$\text{NAD}^+$  (16).  $\text{NMN}^+$  is not an inhibitor, even at a concentration of 5 mM. The probable cellular concentration of  $\text{NMN}^+$  is mid-micromolar (45), since in bacteria  $\text{NMN}^+$  seems to be quickly utilized in a pyridine nucleotide salvage pathway (46). It is unlikely that  $\text{NMN}^+$  has any effect on GHBDH *in vivo*. Therefore, although both of the cleavage products of  $\text{NAD}^+$  by ACT were tested, neither of them is the activator of GHBDH.

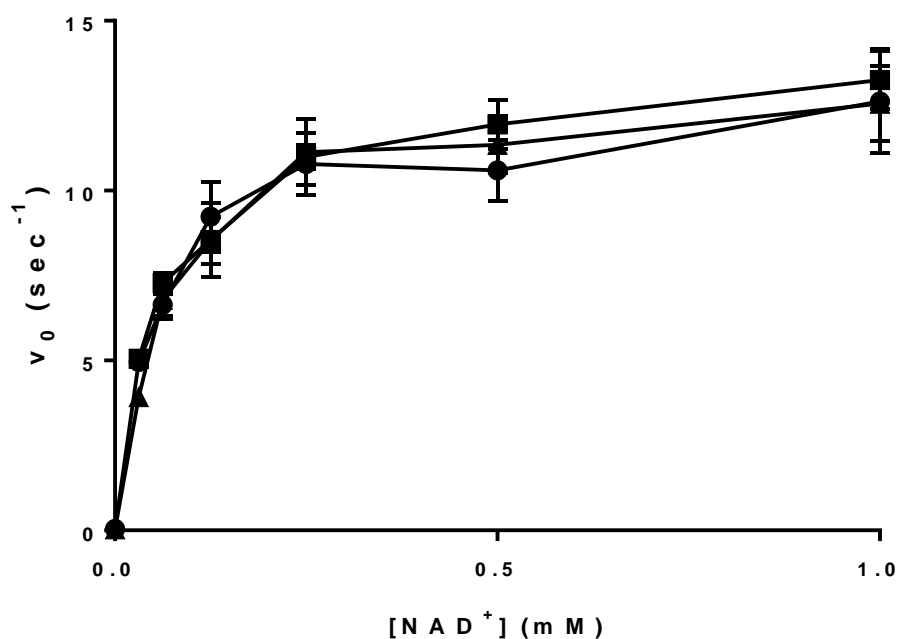


**Figure 21.** The lack of inhibition of GHBDH by  $\text{NMN}^+$ . Error bars are not shown where they would be smaller than the height of the symbol. ● 0 mM  $\text{NMN}^+$ ; ■ 1 mM  $\text{NMN}^+$ ; ▲ 5 mM  $\text{NMN}^+$ .

Kloosterman had suggested that an AMP that remained bound to MDH after nudix hydrolase cleavage was responsible for the activation (22). While adenylation is a well-known mechanism of enzymatic control, this AMP did not appear to be covalently bound to the enzyme, since treatment with urea was able to separate it from MDH. It is hard to imagine a system in which an AMP occupying the AMP binding pocket can be a competitive inhibitor when bound from free solution but is an activator when deposited by a

cleavage of  $\text{NAD}^+$ . Thus far, however, no small-molecule cleavage product has been shown to be the activator.

Although the two expected cleavage products of  $\text{NAD}^+$  are not the true activator, it is possible to make some deductions about what the activator must be.  $\text{NAD}^+$  was the only molecule in solution that contained a pyrophosphate linkage, and therefore had to be the target of ACT, a nudix hydrolase. Thus, if “cleavage” *between* the two phosphates did not produce the activator, then it must be produced by asymmetric cleavage on one side of the pyrophosphate. The two potential pairs of products from asymmetric cleavage are ADP and NR, and adenosine and nicotinamide riboside-5'-pyrophosphate (NRPP). Welch et. al. (16) already found that any compound containing adenosine acted as a competitive inhibitor of NADH in the reduction direction, so ADP and adenosine can be dismissed as candidates for the activator. That leaves only NR and NRPP. What little information is available suggests that NR is not usually found on the *interior* of microbial cells, because the uptake pathway of NR phosphorylates it to  $\text{NMN}^+$  (47), (48). On the other hand, no information about microbial metabolism of NRPP is available at all. While NR is available as a dietary supplement, neither compound is available in pure form for biochemical use and NRPP is difficult even to produce chemically. The next step would be to check each of those compounds individually for ability to activate a Group III ADH.

This leads to an interesting hypothesis: the sole determinant of whether a nudix hydrolase is a Group III ADH activator may be as simple whether that nudix hydrolase is capable of cleaving  $\text{NAD}^+$ . The implication for Group III ADHs in general is that *in vivo*, Group III ADHs may always be activated. Nudix hydrolases are ubiquitous in all cell types, and many of the nudix hydrolases used as activators only incidentally cleave  $\text{NAD}^+$ . From

an evolutionary standpoint, this is probably more a necessary evil than a target, since cells would not wish to be constantly depleting their pool of NAD<sup>+</sup> but need to remove toxic ADPR. Because nudix hydrolases are important in maintaining cellular homeostasis, low but constant background expression is to be expected. In the crowded environment of a bacterial cell, nudix hydrolases would be expected to eventually encounter a Group III ADH. If the activator is actually a small molecule product rather than the enzyme itself, the rate of diffusion and likelihood of interaction only increases. Therefore, is it reasonable to speculate that in a live cell, all molecules of Group III ADH encounter an activator regularly enough that they are maintained in the activated state.

It's also important to make the distinction that activation is probably not one-to-one, but many-to-many. That is, each species probably carries more than one gene for a nudix hydrolase capable of cleaving NAD<sup>+</sup> and thus activating Group III ADHs. It is also likely that many species carry more than one gene for a Group III ADH. *E. coli* carries both 1,2-propanediol dehydrogenase (49) and a protein currently called YqhD (50), which is a Group III ADH with unknown substrate specificity. *B. methanolicus* has at least six different methanol dehydrogenase genes which are all, individually, activated by a nudix hydrolase (23). Even *C. necator*, whence the GHBDH gene was cloned, has a gene for at least one other Group III ADH, whose function is currently unknown but which was crystallized (pdb 3JDZ) (17). Therefore, it's likely that many species which were previously found to have one Group III ADH gene might have more than one, all of which can be activated in the same way by any of the same group of nudix hydrolases.

The experiment to test the hypothesis would be fairly straightforward in a bioreactor. *Bacillus methanolicus*, whose MDH enzyme has already been noted to prefer ethanol as

substrate rather than methanol (23), could be transformed with a vector encoding a native nudix hydrolase under control of an inducible operon. Then the relative amounts of acetaldehyde produced by the bacteria during aerobic growth could be measured when nudix hydrolase was not induced and when it was. If the acetaldehyde production does not improve with induction of nudix hydrolase, then the always-activated theory is correct. If, on the other, acetaldehyde production *does* improve after nudix hydrolase induction, then rather than always being on, nudix hydrolase activator enzymes themselves represent a previously-unrecognized layer of bacterial metabolic control. That too is interesting, as it is a simple plasmid-based genetic modification that has the potential to more than quintuple yields in bioreactors. As the limiting factor in the profitability of many bioreactors is their generally low yield, this would be of general import to the industry.

### ***C. Materials and Methods***

#### **1. Purification of Activator Protein (ACT)**

*E. coli* cells harboring the pET\_21a/ACT plasmid were grown in 200 mL LB supplemented with 100 µg/mL ampicillin. When the culture had reached an OD<sub>600</sub> of 0.4-0.6, ACT was induced by addition of 0.1 mM IPTG. After 5-6 hr of growth, cells were harvested by centrifugation at 4,412 g for 30 minutes. The supernatant was decanted and the cells resuspended in ice-cold ACT Resuspension Buffer (100 mM MOPS, pH 7.4) which had been supplemented with protease inhibitor cocktail (Roche P/N 1873580001). The cell suspension was transferred to a 15 mL Falcon tube and ~3 mg (a spatula load) of lysozyme was added. The tube was then closed and submerged in liquid nitrogen until frozen. The tube was placed in water to thaw, then opened and



supplemented with ~3 mg (a spatula load) of DNase I. The tube was closed and again frozen and thawed. The cell lysate was transferred to a Ti70.1 centrifuge tube and the debris pelleted by centrifugation at 146,550 g for one hour. The supernatant was applied directly to a closed column of 0.5 mL NTA-agarose which had previously been equilibrated with ACT Resuspension Buffer, and allowed to equilibrate for one hour. The column was washed with 10 mL ACT Wash Buffer (100 mM MOPS, pH 7.4, 20 mM imidazole). The protein was eluted with 4 mL ACT Elution Buffer (100 mM MOPS, pH 7.5, 300 mM imidazole, 2 mM DTT) and collected in 0.5 mL fractions. An SDS-PAGE was performed on the fractions to determine which fractions contained the most protein; those fractions (typically 3) were pooled in an Amicon Ultra-4 10 kDa spin column and centrifuged until the volume of retentate was less than 0.1 mL. Then the spin column was filled to 1.5 mL with ACT Resuspension Buffer. The column was spun again, and the retentate again diluted to 1.5 mL with ACT Resuspension Buffer. The protein was aliquoted out in 0.035 mL fractions, frozen in liquid nitrogen, and stored at -80°C.

## 2. Assays of ACT nudix hydrolysis activity

ACT was assayed for nudix hydrolysis via an inorganic phosphate assay (51). The assay mixture contained: a substrate, which was either ADPR or NAD<sup>+</sup>; 1 unit of heat inactivated alkaline phosphatase<sup>5</sup> (HIAP); ACT; and sufficient GHBDH Assay Buffer to bring the total volume to 300 µL. After the desired amount of time, the reaction was

---

<sup>5</sup> Invitrogen P/N 100012546. This product is an active alkaline phosphatase which can be conveniently inactivated by relatively mild warming: 5 minutes at 65°C is enough. It has not already *been* inactivated.

halted and all phosphates complexed by the addition of 600  $\mu\text{L}$  of acid molybdenum consisting of 0.4%  $(\text{NH}_4)_6\text{Mo}_7\text{O}_{24}\cdot 6\text{H}_2\text{O}$  in 1 N  $\text{H}_2\text{SO}_4$ . The molybdenum-phosphate complexes were reduced with 100  $\mu\text{L}$  of 10% ascorbic acid solution. Heating at  $45^\circ\text{C}$  for 20 minutes helped to develop a bright royal blue, which was quantitated by measuring the  $A_{820}$ . The blue color was linearly dependent on the concentration of phosphate, and thus, the efficiency of the initial hydrolysis by ACT. Negative controls included omission of the substrate, ACT (to determine autohydrolysis), and HIAP. Background cleavage accounted for  $\sim 10\%$  of the color change, and was subtracted out to determine actual cleavage by ACT.

### 3. ACT Titration Assays (with pre-incubation)

The assay mixture comprised 16 mM GHB, 1 mM  $\text{NAD}^+$ , 25 pmols GHBDH, the ACT fraction, and enough GHBDH Assay Buffer to bring to total volume to 1 mL. The ratio of ACT to GHBDH (in mols/mol) tested were: 0:1, 0.01:1, 0.02:1, 0.04:1, 0.08:1, 0.1:1, 0.2:1, 0.4:1, 0.8:1, 1:1, 1.5:1, and 2:1. The buffer, reagents, and ACT were mixed together first, and allowed to equilibrate for a minimum of five minutes before the GHBDH fraction was added to initiate the reaction. After quickly mixing by inversion, the absorbance at 340 nm was measured for 60 s. Each assay was performed in triplicate, and one of the replicates used to confirm pH.

### 4. ACT Titration Assays (without pre-incubation)

The ACT titration assays were performed as described in Section 3 above, with minor variations. The ratios of ACT:GHBDH (in mols/mol) tested were 0:1, 0.01:1, 0.01333:1, 0.02:1, 0.04:1, 0.1:1, 0.2:1, 0.4:1, and 1:1. The buffer and reagents were

mixed together first, then ACT and GHBDH added in quick succession to initiate the reaction.

#### 5. GHBDH Assays with AMP and NMN<sup>+</sup>

In order to test whether a product of NAD<sup>+</sup> cleavage by activator protein is the true activator, rather than the protein itself, assays of activated GHBDH were performed in which NAD<sup>+</sup> was the independent variable, and GHB concentration was held constant at 6 mM. Set concentrations of AMP or NMN<sup>+</sup> (0, 1, or 5 mM) were added to these reaction mixes and allowed to equilibrate for at least five minutes prior to addition of the enzyme fraction and data collection.

#### 6. Data Processing

The data were processed as described in Chapter III.

## V. Activated Kinetics of GHBDH

### A. Motivation

The kinetic mechanism of the activated enzyme has never been studied in any member of the Group III ADH family. This is particularly surprising given that activator enzymes appear to work only in one direction (23). Such an odd result bears repeated testing, so the reaction was run in the reverse direction to verify that activators do not activate in the reverse direction.

As the work in Chapter III demonstrated, it is not possible for the activation to be the result of a switch from ping-pong kinetics to ternary complex kinetics, as had been previously proposed; the kinetics of GHBDH in the absence of activator protein follow a Mono-Iso Theorell-Chance mechanism, with  $\text{NAD}^+$  binding first and NADH leaving prior to an isomerization. The question then becomes: does activator protein cause a shift from this mechanism to a different one, and if so, which one?

At least one of the microscopic rate constants ( $k$ ) must have changed (a substrate binds faster, a product dissociates faster, or the covalent reaction itself has increased), and it is entirely possible that the activation has entirely changed which kinetic mechanism the reaction follows. The theoretical basis behind the product inhibition experiments remains as described in Chapter III. Therefore, the simple test is to perform the same experiments as those done to determine the kinetic mechanism of GHBDH a second time, now in the presence of saturating concentrations of activator enzyme.

## B. Results and Discussion

Once functional ACT had been purified, the question of directionality was addressed directly by an assay of the reverse-direction reaction ( $\text{NADH} + \text{SSA} \rightarrow \text{NAD}^+ + \text{GHB}$ ) without and with ACT. The results were identical within error. As a check to make sure that ACT was still turning over under these assay conditions, 0.01 mM ADPR was added to the reverse direction, both without and with ACT. Addition of ADPR lowered the reaction velocity as anticipated, presumably by acting as a competitive inhibitor with respect to NADH. Addition of ACT removed the inhibitory effect, showing that ACT was cleaving essentially all ADPR. Therefore, the lack of activation in the reverse direction was not because ACT was not functional. Why ACT does not seem to activate in the reverse direction is still a mystery.

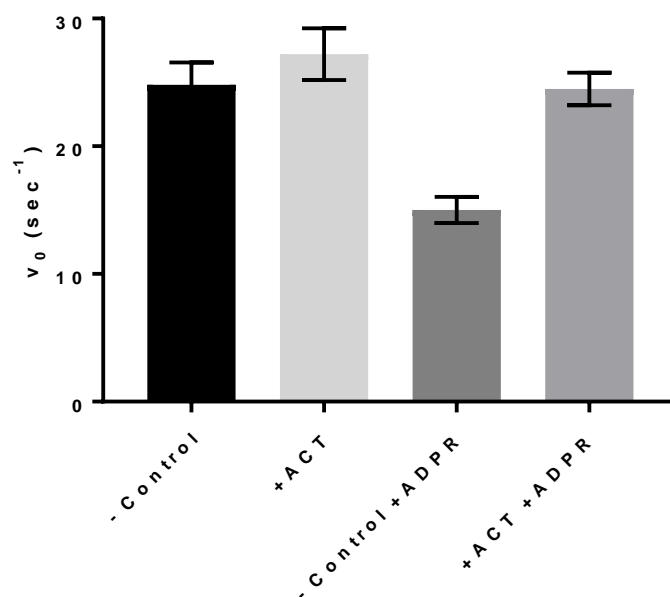


**Figure 22.** Reverse-direction reaction. Even under conditions which should be saturating in the reverse direction (0.15 mM NADH, 0.1 mM SSA), the reverse direction does not become activated (23).

Next, the simple Michaelis-Menten substrate-saturation curves were performed, this time in the presence of ACT. For comparison, the results from Table 1 are reproduced here, along with the results of activated GHBDH (Table 3). Activated GHBDH has a greater affinity for GHB, but a lower affinity for NAD<sup>+</sup>. The concentration of NAD<sup>+</sup> in live *C. necator* has been experimentally measured to be 1.9 mM (52); this experiment was done after bubbling H<sub>2</sub> through the cells, so these cells are expected to be in the most reducing state possible. Therefore, it must be supposed that the NAD<sup>+</sup> concentration in the bacteria is essentially saturating GHBDH, whether or not GHBDH is activated. On the other hand, the lower K<sub>m</sub> for GHB is probably important; 1 mM is a high concentration for a metabolic intermediate.

<b>Table 3.</b> Substrate selectivity of activated GHBDH			
Variable substrate	k <sub>cat</sub> (sec <sup>-1</sup> )	K <sub>m</sub> (mM)	k <sub>cat</sub> /K <sub>m</sub> (mM <sup>-1</sup> sec <sup>-1</sup> )
NAD <sup>+</sup>	8.9 ± 0.2	0.064 ± 0.0063	139 ± 14
NAD <sup>+</sup> + ACT	16.88 ± 0.42	0.14 ± 0.011	120 ± 9.9
GHB	8.4 ± 0.3	0.98 ± 0.11	8.6 ± 1.0
GHB + ACT	15.57 ± 0.48	0.60 ± 0.069	25.9 ± 3.1

To find out if this is physiologically relevant, the activity of GHBDH in the forward direction was measured as a function of pH, both alone and then in combination with ACT. The results show that in the presence of saturating ACT, the pH maximum of GHBDH is unchanged, albeit with higher initial velocity. However, the profile also reveals a more interesting phenomenon that occurs at pH 7.0-7.5. At this physiological pH, although the turnover rate is lower than at pH 9.0, ACT has a greater effect on GHBDH. That is, at the pH maximum, ACT nearly doubles the initial velocity; at pH 7.5, ACT increases the velocity by ~2.75-fold; and at pH 7, this factor increases to 4.5-fold.

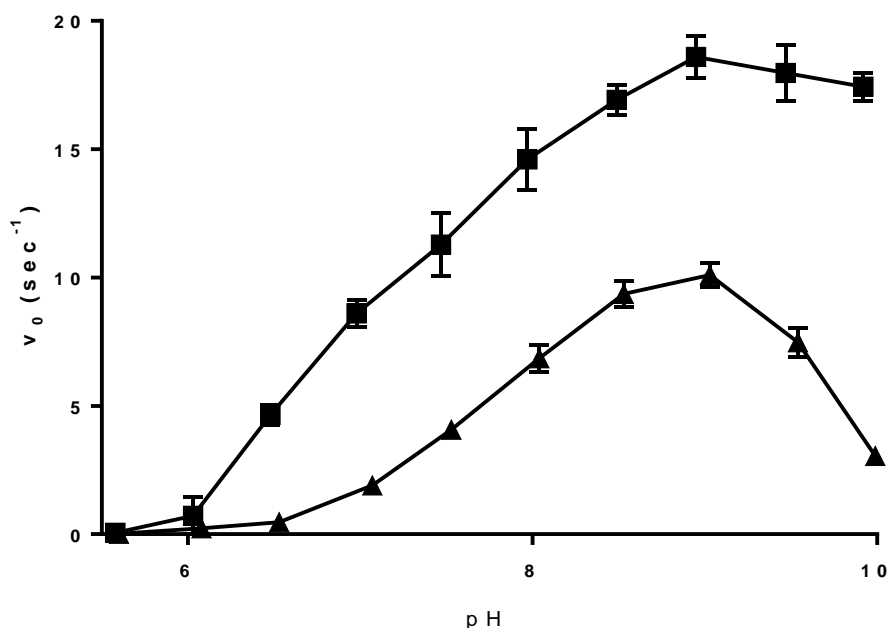


**Figure 23.** GHBDH pH Rate profiles in the absence (▲) and presence (■) of ACT.

The gene for GHBDH was isolated from *C. necator*, a soil bacterium. Despite the prominence of *C. necator* as a source of biodegradable polyhydroxyalkanoate (PHA) plastics, there have been no studies on its internal pH to date. The closest report was in the original paper which described the species (53), where it was found that *C. necator* favors an external pH of 7.0-8.0 but can tolerate a range from 5.5-9.2. Additionally, a study of bacterial pH homeostasis showed that *E. coli*, which has at least three Group III ADHs, maintains an internal pH of 7.4-7.8; *B. subtilis*, another species which produces a Group III ADH, holds its pH at 6.5-7.5. Therefore, it is reasonable to suspect that *C. necator* also is a neutrophile like *E. coli* and *B. subtilis* and has internal pH in the region of 7.0-7.5. The larger activation in the physiological region of internal pH may be important for breaking down stored polymer at a rate sufficient to provide for the energy and carbon needs of the

cell. Certainly, the non-activated rate, might otherwise necessitate a huge GHBDH induction.

When GHBDH activated by saturating ACT is inhibited with NADH, and  $1/\text{NAD}^+$  is the independent variable, NADH displays noncompetitive inhibition (Figure 24). When GHBDH activated by saturating ACT is inhibited with SSA, and  $1/\text{NAD}^+$  is the independent variable, SSA displays noncompetitive inhibition (Figure 25). When GHBDH activated by saturating ACT is inhibited with NADH, and  $1/\text{GHB}$  is the independent variable, NADH displays noncompetitive inhibition (Figure 26). When GHBDH activated by saturating ACT is inhibited with SSA, and  $1/\text{GHB}$  is the independent variable, SSA displays competitive inhibition (Figure 27).

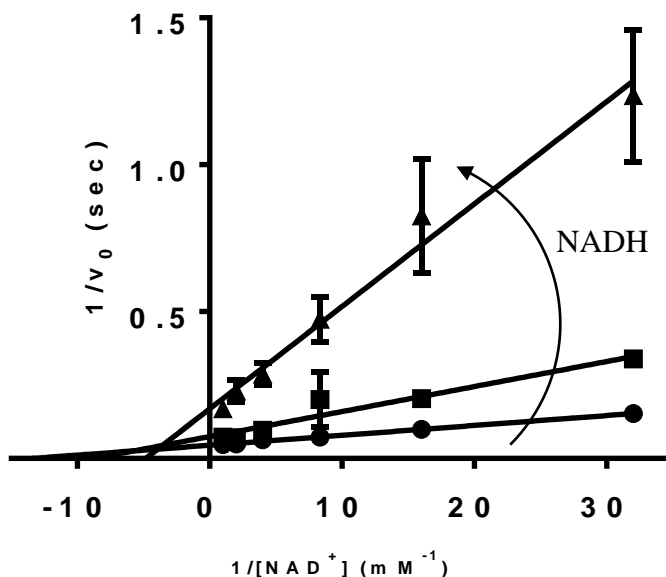


**Figure 24.** Lineweaver-Burke plot of activated GHBDH inhibition by NADH with  $\text{NAD}^+$  as the variable substrate. Error bars are not shown where they would be smaller than the height of the symbol. ● 0 mM NADH; ■ 0.04 mM NADH; ▲ 0.125 mM NADH.



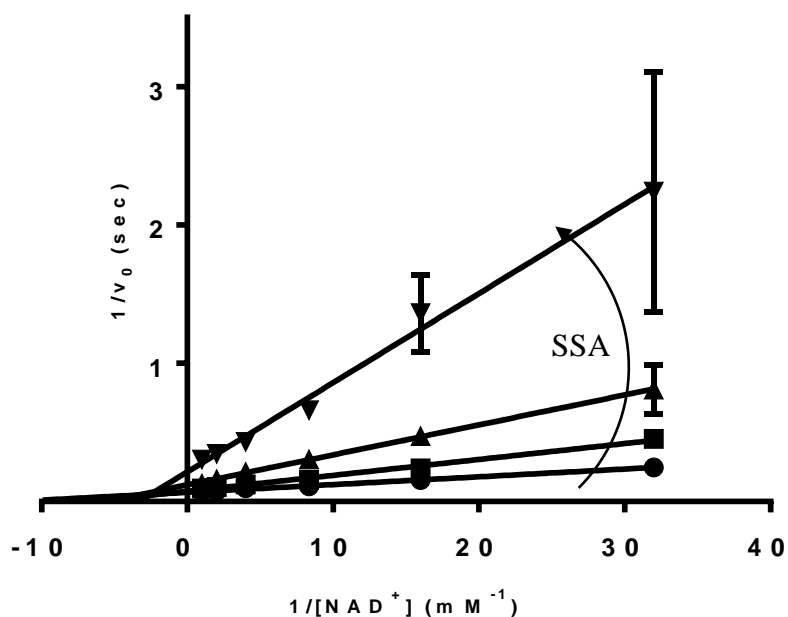


**Figure 25.** Lineweaver-Burke plot of activated GHBDH inhibition by SSA with NAD<sup>+</sup> as the variable substrate. Error bars are not shown where they would be smaller than the height of the symbol. ● 0 mM SSA; ■ 0.1 mM SSA; ▲ 0.3 mM SSA; ▼ 1 mM SSA.

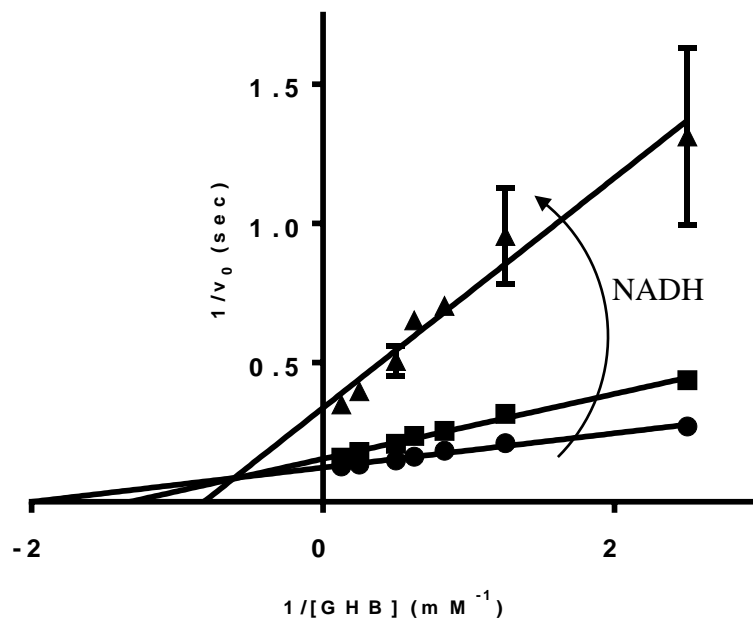


**Figure 26.** Lineweaver-Burke plot of activated GHBDH inhibition by NADH with GHB as the variable substrate. Error bars are not shown where they would be smaller than the height of the symbol. ● 0 mM NADH; ■ 0.01 mM NADH; ▲ 0.04 mM NADH.

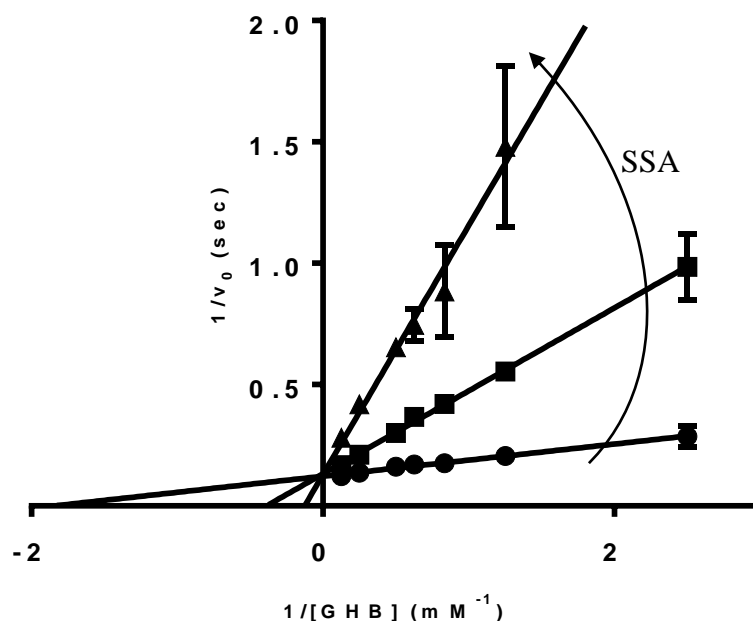


**Figure 27.** Lineweaver-Burke plot of activated GHBDH inhibition by SSA with GHB as the variable substrate. Error bars are not shown where they would be smaller than the height of the symbol. ● 0 mM SSA; ■ 0.1 mM SSA; ▲ 0.3 mM SSA.

These results show that, despite the presence of ACT almost doubling the initial velocity at pH 9, activated GHBDH follows the same Mono-Iso Theorell-Chance kinetic mechanism as does unactivated GHBDH. Which microscopic rate increased is unclear at this time, and this assay cannot easily determine the answer. This is because  $A_{340}$ , which is really just a measure of NADH in solution, cannot unambiguously determine which microscope step is faster, only that NADH is appearing more rapidly than previously. Because the activation does not appear to work in the reverse direction, it's impossible to perform both forward- and reverse-direction kinetics and accurately determine every rate constant in activated GHBDH.

However, it is now possible to hypothesize what occurs during activation, and why the activation doesn't occur in the reverse direction. In a single-step reaction, the Group III

ADH would lower the activation energy. In such a system, activation would occur in both directions. This is not observed in Group III ADHs, so the reaction cannot have only a single step. Thus, a multi-step reaction is hypothesized, where there is an energy barrier prior to the binding of the first substrate:

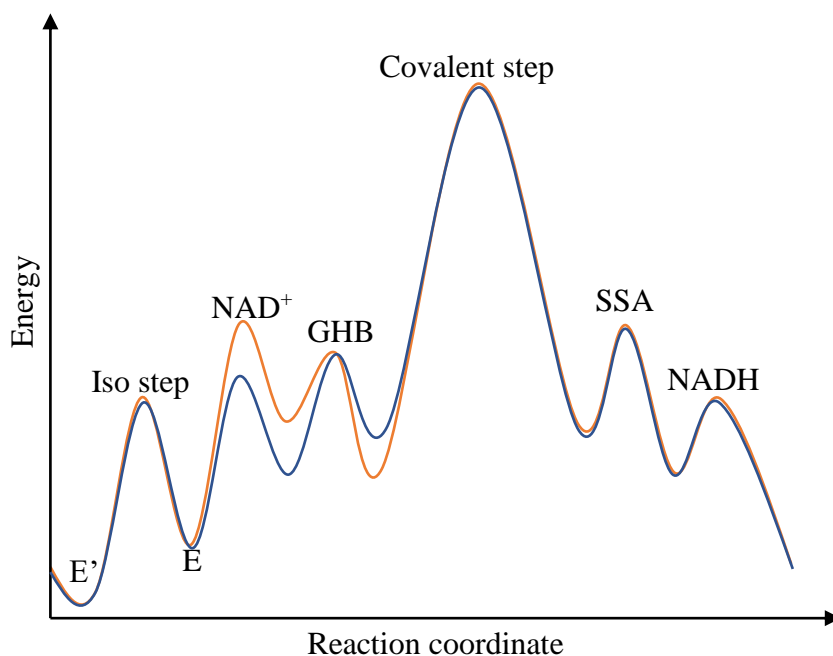


**Figure 28.** Energy schematic of the oxidation of GHB by GHBDH when unactivated (blue) and activated (orange).

The equilibrium between initial enzyme and enzyme that has gone over the first small energy barrier is a direct function of the energy difference between the two states. This is a pre-equilibrium before the rate determining step. If the intrinsic rate constant in one direction, here shown as the forward direction, is much smaller than the intrinsic rate constant in the other direction, here shown as the reverse direction, then the concentration of enzyme in the intermediate transition state can be very low. Any enzyme in this state can either (a) return back over the initial energy barrier or (b) proceed forward toward the large energy barrier.

In any isomerization mechanism, there is at least one slow isomerization step, in addition to a slow chemical step (36). In GHBDH, slow is comparable or slower than the turnover rate of  $\sim 10/\text{sec}$  in unactivated enzyme at pH 9. If the isomerization step is assigned to the first energy barrier, and the covalent step assigned to the highest energy barrier, then this multi-step model is brought into harmony with the Mono-Iso Theorell-Chance mechanism. The initial enzyme form is not E, in this case, but isomerized E'. This E' must first isomerize into E in a relatively slow step. Then it becomes able to bind  $\text{NAD}^+$  etc. and perform enzymatic turnover. The hydride transfer step is the likely step for E to isomerize to E' before release of SSA and NADH. The slowness of the initial isomerization from E' to E is partially rate-limiting *in this direction*. On the other hand, as has already been established, the isomerization from E to E' is more favorable; consequently, it is either much less rate-limiting or not rate limiting at all *in the reverse direction*.

It is easy to imagine that the binding of some other moiety, either the ACT protein itself or some small molecule that ACT is producing, to allosterically regulate the enzyme. This results in a decreased affinity for  $\text{NAD}^+$ , but an increased affinity for GHB. Because  $\text{NAD}^+$  is always saturating but GHB isn't, the result is a faster reaction cycle, thus, a higher initial velocity. The activation still can't be observed in the reverse direction because, although the reaction coordinate has changed, the binding of  $\text{NAD}^+$  and GHB, and the apparent flux through the isomerization step will not be rate limiting in the reverse direction.

The challenge now lies in experimentally proving the hypothesis. It would, at a minimum, require some way to determine the overall E/E' ratio of the enzyme ensemble in solution, and some way to reliably "push" the solution ensemble toward E or E', thus changing that ratio in predictable ways. Then application of ACT can be compared to the

effect of the “push” to see if it really does change propensity toward isomerization. EPR analysis might work, if the geometry of chelator residues around the  $\text{Fe}^{2+}$  changes as a function of isomerization. Alternatively, intrinsic protein absorbance at 280 nm could also be a readout if the isomerization results in rearrangement of aromatic rings. For changing the E/E' ratio, pH, ionic strength, and solution viscosity are all possible ways to make the isomerization more or less likely. However, none of these methods is certain to work, since very little is known about the conformations of the protein in solution.

### ***C. Materials and Methods***

#### **1. GHBDH Activation Assay in the Reduction of Aldehyde**

The assay mixture comprised 0.1 mM SSA, 0.15 mM NADH, the enzyme fraction, and sufficient Reverse Assay Buffer to bring the total volume to 1 mL. Reverse Assay Buffer comprised 0.1 M potassium phosphate, pH 7, and 5 mM  $\text{Mg}_2\text{SO}_4$ . The buffer and reagents were mixed together first, and the enzyme fraction added last to initiate the reaction. In activated samples, a total of 0.5  $\mu\text{g}/\text{mL}$  ACT protein was added and allowed to incubate with solution for a minimum of five minutes prior to addition of GHBDH. In assays containing ADPR, 0.01 mM ADPR was added. After quickly mixing by inversion, the absorbance at 340 nm was measured for 60 s. Each assay was performed in triplicate. Fitting was accomplished essentially as described in Chapter III, but because an absorbance *decrease* was measured, the absolute value of the zero-time derivative was used for initial reaction velocity.

## 2. GHBDH pH Rate Profiles

The assay mixture comprised 16 mM GHB, 1 mM NAD<sup>+</sup>, the enzyme fraction, and enough GHBDH Assay Buffer to bring to total volume to 1 mL. The pHs tested were 4.5, 5, 5.5, 6, 6.5, 7, 7.5, 8, 8.5, 9, 9.5, and 10; however, no activity was observed below pH 5.5. The buffer and reagents were mixed together first, and the enzyme fraction added last to initiate the reaction. In activated samples, a total 0.5 µg/mL ACT protein was added and allowed to incubate with solution for a minimum of five minutes prior to addition of GHBDH. After quickly mixing by inversion, the absorbance at 340 nm was measured for 60 s. Each assay was performed in triplicate, and one of the replicates used to confirm pH. While the pH was maintained well at high pH, the large addition of pH 7.0 enzyme fractions tended to raise the pH a little on the low end of the pH range. The true recorded pH was used for all further analysis.

## 3. Activated GHBDH Product Inhibition Assays

The assay was performed as described in Chapter III, with the addition of 0.5 µg/mL ACT to the assay mixture and a pre-incubation of at least five minutes prior to addition of GHBDH.

## 4. Data Processing

The data were processed as described in Chapter III.

## VI. GHBDH Mutations

### A. Motivation

The amino acids responsible for GHBDH's catalytic activity, and therefore to that of Group III ADHs as a whole, have been partially determined. The four amino acids which chelate the  $\text{Fe}^{2+}$  ion in place are absolutely necessary in other Group III ADHs.

Accordingly, to verify that GHBDH is not acting in any unusual way, these amino acids were mutated to non-binding residues and the effect on GHBDH observed.

In order for the amino acids which bind  $\text{Fe}^{2+}$  to do so, however, they must remain in the deprotonated state. As such, they cannot then also be responsible for the removal of the primary hydroxyl proton which initiates the dehydrogenation. The only other ionizable group located within the active site is a histidine residue. This residue is located on the same  $\alpha$ -helix as one of the  $\text{Fe}^{2+}$ -binding histidines (H261), but is one turn of the helix further along. In prior work on the *E. coli* enzyme FucO, mutation of the homologous residue (H267) to an alanine generated inactive enzyme (6). At the time, this was believed to therefore be another  $\text{Fe}^{2+}$ -binding residue. Subsequent crystal-structure work indicated that the residue was not close enough to interact with the  $\text{Fe}^{2+}$ , and instead suggested a catalytic role through a proton wire (49). Accordingly, this amino acid was chosen for multiple mutations. In the case that this residue is catalytic, mutation to an alanine should remove all GHBDH activity. Mutation to other potential general bases can still allow activity that differs in pH preference. Therefore, this amino acid was mutated to alanine, aspartate, and cysteine.

C. necator GHB DH	GMDAIAHCIETFLA-----PAFNPPADGIALDGLERGWGHTERATR
E. coli FucO	GVDALTHAIEGYIT-----RGAWALTDALHIKAIEIIAGALRGSVA
B. methanolicus MDH	GMDALSHAIEAYVA-----KGATPVTDAFAIQAMKLINEYLPKAVA
Z. mobilis ADH2O	GMDALTHAFEAYSS-----TAATPITDACALKAASMIAKNLKTCAD
S. cerevisiae ADH4	GLDALTHCIEAYVS-----TASNPIITDACALKGIDLINESLVAAYK
D. melanogaster HOT	GFDVFCHALESEFTAVDYRERGLAPSDPSLRPTYQGRNPVSDVWARFALETIRKNEVNAIY
Xenopus HOT	GFDVLCHSLESY TALPYNMRSPCPTNPINRPAYQGSNPISDVWAKHALRIVAKFLKRAVR
Human HOT	GFDVLCHALESYTTLPLYHLRSPCPSNPITRPAYQGSNPISDIWAIHALRIVAKYLKRAVR
Rat HOT	GFDVLCHALESYTAIPYSMRSPCPSNP IQRPAYQGSNPISDIWAVHALRIVAKYLKRAVR
	⊗ ⊗
C. necator GHB DH	DGQDRDARLNMMSASMQGAMAFQ-KGLGCVHSLSHPLGGLKID-----GRTGLHHGT
E. coli FucO	G--DKDAGEEMALGQYVAGMGFSNVGLGLVHGMAHPLGAFY-----NTPHGV
B. methanolicus MDH	NGEDIEAREAMAYAQMAGVAFNNGGLGLVHSISHQVGGVY-----KLQHGI
Z. mobilis ADH2	NGKDMPAREAMAYAQFLAGMAFNNASLGYVHAMAHQLGGYY-----NLPHGV
S. cerevisiae ADH4	DGKDKKARTDMCYAEYLAGMAFNNASLGYVHALAHQLGGFY-----HLPHGV
D. melanogaster HOT	QPDNLEARSQMHLASTMAGVGFGNAGVHLC HGLSYPISGNVRDYKPKGYSADHALIPHGL
Xenopus HOT	NPDDREARFAMHLASSFAGVGFGNAGVHLC HGMSPYIAGHVKTYRAKDYKVDHPLVPHGL
Human HOT	NPDDLEARSMHHLASAFAGIGFGNAGVHLC HGMSPYISGLVKMYKAKDYNVDHPLVPHGL
Rat HOT	NPDDLEARS SMHLASAFAGIGFGNAGVHLC HGMSPYISGLVKTYKAKEYNVDHPLVPHGL
	⊗ ↑ ⊗

**Figure 29.** Partial sequence alignment of selected Group III ADHs and hydroxyacid-oxoacid transhydrogenases (HOTs). The sequences were aligned using Clustal Omega (Sievers, et al., 2014). The proteins are:  $\gamma$ -hydroxybutyrate dehydrogenase from *Cupriavidus necator* (UniProt Q0KBD6); methanol dehydrogenase from *Bacillus methanolicus* (UniProt P31005); lactaldehyde reductase from *Escherisia coli* (UniProt P08971); alcohol dehydrogenase II from *Zymomonas mobilis* (UniProt P0DJA2); alcohol dehydrogenase IV from *Saccharomyces cerevisia* (UniProt P10127); hydroxyacid-oxoacid transhydrogenase from *Drosophila melanogaster* (UniProt Q9W265); hydroxyacid-oxoacid transhydrogenase from *Xenopus laevis* (UniProt Q08B39); hydroxyacid-oxoacid transhydrogenase from *Homo spaiens* (UniProt Q8IWW8); and hydroxyacid-oxoacid transhydrogenase from *Rattus norvegicus* (UniProt Q4QQW3). The four iron-coordinating residues are marked “⊗”. The histidine that was proposed to be catalytic, as well as the tyrosine residue that replaces it in higher organisms, is marked “↑”. Residues that are identical in all sequences are shaded dark grey. Residues that have conservative substitutions are shaded medium grey. Residues that have only semi-conservative substitutions are shaded light grey. “-” indicates no corresponding amino acid.

The final mutation of this histidine was made to explore the evolution of Group III ADHs. Amongst higher organisms, there exist no “true” Group III ADHs; that is, enzymes which transfer a hydride from an alcohol substrate to an NAD(P). However, one family of sequentially-similar enzymes exists: the hydroxyacid-oxoacid transhydrogenases (HOTs). In the HOT family, a hydride is transferred between two substrates. Human ADHFe1, a HOT enzyme, removes a hydride from a hydroxyacid, GHB, and places it on an oxoacid,  $\alpha$ -ketoglutarate. It is suspected, but unconfirmed, that HOTs have a bound non-dissociable NAD(H) that serves as the electron sink and the enzyme therefore follows ping-pong reaction kinetics, as substrates are sequentially oxidized and reduced. In all known HOTs,



the amino acid present in the position occupied by conserved H265 of GHBDH is a tyrosine, not a histidine. It is possible for tyrosine residues to serve as general bases/acids, but it is unknown whether it does so in HOTs. Because it has (thus far) been all but impossible to express and purify cloned HOT, probing this residue in the original enzyme isn't feasible. However, the GHBDH expression system already works well. Therefore, it was decided to try the H265Y mutation, and see if any insight could be gained into the related HOT enzymes.

### ***B. Results and Discussion***

As expected, alanine mutants in any of the four Fe<sup>2+</sup>-binding amino acids resulted in enzyme with very little of the original wild-type activity remaining. The mutant with the most remaining activity was H280A, with almost 0.6% of wild-type activity. Next was D193A, with a bit over 0.2%, and finally H197A and H261A, both of which had only about 0.04% of original activity. Clearly, not all of the Fe<sup>2+</sup>-binding amino acids are of equal import, but changing even one of them is sufficient to substantially reduce activity.

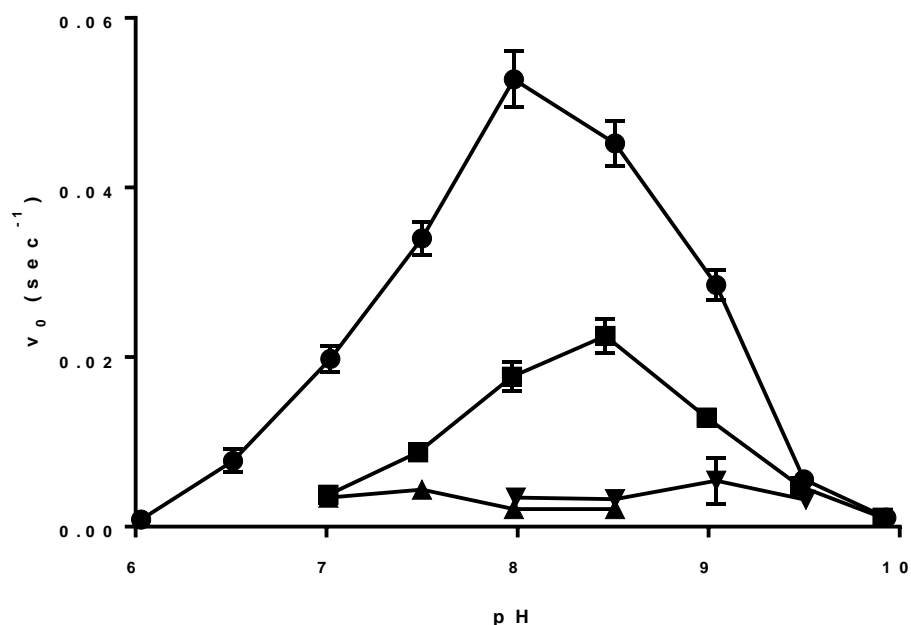


**Figure 30.** pH rate profiles of GHBDH chelator mutants. Wild type is not shown due to scaling issues. ● H280A; ■ D193A; ▲ H197A; ▼ H261A.

For comparison, a protocol for on-column removal of  $\text{Fe}^{2+}$  from wild-type GHBDH was developed. This protocol turned out to have an unexpected visual confirmation of  $\text{Fe}^{2+}$  removal: within 5 minutes of adding the chelation buffer, a pink-orange color developed on the column. This color was not bound to the column, but neither did it travel with the buffer, indicating some weak equilibrium binding. Further research suggested the pink color to be the result of a three-step process. First, the *ortho*-phenanthroline removed  $\text{Fe}^{2+}$  from the GHBDH. Then, since GHBDH is not oxygen-sensitive and nothing in particular had been done to reduce  $\text{O}_2$  concentration in any of the buffers, the  $\text{Fe}^{2+}$  oxidized to  $\text{Fe}^{3+}$ ; this was probably the slow step, as the inactivation of GHBDH by 10 mM *o*-phenanthroline is complete within 1 minute. Finally, this  $\text{Fe}^{3+}$  interacted with some species in solution, quite probably the EDTA itself. The predominant form at near-neutral pH is  $[\text{Fe}(\text{EDTA})(\text{H}_2\text{O})]^-$ ,

and the salt of this complex ion with  $\text{Na}^+$  is known to be yellowish-brown. Addition of solid  $\text{FeCl}_3$  to a solution of chelation buffer in quantities which matched the probable on-column  $\text{Fe}^{3+}$  concentrations resulted in a solution of the same pink-orange as the wash-through from the column. The complex was all washed from the column before the elution buffer was applied. The ApoGHBDH thus formed was tested for native GHBDH activity. It had ~6% residual activity, almost ten times more as the H280A mutants. Therefore, it is reasonable to estimate that *ortho*-phenanthroline is not completely effective at removing bound  $\text{Fe}^{2+}$ , and the lack of activity in the mutants was directly due to impaired  $\text{Fe}^{2+}$  binding during protein synthesis.

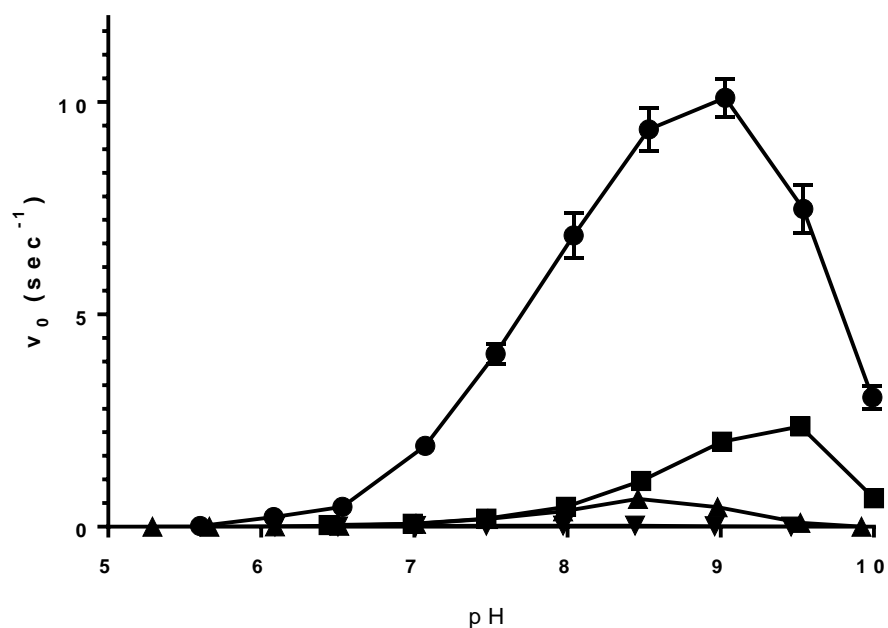


**Figure 31.** pH rate profiles of GHBDH H265 mutants. ● Wild-type; ■ H265A; ▲ H265C; ▼ H265D; ◆ H265Y.

The case of the non- $\text{Fe}^{2+}$ -binding mutants is somewhat more confusing. All of the H265 mutants performed less well than wild-type, but the *most* active of these mutants was

H265A, which had a maximum activity about one-third that of wild-type and a slightly higher pH preference before becoming unstable at pH 10. This was followed by H265C, which had activity of 6.5% that of wild-type. H265C also had a different pH preference and favored pH 8.5. The H265D mutant had extremely low activity, but when the enzyme fraction in the assay was increased from 5 to 50  $\mu\text{L}$ , there was enough  $\Delta A_{340}$  to make some conclusions. H265D has a pH preference of about 8, but a very broad peak, going from pH 7.5 up to pH 8.5 at about the same activity. This activity, however, was still only 0.3% that of wild-type. Finally, the H265Y mutant behaved no better than a water blank, indicating that this enzyme is totally inactive. The bulky side-chain was probably interfering, and possibly had prevented the enzyme from even folding properly in the first place. Therefore, it can be concluded that the eukaryotic HOTs, while probably having a similar overall fold to Group III ADHs, must have a somewhat different active site in order to accommodate a tyrosine residue at this position.

### ***C. Materials and Methods***

#### **1. Mutagenesis**

*E. coli* bearing the pGEX-2T/GHB-DH vector (54) were grown overnight in 5mL LB supplemented with 1  $\mu\text{g}/\text{mL}$  ampicillin. Plasmid was harvested using a StrataPrep Plasmid miniprep kit according the manufacturer's instruction. Then the Agilent Technologies QuikChange Lightning site-directed mutagenesis kit was used according to the manufacturer's direction to generate mutants. See Table 4 for primers. Primers were designed using a least-mismatch approach. Two of the sequences encountered low efficiency mutations: H265Y and H280A. H265Y probably had issues due to the two

<b>Table 4. Primers used for site-directed mutagenesis. Mutated nucleotides are in bold.</b>		
Name	Nucleotide sequence	Amino acid exchange
D193A Forward	5'-GCC ACC GGC ATG GCT GCG ATC GCG CAC-3'	D193 → A
D193A Reverse	5'-GTG CGC GAT CGC AGC CAT GCC GGT GGC-3'	
H197A Forward	5'-C ATG GAT GCG ATC GCG <b>GCC</b> TGC ATC GAG ACC TTC-3'	H197 → A
H197A Reverse	5'-GAA GGT CTC GAT GCA <b>GGC</b> CGC GAT CGC ATC CAT G-3'	
H261A Forward	5'-CTG GGC TGC GTG <b>GCT</b> TCG CTG TCG CAC-3'	H261 → A
H261A Reverse	5'-GTG CGA CAG CGA <b>AGC</b> CAC GCA GCC CAG-3'	
H280A Forward	5'-C ACC GGC CTG CAC <b>GCC</b> GGC ACG CTC AAC-3'	H280 → A
H280A Reverse	5'-GTT GAG CGT GCC <b>GGC</b> GTG CAG GCC GGT G-3'	
H265A Forward	5'-G CAT TCG CTG TCG <b>GCC</b> CCG CTG GGC GGG-3'	H265 → A
H265A Reverse	5'-CCC GCC CAG CGG <b>GGC</b> CGA CAG CGA ATG C-3'	
H265C Forward	5'-G CAT TCG CTG TCG <b>TGC</b> CCG CTG GGC GGG-3'	H265 → C
H265C Reverse	5'-CCC GCC CAG CGG <b>GCA</b> CGA CAG CGA ATG C-3'	
H265D Forward	5'-G CAT TCG CTG TCG <b>GAC</b> CCG CTG GGC GG-3'	H265 → D
H265D Reverse	5'-CC GCC CAG CGG <b>GTC</b> CGA CAG CGA ATG C-3'	
H265Y Forward	5'-G CAT TCG CTG TCG <b>TAT</b> CCG CTG GGC GGG C-3'	H265 → Y
H265Y Reverse	5'-G CCC GCC CAG CGG <b>ATA</b> CGA CAG CGA ATG C-3'	

mismatched nucleotides being non-adjacent. However, there were still sufficient colonies to recover mutant plasmid and proceed. H280A was more severe, initially generating no mutant colonies. Sequence analysis showed that the problem was likely high GC content preventing denaturation during the thermal cycling, but switching to the manufacturer's high GC content protocol did not ameliorate the issue. Addition of a small quantity of DMSO to the PCR tubes produced

viable mutant colonies. Plasmids were isolated from all mutant colonies and sequenced

to confirm mutations. Mutant plasmids were transformed into BL21(DE3) cells and cultures flash frozen in liquid nitrogen before long-term storage at  $-80^{\circ}\text{C}$ .

## 2. Mutant Protein Expression and Purification

Protein was grown and purified as described in Chapter III. However, since mutant proteins were either less active than wild-type or completely inactive, fractions were pooled on the basis of an SDS-PAGE gel of eluted fractions rather than activity. Pooled protein was divided into 1.2 mL aliquots, flash-frozen in liquid nitrogen, and stored at  $-80^{\circ}\text{C}$ .

## 3. ApoGHBDH Expression and Purification

Cells were grown, induced, harvested, lysed, and loaded onto the column as described in Chapter III. The column was washed with 20 mL of GHBDH Wash Buffer #1 to remove nonspecifically bound proteins. Next, 20 mL of GHBDH Chelation buffer (30 mM MOPS, pH 7.4, 10 mM *ortho*-phenanthroline, 100 mM ethylenediaminetetraacetic acid (EDTA)) was flowed onto the column. While some Group III ADHs are completely inactivated by EDTA (2), (11), others are not (4), (14) and require the planar structure of *o*-phenanthroline to remove the ion; GHBDH was found to be of this latter type. The EDTA was added to complex  $\text{Fe}^{2+}$  ions removed by *o*-phenanthroline, thus regenerating it and keeping the overall *o*-phenanthroline concentration steady. The column was stopped for 20 minutes while the chelation buffer removed  $\text{Fe}^{2+}$ . Then, this buffer was flowed out of the column. An additional 20 mL of chelation buffer was flowed onto the column and allowed to rest for 20 minutes to remove  $\text{Fe}^{2+}$  as previously. Then, 20 mL of GHBDH Wash Buffer #2, was flowed through the column to remove the chelation buffer and  $\text{Fe}^{2+}$  ions. Finally, 50 mL of

GHBDH Elution Buffer was used to elute the protein. Fractions of 5 mL were collected, and these fractions were run on an SDS-PAGE gel to determine which fractions contained the (now Fe<sup>2+</sup>-deficient) enzyme. The three fractions containing the most ApoGHBDH were pooled, divided into 1.2 mL aliquots, flash-frozen in liquid nitrogen, and stored at -80°C.

#### 4. Wild-type and Mutant GHBDH Assays

The assay mixture comprised 16 mM GHB, 1 mM NAD<sup>+</sup>, the enzyme fraction, and enough GHBDH Assay Buffer to bring to total volume to 1 mL. The pHs tested were 4.5, 5, 5.5, 6, 6.5, 7, 7.5, 8, 8.5, 9, 9.5, and 10. The buffer and reagents were mixed together first, and the enzyme fraction added last to initiate the reaction. Due to low activity in the mutants, the enzyme fraction of all mutants except H265A was 50 µL rather than 5 µL. After quickly mixing by inversion, the absorbance at 340 nm was measured for 60 s. Each assay was performed in triplicate, and one of the replicates used to confirm pH. While the pH was maintained well at high pH, the large addition of pH 7.0 enzyme fractions tended to raise the pH a little on the low end. The true recorded pH was used for all further analysis.

#### 5. Data Processing

The data were processed as described in Chapter III.

## **VII. Conclusions**

### ***A. GHBDH Homology Model***

GHBDH has homology to other Group III ADH, some of which have been crystallized. Using MODELLER, a homology model of GHBDH was built from these solved crystal structures. The homology model showed the  $\text{Fe}^{2+}$  ion held in the correct orientation by its four chelators, as well as the binding sites of  $\text{NAD}^+$  and GHB. When DOCK was used to place the two substrates in the homology model, the substrates were found to occupy the binding site at separation distances less than the van Der Waals radius, indicating that hydride transfer is possible. The model also allowed identification of a possible disulfide linkage, which would explain why thiols inactivate GHBDH.

### ***B. GHBDH Product Inhibition Assays***

GHBDH displays a Mono-Iso Theorell-Chance Mechanism at pH 9. This is an extremely unusual reaction mechanism, but the two findings that (a)  $\text{NAD}^+$  can bind to enzyme in the absence of alcohol substrate and (b)  $\text{NAD}^+$  and NADH are not competitive require an isomerization step to prevent them from binding to the same form of free enzyme.

### ***C. Activator Assays***

ACT was found to cleave ADPR and, to a much lesser extent,  $\text{NAD}^+$ . The activation was found to require quantities of ACT far below stoichiometric when ACT was pre-incubated with  $\text{NAD}^+$ , but approximately stoichiometric quantities when ACT was added just prior to GHBDH. The conclusion was that the true activator is not ACT, but a product of the  $\text{NAD}^+$  cleavage that ACT can perform. The two expected  $\text{NAD}^+$  cleavage products, AMP and



NMN<sup>+</sup>, were tested to see if they are stimulatory. Neither is; AMP is an inhibitor. Therefore, while a small-molecule cleavage product makes sense as the stimulant, so far nudix hydrolase protein is required to stimulate GHBDH. The effect of operon-inducible nudix hydrolase expression on acetone production in live culture remains to be seen.

#### ***D. Activated GHBDH Product Inhibition Assays***

GHBDH is activated by a *Bacillus methanolicus* nudix hydrolase, here termed ACT, in the direction of oxidizing substrate. It is not activated in the direction of reduction of substrate, an unusual fact which does not match simple models of protein activation. Activated GHBDH was found to have a similar pH rate profile to unactivated GHBDH. Interestingly, the profile shows that the activation starts at around pH 6, and the activation factor is higher at lower pH. This suggests that the activation has a larger effect in the physiological context.

Activated GHBDH was found to proceed by the same unusual Mono-Iso Theorell-Chance mechanism as unactivated GHBDH. This, in turn, leads to the hypothesis that it's the rate-limiting *isomerization*, rather than any of the chemical steps, that ACT improves. This theory might also explain why there is no apparent activation in the reverse direction: the isomerization precedes the rate-limiting step in the forward direction. Changing the propensity of GHBDH to isomerize doesn't really change the reaction velocity in the reverse direction because it follows the rate-limiting step in the direction.

#### ***E. GHBDH Mutations***

GHBDH was mutated in five residues. As expected, mutations in the residues responsible for chelation of the active-site Fe<sup>2+</sup> reduced GHBDH activity, presumably by

interfering with proper Fe<sup>2+</sup> loading during synthesis. Mutations in the proposed catalytic histidine did not produce inactive enzyme. If this histidine acts as a general base to promote formation of aldehyde from the alcohol of GHB, its mutation should greatly reduce activity. Instead, GHBDH remains most active with an alanine in place of this histidine. Both the cysteine and aspartate mutant were also active, albeit less than wild-type. The tyrosine mutant was the only totally inactive protein, indicating that eukaryotic HOTs must have a different binding pocket in order to accommodate this bulky residue.

#### ***F. Final Remarks***

Although Group III ADHs have been known for over a decade, intensive study of their roles in microbial metabolism has not yet occurred. This is a gross oversight, considering their role in metabolism – for example *E. coli* 1,2-propanediol dehydrogenase – and their ability to produce valuable industrial chemicals from non-petroleum feedstock. This work was an attempt to correct some of that oversight by determining the kinetic mechanism of a Group III ADH, GHBDH, in the oxidation direction, while inactivated and activated. This work has been successful, inasmuch as the kinetic mechanism of both systems is now known. More work remains, however, to determine what the actual activator molecule is and especially why it activates in the oxidation of alcohol substrate, but not the reduction of aldehyde.

Also remaining is the task of determining if the activation described here is observed in live cells. If it is, then much of the *in vitro* work that has been done to date is unfortunately irrelevant to the kind of metabolically engineered bacterial systems that are under development for production of a variety of chemicals. On the other hand, if activation is not

common *in vivo*, then inducible activation represents an opportunity to vastly improve yields with a relatively minor change in the engineered cells. Either way, activating nudix hydrolyses, and their relationships to the Group III ADHs they activate, should remain an area of active research for some time to come.

## VIII. Bibliography

1. *Molecular characterization of microbial alcohol dehydrogenases*. **Reid, Matthew F. and Fewson, Charles A.** 1, 1994, *Critical Reviews in Microbiology*, Vol. 20, pp. 13-56.
2. *Isolation and characterisation of the glycerol dehydrogenase from Bacillus stearothermophilus*. **Spencer, P., et al.** 3, 1989, *Biochimica et Biophysica Acta (BBA) - Protein Structure and Molecular Enzymology*, Vol. 994, pp. 270–279.
3. *Overexpression, purification and properties of alcohol dehydrogenase IV from Saccharomyces cerevisiae*. **Drewke, Christel and Ciriacy, Michael.** 1, May 6, 1988, *Biochimica et Biophysica Acta*, Vol. 950, pp. 54-60.
4. *Ferrous-activated Nicotinamide Adenine Dinucleotide-linked Dehydrogenase from a Mutant of Escherichia coli Capable of Growth on 1,2-Propanediol*. **Sridhara, S., et al.** 1, 1969, *Journal of Bacteriology*, Vol. 98, pp. 87-95.
5. *The two alcohol dehydrogenases of Zymomonas mobilis: purification by differential dye ligand chromatography, molecular characterisation and physiological roles*. **Neale, Alan D., et al.** 1, 1986, *FEBS Journal*, Vol. 154, pp. 119-124.
6. *Site-directed mutagenesis studies of the metal-binding center of the iron-dependent propanediol oxidoreductase from Escherichia coli*. **Obradors, Nuria, et al.** 1, November 15, 1998, *FEBS Journal*, Vol. 258, pp. 207-213.
7. *Characterization of a Thermostable Xylanase from the Extremely Thermophilic Bacterium Thermotoga hypogea*. **Dhanjoon, Jasleen, et al.** 4, 2013, *Current biotechnology*, Vol. 2, pp. 325-333.
8. *A method of expression for an oxygen-tolerant group III alcohol dehydrogenase from Pyrococcus horikoshii OT3*. **Sugimoto, Chikanobu, et al.** 4, 2017, *Journal of Biological Inorganic Chemistry*, Vol. 22, pp. 527-534.

9. *In vitro* activation of NAD-dependent alcohol dehydrogenases by Nudix hydrolases is more widespread than assumed. **Ochsner, Andrea M., et al.** 17, August 25, 2014, FEBS Letters, Vol. 588, pp. 2993-2999.
10. Expression and characterization of a novel 1,3-propanediol dehydrogenase from *Lactobacillus brevis*. **Qi, Xianghui, et al.** 6, July 2016, Biotechnology and Applied Biochemistry, Vol. 179, pp. 959-972.
11. Purification and characterization of an iron-containing alcohol dehydrogenase in extremely thermophilic bacterium *Thermotoga hypogea*. **Ying, Xiangxian, et al.** 6, 2007, Archives of Microbiology, Vol. 187, pp. 499-510.
12. Molecular characterization of the recombinant iron-containing alcohol dehydrogenase from the hyperthermophilic Archaeon, *Thermococcus* strain ES1. **Ying, Xiangxian, et al.** 2, 2009, Extremophiles, Vol. 13, pp. 299-311.
13. Structural and biochemical characterisation of a NAD<sup>+</sup>-dependent alcohol dehydrogenase from *Oenococcus oeni* as a new model molecule for industrial biotechnology applications. **Elleuche, Skander, et al.** 20, October 2013, Applied Microbiology and Biotechnology, Vol. 97, pp. 8963-8975.
14. Characterization of 1,3-propanediol oxidoreductase (*DhaT*) from *Klebsiella pneumoniae* J2B. **Lama, Suman, et al.** 6, 2015, Biotechnology and Bioprocess Engineering, Vol. 20, pp. 971-979.
15. Comparative analysis of two members of the metal ion-containing group III-alcohol dehydrogenases from *Dickeya zea*. **Elleuche, Skander, et al.** 5, 2013, Biotechnology Letters, Vol. 35, pp. 725-733.
16. Purification and Characterization of the NADH-Dependent Butanol Dehydrogenase from *Clostridium acetobutylicum* (ATCC 824). **Welch, Richard W., Rudolph, Frederick B. and Papoustakis, E. Terry.** 2, September 1989, Archives of Biochemistry and Biophysics, Vol. 273.

17. *Diversity and Evolutionary Analysis of Iron-Containing (Type-III) Alcohol Dehydrogenases in Eukaryotes*. **Gaona-López, Carlos, Julián-Sánchez, Adriana and Riveros-Rosas, Héctor**. 11, 2016, PLOS ONE, Vol. 11.
18. *Glycerol dehydrogenase: structure, specificity, and mechanism of a family III polyol dehydrogenase*. **Ruzheinikov, Sergey N., et al.** 9, September 2001, Structure, Vol. 9, pp. 789-802.
19. *1,3-Propanediol Dehydrogenase from Klebsiella pneumoniae: Decameric Quaternary Structure and Possible Subunit Cooperativity*. **Marçal, David, et al.** 4, February 2009, Journal of Bacteriology, Vol. 191, pp. 1143-1151.
20. *Structures and mechanisms of Nudix hydrolases*. **Mildvan, Albert S., et al.** 1, January 1, 2005, Archives of Biochemistry and Biophysics, Vol. 433, pp. 129-143.
21. *Functional characterization of the mammalian mRNA decapping enzyme hDcp2*. **Piccirillo C, Khanna R, Kiledjian M.** 9, 2003, RNA, Vol. 9, pp. 1138–47.
22. *Molecular, Biochemical, and Functional Characterization of a Nudix Hydrolase Protein That Stimulates the Activity of a Nicotinoprotein Alcohol Dehydrogenase*. **Kloosterman, Harm, Vrijbloed, Jan W. and Dijkhuizen, Lubbert.** 38, September 20, 2002, Journal of Biological Chemistry, Vol. 277, pp. 34785-34792.
23. *Methylophilic Bacillus methanolicus Encodes Two Chromosomal and One Plasmid Born NAD<sup>+</sup> Dependent Methanol Dehydrogenase Paralogs with Different Catalytic and Biochemical Properties*. **Krog, Anne, et al.** 3, March 19, 2013, PLOS ONE, Vol. 8.
24. *Metabolic Pathway for Biosynthesis of Poly (3-Hydroxybutyrate-co-4-Hydroxybutyrate) from 4-Hydroxybutyrate by Alcaligenes eutrophus*. **Valentin, Henry E, et al.** 1-2, January 1995, European Journal of Biochemistry, Vol. 227, pp. 43-60.
25. *Genomic View of Energy Metabolism in "Ralstonia eutropha" H16*. **Cramm, R.** 1–2, 2009, J Mol Microbiol Biotechnol, Vol. 16, pp. 38–52.

26. *Green Technology for Conversion of Food Scraps to Biodegradable Thermoplastic Polyhydroxyalkanoates*. **Du, Guocheng and Yu, Jian**. 24, Novembr 7, 2002, Environmental Science and Technology, Vol. 36, pp. 5511-5516.
27. *Microbial production of polyhydroxyalkanoates (PHAs) and its copolymers: A review of recent advancements*. **Anjum, Anbreen, et al**. 2016, International Journal of Biological Macromolecules, Vol. 89, pp. 161-174.
28. *Comparative Protein Modelling by Satisfaction of Spatial Restraints*. **Sali, Andrej and Blundell, Tom L**. 3, 1993, Journal of Molecular Biology, Vol. 234, pp. 779-815.
29. *UCSF Chimera - A Visualization System for Exploratory Research and Analysis*. **Pettersen, E.F., et al**. 2004, J. Comput. Chem., Vol. 25, pp. 1605–1612.
30. *Statistical potential for assessment and prediction of protein structures*. **Shen, Min-yi and Sali, Andrej**. 11, 2006, Protein Science, Vol. 15, pp. 2507-2524.
31. *ZINC: A Free Tool to Discover Chemistry for Biology*. **Irwin, John J., et al**. 7, 2012, Journal of Chemical Information and Modeling, Vol. 52, pp. 1757-1768.
32. *A geometric approach to macromolecule-ligand interactions*. **Kuntz, ID, et al**. 2, 1982, Journal of Molecular Biology, Vol. 161, pp. 269–88.
33. *DOCK 6: Impact of new features and current docking performance*. **Allen, William J., et al**. 15, 2015, Journal of Computational Chemistry, Vol. 36, pp. 1132-1156.
34. *Functional characterization of a stereospecific diol dehydrogenase, FucO, from Escherichia coli: Substrate specificity, pH dependence, kinetic isotope effects and influence of solvent viscosity*. **Blikstad, Cecilia and Widersten, Mikael**. September 2010, Journal of Molecular Catalysis B-enzymatic, Vol. 66, pp. 148-155.
35. *The kinetics of enzyme-catalyzed reactions with two or more substrates or products. I. Nomenclature and rate equations*. **Cleland, W. Wallace**. 1963, Biochimica et Biophysica Acta, Vol. 67, pp. 104-137.

36. **Purich, Daniel L.** *Enzyme Kinetics: Catalysis and Control: A Reference of Theory and Best-Practice Methods*. s.l. : Elsevier.
37. *Studies on Liver Alcohol Dehydrogenase. II. The Kinetics of the Compound of Horse Liver Alcohol Dehydrogenase and Reduced Diphosphopyridine Nucleotide.* **Theorell, Hugo and Chance, Britton.** 1951, *Acta Chemica Scandinavica*, Vol. 5, pp. 1127-1144.
38. *ATP sulfurylase from *Penicillium chrysogenum*: Measurements of the true specific activity of an enzyme subject to potent product: Inhibition and a reassessment of the kinetic mechanism.* **Seubert, Peter A., et al.** 2, 1983, *Archives of Biochemistry and Biophysics*, Vol. 225, pp. 679-691.
39. *The adenine phosphoribosyltransferase from *Giardia lamblia* has a unique reaction mechanism and unusual substrate binding properties.* **Sarver AE, Wang CC.** 42, *The Journal of Biological Chemistry*, Vol. 277, pp. 39973–80.
40. *Structural and Kinetic Properties of a beta-Hydroxyacid Dehydrogenase Involved in Nicotinate Fermentation.* **Reitz, Simon, et al.** 3, 2008, *Journal of Molecular Biology*, Vol. 382, pp. 802-811.
41. *Reaction mechanism and specificity of human GMP reductase. Substrates, inhibitors, activators, and inactivators.* **T, Spector, Te, Jones and RI, Miller.** 7, 1979, *Journal of Biological Chemistry*, Vol. 254, pp. 2308-2315.
42. *Purification, characterization, and kinetic mechanism of S-adenosyl-L-methionine: vitexin 2''-O-rhamnoside 7-O-methyltransferase of *Avena sativa* L.* **Knogge, Wolfgang and Weissenböck, Gottfried.** 1, 1984, *FEBS Journal*, Vol. 140, pp. 113-118.
43. *Mechanism of the *Escherichia coli* ADP-Ribose Pyrophosphatase, a Nudix Hydrolase.* **Gabelli, Sandra B., et al.** 30, 2002, *Biochemistry*, Vol. 41, pp. 9279-9285.
44. *Cellular concentrations of enzymes and their substrates.* **Albe, Kathy R., Butler, Margaret Husta and Wright, Barbara E.** 2, 1990, *Journal of Theoretical Biology*, Vol. 143, pp. 163-195.



45. *Marinescu, G. C., Popescu, R.-G., Stoian, G., & Dinischiotβ-nicotinamide mononucleotide (NMN) production in Escherichia coli.* **Mainescu, G. C., et al.** 12278, s.l. : Scientific Reports, 2018, Vol. 8.
46. *Nicotinamide adenine dinucleotide biosynthesis and pyridine nucleotide cycle metabolism in microbial systems.* **Foster, J W and Moat, A G.** 1, 1980, Microbiological Research, Vol. 44, pp. 83-105.
47. *Ribosylnicotinamide kinase domain of NadR protein: identification and implications in NAD biosynthesis.* **Kurnasov OV, Polanuyer BM, Ananta S, Sloutsky R, Tam A, Gerdes SY, Osterman AL.** 24, Journal of Bacteriology, Vol. 184, pp. 6906–17.
48. *Saccharomyces cerevisiae YOR071C encodes the high affinity nicotinamide riboside transporter Nrt1.* **Belenky PA, Moga TG, Brenner C.** 13, The Journal of Biological Chemistry, Vol. 283, pp. 8075–9.
49. *Crystal structure of an Iron-dependent group III dehydrogenase that Interconverts L-Lactaldehyde and L-1,2-Propanediol in Escherichia coli.* **Montella, Christina, et al.** July 2005, Journal of Bacteriology, pp. 4957-4966.
50. *Crystal Structure of E.Coli Alcohol Dehydrogenase Yqhd: Evidence of a Covalently Modified Nadp Coenzyme.* **Sulzenbacher, Gerlind, et al.** 2, 2004, Journal of Molecular Biology, Vol. 342, pp. 489-502.
51. *Microdetermination of Phosphorous.* **Chen, P. S., Toriyaba, T. Y, and Warner, Huber.** 11, November 1, 1956, Analytical Chemistry, Vol. 28, pp. 1756-1758.
52. *Investigation of the NADH/NAD(+) ratio in Ralstonia eutropha using the fluorescence reporter protein Peredox.* **Tejwani, Vijay, et al.** 1, 2017, Biochimica et Biophysica Acta, Vol. 1858, pp. 86-94.
53. *Cupriavidus necator gen. nov., sp. nov.: a nonobligate bacterial predator of bacteria in soil.* **Makkar, N.S. and Casida, L.E.** 4, 1987, International Journal of Systematic and Evolutionary Microbiology, Vol. 37, pp. 323-326.

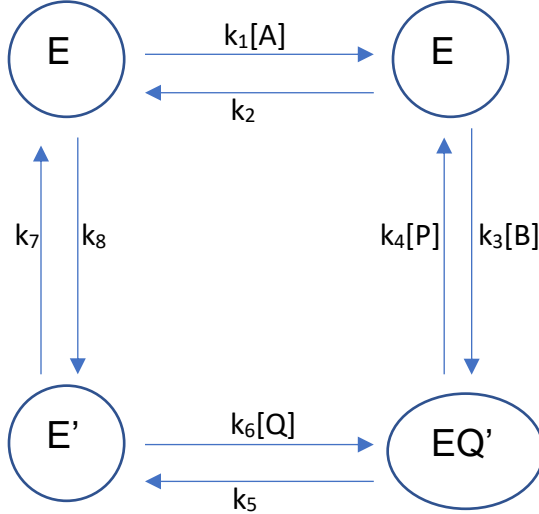
54. *Reliable, sensitive, rapid, and quantitative enzyme-based assay for gamma-hydroxybutyric acid (GHB)*. **Bravo, Dawn T., Harris, David O. and Parsons, Stanley M.** 2, March 2004, Journal of Forensic Science, Vol. 49, pp. 1-9.
55. *Group III alcohol dehydrogenase from Pectobacterium atrosepticum: insights into enzymatic activity and organization of the metal ion-containing region*. **Elleuche, Skander, et al.** 9, May 2014, Applied Microbiology and Biotechnology, Vol. 98, pp. 4041-4051.
56. *Properties of an NAD(H)-containing methanol dehydrogenase and its activator protein from Bacillus methanolicus*. **Arfman, Nico, et al.** 2, March 1, 1997, FEBS Journal, Vol. 244, pp. 426-433.
57. *Purification, crystallization and quaternary structure analysis of a glycerol dehydrogenase S305C mutant from Bacillus stearothermophilus*. **Burke, Jacky, et al.** 1, January 2001, Acta Crystallographica Section D-biological Crystallography, Vol. 57, pp. 165-167.
58. *Enhanced 1,3-propanediol production in recombinant Klebsiella pneumoniae carrying the gene yqhD encoding 1,3-propanediol oxidoreductase isoenzyme*. **Zhu, Jian-Guo, et al.** 7, July 2009, World Journal of Microbiology & Biotechnology, Vol. 25, pp. 1217-1223.
59. *Improved isolation of proteins tagged with glutathione S-transferase*. **Vinckier, Nicholas K., Chworos, Arkadiusz and Parsons, Stanley M.** February 2011, Protein Expression and Purification, Vol. 75, pp. 161-164.
60. *Investigation of the NADH/NAD(+) ratio in Ralstonia eutropha using the fluorescence reporter protein Peredox*. **Tejwani, Vijay, et al.** 1, 2017, Biochimica et Biophysica Acta, Vol. 1858, pp. 86-94.

61. *Crystal structure of an iron-containing 1,3-propanediol dehydrogenase (TM0920) from Thermotoga maritima at 1.3 Å resolution.* **Schwarzenbacher, Robert, et al.** 1, January 1, 2004, *Proteins*, Vol. 54, pp. 174-177.
62. *Structures of iron-dependent alcohol dehydrogenase 2 from Zymomonas mobilis ZM4 with and without NAD<sup>+</sup> cofactor.* **Moon, Ji-Hyun, et al.** 3, April 1, 2011, *Journal of Molecular Biology*, Vol. 407, pp. 413-424.
63. *Purification of two alcohol dehydrogenases from Zymomonas mobilis and their properties.* **Kinoshita, Shinichi, et al.** 4, August 1985, *Applied Microbiology and Biotechnology*, Vol. 22, pp. 249-254.
64. *Mechanism of the Escherichia coli ADP-Ribose Pyrophosphatase, a Nudix Hydrolase.* **Gabelli, Sandra M., et al.** 30, July 2, 2002, *Biochemistry*, Vol. 41, pp. 9279-9285.
65. *Mutations in adenine-binding pockets enhance catalytic properties of NAD(P)H-dependent enzymes.* **Cahn, Jackson K. B., et al.** 1, October 27, 2015, *Protein Engineering Design & Selection*, Vol. 29, pp. 31-38.
66. *Taxonomy of the genus Cupriavidus: a tale of lost and found.* **Vandamme, Peter and Coenye, Tom.** November 2004, *International Journal of Systematic and Evolutionary Microbiology*, Vol. 54, pp. 2285-2289.
67. **Vinckier, Nicholas K., et al.** *Metal ions. chelators. alternative substrates, and kinetic mechanism for Fe(II)-dependent gamma-hydroxybutyrate dehydrogenase of Type III from Cupriavidus necator.* 2018.
68. *Bacterial group III alcohol dehydrogenases-function, evolution, and biotechnological applications.* **Elleuche, S. and Antranikian, G.** 1, March 01, 2013, *Open Access Alcohol*, Vol. 1.
69. *Reduced surface: An efficient way to compute molecular surfaces.* **Sanner, Michel F., Olson, Arthur J. and Spehner, Jean-Claude.** 3, 1996, *Biopolymers*, Vol. 38, pp. 305-320.

70. *Fast, scalable generation of high-quality protein multiple sequence alignments using Clustal Omega.* **Sievers, Fabian, et al.** 1, 2014, *Molecular Systems Biology*, Vol. 7.

## IX. Appendix

### A. Derivation of Mono-Iso Theorell-Chance Inhibition Equations:



$$E = \frac{k_6[Q] \cdot k_4[P] \cdot k_2 + k_4[P] \cdot k_2 \cdot k_7 + k_2 \cdot k_5 \cdot k_7 + k_3[B] \cdot k_5 \cdot k_7}{k_1[A] \cdot k_6[Q] \cdot k_4[P] + k_8 \cdot k_6[Q] \cdot k_4[P] + k_7 \cdot k_1[A] \cdot k_4[P] + k_5 \cdot k_7 \cdot k_1[A]}$$

$$EA = \frac{k_1[A] \cdot k_6[Q] \cdot k_4[P] + k_8 \cdot k_6[Q] \cdot k_4[P] + k_7 \cdot k_1[A] \cdot k_4[P] + k_5 \cdot k_7 \cdot k_1[A]}{k_1[A] \cdot k_3[B] \cdot k_5 + k_3[B] \cdot k_5 \cdot k_8 + k_5 \cdot k_2 \cdot k_8 + k_4[P] \cdot k_2 \cdot k_8}$$

$$EQ' = \frac{k_7 \cdot k_1[A] \cdot k_3[B] + k_1[A] \cdot k_3[B] \cdot k_6[Q] + k_8 \cdot k_6[Q] \cdot k_3[B] + k_2 \cdot k_8 \cdot k_6[Q]}{k_2 \cdot k_5 \cdot k_7 + k_5 \cdot k_2 \cdot k_8 + k_5 \cdot k_7 \cdot k_1[A] + k_3[B] \cdot k_5 \cdot k_8 + k_3[B] \cdot k_5 \cdot k_7 + k_1[A] \cdot k_3[B] \cdot k_5 + k_7 \cdot k_1[A] \cdot k_3[B] + k_7 \cdot k_1[A] \cdot k_4[P] + k_8 \cdot k_6[Q] \cdot k_3[B] + k_2 \cdot k_8 \cdot k_6[Q] + k_4[P] \cdot k_2 \cdot k_7 + k_4[P] \cdot k_2 \cdot k_8 + k_6[Q] \cdot k_4[P] \cdot k_2 + k_8 \cdot k_6[Q] \cdot k_4[P] + k_1[A] \cdot k_6[Q] \cdot k_4[P] + k_1[A] \cdot k_3[B] \cdot k_6[Q]}$$

$$E' = \frac{k_1[A] \cdot k_3[B] \cdot k_5 + k_3[B] \cdot k_5 \cdot k_8 + k_5 \cdot k_2 \cdot k_8 + k_4[P] \cdot k_2 \cdot k_8}{k_2 \cdot k_5 \cdot k_7 + k_5 \cdot k_2 \cdot k_8 + k_5 \cdot k_7 \cdot k_1[A] + k_3[B] \cdot k_5 \cdot k_8 + k_3[B] \cdot k_5 \cdot k_7 + k_1[A] \cdot k_3[B] \cdot k_5 + k_7 \cdot k_1[A] \cdot k_3[B] + k_7 \cdot k_1[A] \cdot k_4[P] + k_8 \cdot k_6[Q] \cdot k_3[B] + k_2 \cdot k_8 \cdot k_6[Q] + k_4[P] \cdot k_2 \cdot k_7 + k_4[P] \cdot k_2 \cdot k_8 + k_6[Q] \cdot k_4[P] \cdot k_2 + k_8 \cdot k_6[Q] \cdot k_4[P] + k_1[A] \cdot k_6[Q] \cdot k_4[P] + k_1[A] \cdot k_3[B] \cdot k_6[Q]}$$

$$E_T = \frac{k_6[Q] \cdot k_4[P] \cdot k_2 + k_4[P] \cdot k_2 \cdot k_7 + k_2 \cdot k_5 \cdot k_7 + k_3[B] \cdot k_5 \cdot k_7 + k_1[A] \cdot k_6[Q] \cdot k_4[P] + k_8 \cdot k_6[Q] \cdot k_4[P] + k_7 \cdot k_1[A] \cdot k_4[P] + k_5 \cdot k_7 \cdot k_1[A] + k_7 \cdot k_1[A] \cdot k_3[B] + k_1[A] \cdot k_3[B] \cdot k_6[Q] + k_8 \cdot k_6[Q] \cdot k_3[B] + k_2 \cdot k_8 \cdot k_6[Q] + k_1[A] \cdot k_3[B] \cdot k_5 + k_3[B] \cdot k_5 \cdot k_8 + k_5 \cdot k_2 \cdot k_8 + k_4[P] \cdot k_2 \cdot k_8}{k_2 \cdot k_5 \cdot k_7 + k_5 \cdot k_2 \cdot k_8 + k_5 \cdot k_7 \cdot k_1[A] + k_3[B] \cdot k_5 \cdot k_8 + k_3[B] \cdot k_5 \cdot k_7 + k_1[A] \cdot k_3[B] \cdot k_5 + k_7 \cdot k_1[A] \cdot k_3[B] + k_7 \cdot k_1[A] \cdot k_4[P] + k_8 \cdot k_6[Q] \cdot k_3[B] + k_2 \cdot k_8 \cdot k_6[Q] + k_4[P] \cdot k_2 \cdot k_7 + k_4[P] \cdot k_2 \cdot k_8 + k_6[Q] \cdot k_4[P] \cdot k_2 + k_8 \cdot k_6[Q] \cdot k_4[P] + k_1[A] \cdot k_6[Q] \cdot k_4[P] + k_1[A] \cdot k_3[B] \cdot k_6[Q]}$$

$$E_T = \frac{k_2 \cdot k_5 \cdot k_7 + k_5 \cdot k_2 \cdot k_8 + k_5 \cdot k_7 \cdot k_1[A] + k_3[B] \cdot k_5 \cdot k_8 + k_3[B] \cdot k_5 \cdot k_7 + k_1[A] \cdot k_3[B] \cdot k_5 + k_7 \cdot k_1[A] \cdot k_3[B] + k_7 \cdot k_1[A] \cdot k_4[P] + k_8 \cdot k_6[Q] \cdot k_3[B] + k_2 \cdot k_8 \cdot k_6[Q] + k_4[P] \cdot k_2 \cdot k_7 + k_4[P] \cdot k_2 \cdot k_8 + k_6[Q] \cdot k_4[P] \cdot k_2 + k_8 \cdot k_6[Q] \cdot k_4[P] + k_1[A] \cdot k_6[Q] \cdot k_4[P] + k_1[A] \cdot k_3[B] \cdot k_6[Q]}{k_2 \cdot k_5 \cdot (k_7 + k_8) + k_1 \cdot k_5 \cdot k_7 \cdot [A] + k_3 \cdot k_5 \cdot (k_7 + k_8) \cdot [B] + k_1 \cdot k_3 \cdot (k_5 + k_7) \cdot [A] \cdot [B] + k_2 \cdot k_4 \cdot (k_7 + k_8) \cdot [P] + k_2 \cdot k_6 \cdot k_8 \cdot [Q] + k_4 \cdot k_6 \cdot (k_2 + k_8) \cdot [P] \cdot [Q] + k_3 \cdot k_6 \cdot k_8 \cdot [B] \cdot [Q] + k_1 \cdot k_4 \cdot k_7 \cdot [A] \cdot [P] + k_1 \cdot k_4 \cdot k_6 \cdot [A] \cdot [P] \cdot [Q] + k_1 \cdot k_3 \cdot k_6 \cdot [A] \cdot [B] \cdot [Q]}$$

$$E_T = \frac{k_2 \cdot k_5 \cdot (k_7 + k_8) + k_1 \cdot k_5 \cdot k_7 \cdot [A] + k_3 \cdot k_5 \cdot (k_7 + k_8) \cdot [B] + k_1 \cdot k_3 \cdot (k_5 + k_7) \cdot [A] \cdot [B] + k_2 \cdot k_4 \cdot (k_7 + k_8) \cdot [P] + k_2 \cdot k_6 \cdot k_8 \cdot [Q] + k_4 \cdot k_6 \cdot (k_2 + k_8) \cdot [P] \cdot [Q] + k_3 \cdot k_6 \cdot k_8 \cdot [B] \cdot [Q] + k_1 \cdot k_4 \cdot k_7 \cdot [A] \cdot [P] + k_1 \cdot k_4 \cdot k_6 \cdot [A] \cdot [P] \cdot [Q] + k_1 \cdot k_3 \cdot k_6 \cdot [A] \cdot [B] \cdot [Q]}{k_2 \cdot k_5 \cdot (k_7 + k_8) + k_1 \cdot k_5 \cdot k_7 \cdot [A] + k_3 \cdot k_5 \cdot (k_7 + k_8) \cdot [B] + k_1 \cdot k_3 \cdot (k_5 + k_7) \cdot [A] \cdot [B] + k_2 \cdot k_4 \cdot (k_7 + k_8) \cdot [P] + k_2 \cdot k_6 \cdot k_8 \cdot [Q] + k_4 \cdot k_6 \cdot (k_2 + k_8) \cdot [P] \cdot [Q] + k_3 \cdot k_6 \cdot k_8 \cdot [B] \cdot [Q] + k_1 \cdot k_4 \cdot k_7 \cdot [A] \cdot [P] + k_1 \cdot k_4 \cdot k_6 \cdot [A] \cdot [P] \cdot [Q] + k_1 \cdot k_3 \cdot k_6 \cdot [A] \cdot [B] \cdot [Q]}$$

$$v = (EA*k_3[B] - FQ*k_4[P])/E_T$$

$$v = ((k_1[A]*k_6[Q]*k_4[P] + k_8*k_6[Q]*k_4[P] + k_7*k_1[A]*k_4[P] + k_5*k_7*k_1[A]*k_3[B] - (k_7*k_1[A]*k_3[B] + k_1[A]*k_3[B]*k_6[Q] + k_8*k_6[Q]*k_3[B] + k_2*k_8*k_6[Q])*k_4[P])/E_T$$

$$v = (k_1k_3k_4k_6[A][B][P][Q] + k_3k_4k_6k_8[B][P][Q] + k_1k_3k_4k_7[A][B][P] + k_1k_3k_5k_7[A][B] - k_1k_3k_4k_7[A][B][P] - k_1k_3k_4k_6[A][B][P][Q] - k_3k_4k_6k_8[B][P][Q] - k_2k_4k_6k_6[P][Q])/E_T$$

$$v = (k_1k_3k_5k_7[A][B] - k_2k_4k_6k_6[P][Q]) / ((k_2k_5(k_7 + k_8) + k_1k_5k_7[A] + k_3k_5(k_7 + k_8)[B] + k_1k_3(k_5 + k_7)[A][B] + k_2k_4(k_7 + k_8)[P] + k_2k_6k_8[Q] + k_4k_6(k_2 + k_8)[P][Q] + k_3k_6k_8[B][Q] + k_1k_4k_7[A][P] + k_1k_4k_6[A][P][Q] + k_1k_3k_6[A][B][Q])$$

$$v/E_T = (k_1k_3k_5k_7[A][B] - k_2k_4k_6k_6[P][Q]) / ((k_2k_5(k_7 + k_8) + k_1k_5k_7[A] + k_3k_5(k_7 + k_8)[B] + k_1k_3(k_5 + k_7)[A][B] + k_2k_4(k_7 + k_8)[P] + k_2k_6k_8[Q] + k_4k_6(k_2 + k_8)[P][Q] + k_3k_6k_8[B][Q] + k_1k_4k_7[A][P] + k_1k_4k_6[A][P][Q] + k_1k_3k_6[A][B][Q])$$

Defining Coefficients and Constants:

num1 =	$k_1k_3k_5k_7$	Coeff <sub>Q</sub> =	$k_2k_6k_8$
num2 =	$k_2k_4k_6k_8$	Coeff <sub>PQ</sub> =	$k_4k_6(k_2 + k_8)$
constant =	$k_2k_5(k_7 + k_8)$	Coeff <sub>BQ</sub> =	$k_3k_6k_8$
Coeff <sub>A</sub> =	$k_1k_5k_7$	Coeff <sub>AP</sub> =	$k_1k_4k_7$
Coeff <sub>B</sub> =	$k_3k_5(k_7 + k_8)$	Coeff <sub>APQ</sub> =	$k_1k_4k_6$
Coeff <sub>AB</sub> =	$k_1k_3(k_5 + k_7)$	Coeff <sub>ABQ</sub> =	$k_1k_3k_6$
Coeff <sub>P</sub> =	$k_2k_4(k_7 + k_8)$	K <sub>eq</sub> =	num1/num2

Defining V, K<sub>ms</sub>, K<sub>is</sub>, and K<sub>ii</sub>s

$V_{\max f} = \frac{num1}{Coeff_{AB}}$	$V_{\max r} = \frac{num2}{Coeff_{PQ}}$
$K_a = \frac{Coeff_B}{Coeff_{AB}}$	$K_{ia} = \frac{constant}{Coeff_A} = \frac{Coeff_P}{Coeff_{AP}}$
$K_b = \frac{Coeff_A}{Coeff_{AB}}$	$K_{iq} = \frac{constant}{Coeff_Q} = \frac{Coeff_B}{Coeff_{BQ}}$
$K_p = \frac{Coeff_Q}{Coeff_{PQ}}$	$K_{iia} = \frac{Coeff_{PQ}}{Coeff_{APQ}}$
$K_q = \frac{Coeff_P}{Coeff_{PQ}}$	$K_{iiq} = \frac{Coeff_{AB}}{Coeff_{ABQ}}$

Multiply the whole equation by  $\frac{num2}{Coeff_{AB} * Coeff_{PQ}}$ , and also sometimes by  $\frac{num1}{num1}$  (1):

$$v = \frac{\frac{num1 * num2 [A][B]}{Coeff_{AB} * Coeff_{PQ}} - \frac{num1 * num2 * num2 [P][Q]}{num1 * Coeff_{AB} * Coeff_{PQ}}}{\frac{constant * num2}{Coeff_{AB} * Coeff_{PQ}} + \frac{num2 * Coeff_A [A]}{Coeff_{AB} * Coeff_{PQ}} + \frac{num2 * Coeff_A [B]}{Coeff_{AB} * Coeff_{PQ}} + \frac{num2 * Coeff_{AB} [A][B]}{Coeff_{AB} * Coeff_{PQ}} + \frac{num1 * num2 * Coeff_P [P]}{num1 * Coeff_{AB} * Coeff_{PQ}} + \frac{num1 * num2 * Coeff_Q [Q]}{num1 * Coeff_{AB} * Coeff_{PQ}} + \frac{num1 * num2 * Coeff_{PQ} [P][Q]}{num1 * Coeff_{AB} * Coeff_{PQ}} + \frac{num2 * Coeff_{BQ} [B][Q]}{Coeff_{AB} * Coeff_{PQ}} + \frac{num1 * num2 * Coeff_{AP} [A][P]}{num1 * Coeff_{AB} * Coeff_{PQ}} + \frac{num1 * num2 * Coeff_{APQ} [A][P][Q]}{num1 * Coeff_{AB} * Coeff_{PQ}} + \frac{num2 * Coeff_{ABQ} [A][B][Q]}{Coeff_{AB} * Coeff_{PQ}}}$$

Replace:

$$v = \frac{V_{maxf} V_{maxr} [A][B] - \frac{V_{maxf} V_{maxr} [P][Q]}{K_{eq}}}{\frac{V_{maxr} constant}{Coeff_{AB}} + V_{maxr} K_b [A] + V_{maxr} K_a [B] + V_{maxr} [A][B] + \frac{V_{maxf} K_q [P]}{K_{eq}} + \frac{V_{maxf} K_p [Q]}{K_{eq}} + \frac{V_{maxf} [P][Q]}{K_{eq}} + \frac{V_{maxr} K_B [B][Q]}{Coeff_{AB} K_{iq}} + \frac{V_{maxf} K_P [A][P]}{K_{ia} K_{eq} Coeff_{PQ}} + \frac{V_{maxf} [A][P][Q]}{K_{eq} K_{iia}} + \frac{V_{maxr} [A][B][Q]}{K_{iia}}}$$

$$v = \frac{V_{maxf} V_{maxr} [A][B] - \frac{V_{maxf} V_{maxr} [P][Q]}{K_{eq}}}{K_{ia} K_b + V_{maxr} K_b [A] + V_{maxr} K_a [B] + V_{maxr} [A][B] + \frac{V_{maxf} K_q [P]}{K_{eq}} + \frac{V_{maxf} K_p [Q]}{K_{eq}} + \frac{V_{maxf} [P][Q]}{K_{eq}} + \frac{V_{maxr} K_a [B][Q]}{K_{iq}} + \frac{V_{maxf} K_q [A][P]}{K_{ia} K_{eq}} + \frac{V_{maxf} [A][P][Q]}{K_{eq} K_{iia}} + \frac{V_{maxr} [A][B][Q]}{K_{iia}}}$$

Divide the whole equation by  $V_{maxr}$ :

$$v = \frac{V_{maxf} [A][B] - \frac{V_{maxf} [P][Q]}{K_{eq}}}{K_{ia} K_b + K_b [A] + K_a [B] + [A][B] + \frac{V_{maxf} K_q [P]}{V_{maxr} K_{eq}} + \frac{V_{maxf} K_p [Q]}{V_{maxr} K_{eq}} + \frac{V_{maxf} [P][Q]}{V_{maxr} K_{eq}} + \frac{K_a [B][Q]}{K_{iq}} + \frac{V_{maxf} K_q [A][P]}{V_{maxr} K_{ia} K_{eq}} + \frac{V_{maxf} [A][P][Q]}{V_{maxr} K_{eq} K_{iia}} + \frac{[A][B][Q]}{K_{iia}}}$$

Haldane Relationships:

$$\frac{K_{ia}K_bV_{maxr}K_{eq}}{V_{maxf}} = \left(\frac{\text{constant}}{Coef_{f_{AB}}}\right) \left(\frac{\text{num2}}{Coef_{f_{PQ}}}\right) \left(\frac{\text{num1}}{\text{num2}}\right) \left(\frac{Coef_{f_{AB}}}{\text{num1}}\right) = \frac{\text{constant}}{Coef_{f_{PQ}}} = K_{iq}K_p$$

$$= K_{ip}K_q$$

$$\frac{V_{maxf}}{V_{maxr}K_{eq}} = \frac{K_{ia}K_b}{K_{iq}K_p} = \frac{K_{ia}K_b}{K_{ip}K_q} = \frac{K_aK_{ib}}{K_{iq}K_p} = \frac{K_aK_{ib}}{K_{ip}K_q}$$

Replace:

$$v = \frac{V_{maxf}[A][B] - \frac{V_{maxf}[P][Q]}{K_{eq}}}{K_{ia}K_b + K_b[A] + K_a[B] + [A][B] + \frac{K_{ia}K_b[P]}{K_{ip}} + \frac{K_{ia}K_b[Q]}{K_{iq}} + \frac{K_{ia}K_b[P][Q]}{K_{ip}K_q} + \frac{K_a[B][Q]}{K_{iq}} + \frac{K_b[A][P]}{K_{ip}} + \frac{K_{ia}K_b[A][P][Q]}{K_{iq}K_p * K_{iia}} + \frac{[A][B][Q]}{K_{iiq}}}$$

Take the reciprocal on both sides:

$$\frac{1}{v_0} = \frac{K_{ia}K_b + K_b[A] + K_a[B] + [A][B] + \frac{K_{ia}K_b[P]}{K_{ip}} + \frac{K_{ia}K_b[Q]}{K_{iq}} + \frac{K_{ia}K_b[P][Q]}{K_{ip}K_q} + \frac{K_a[B][Q]}{K_{iq}} + \frac{K_b[A][P]}{K_{ip}} + \frac{K_{ia}K_b[A][P][Q]}{K_{iq}K_p * K_{iia}} + \frac{[A][B][Q]}{K_{iiq}}}{V_{maxf}[A][B] - \frac{V_{maxf}[P][Q]}{K_{eq}}}$$

If there is Q but no P:

$$\frac{1}{v_0} = \frac{K_{ia}K_b + K_b[A] + K_a[B] + [A][B] + \frac{K_{ia}K_b[Q]}{K_{iq}} + \frac{K_a[B][Q]}{K_{iq}} + \frac{[A][B][Q]}{K_{iiq}}}{V_{maxf}[A][B]}$$

$$\frac{1}{v_0} = \frac{K_{ia}K_b}{V_{maxf}[A][B]} + \frac{K_b}{V_{maxf}[B]} + \frac{K_a}{V_{maxf}[A]} + \frac{1}{V_{maxf}} + \frac{K_{ia}K_b[Q]}{V_{maxf}[A][B]K_{iq}} + \frac{K_a[Q]}{V_{maxf}[A]K_{iq}}$$

$$+ \frac{[Q]}{V_{maxf}K_{iiq}}$$

$$\frac{1}{v_0} = \frac{1}{V_{maxf}} \left[ 1 + \frac{[Q]}{K_{iiq}} \right] + \frac{K_a}{V_{maxf}[A]} \left[ 1 + \frac{[Q]}{K_{iq}} \right] + \frac{K_b}{V_{maxf}[B]} + \frac{K_{ia}K_b}{V_{maxf}[A][B]} \left[ 1 + \frac{[Q]}{K_{iq}} \right]$$



If there is P but no Q:

$$\frac{1}{v_0} = \frac{K_{ia}K_b + K_b[A] + K_a[B] + [A][B] + \frac{K_{ia}K_b[P]}{K_{ip}} + \frac{K_b[A][P]}{K_{ip}}}{V_{maxf}[A][B]}$$

$$\frac{1}{v_0} = \frac{K_{ia}K_b}{V_{maxf}[A][B]} + \frac{K_b}{V_{maxf}[B]} + \frac{K_a}{V_{maxf}[A]} + \frac{1}{V_{maxf}} + \frac{K_{ia}K_b[P]}{V_{maxf}[A][B]K_{ip}} + \frac{K_b[P]}{V_{maxf}[B]K_{ip}}$$

$$\frac{1}{v_0} = \frac{1}{V_{maxf}} + \frac{K_a}{V_{maxf}[A]} + \frac{K_b}{V_{maxf}[B]} \left[ 1 + \frac{[P]}{K_{ip}} \right] + \frac{K_{ia}K_b}{V_{maxf}[A][B]} \left[ 1 + \frac{[P]}{K_{ip}} \right]$$

### B. Sample Mathematica Fitting Script

Import data from .xls spreadsheet.

```
sheet7=Import["C:\\Users\\Esther
Taxon\\Documents\\Parsons\\Mathematica Manipulations\\2017-7-
28 GHB 0.3 mM SSA.xls",{"Data",7}]
```

```
{{Time ( Second ),4 mM GHB #1,4 mM GHB #2,4 mM GHB #3,,Time (
Second ),4 mM GHB #1,4 mM GHB #2,4 mM GHB
#3},{0.,0.0105,0.0167,0.0129,,0.,20.0784,31.9341,24.6677},{1.
,0.0129,0.0184,0.0148,,1.,24.6677,35.1849,28.3009},{2.,0.0149
,0.0212,0.0167,,2.,28.4921,40.5392,31.9341},{3.,0.0178,0.0232
,0.0187,,3.,34.0376,44.3636,35.7586},{4.,0.0175,0.024,0.0182,
,4.,33.4639,45.8934,34.8025},{5.,0.019,0.0271,0.0226,,5.,36.3
323,51.8213,43.2163},{6.,0.02,0.0255,0.0219,,6.,38.2445,48.76
17,41.8777},{7.,0.0225,0.0287,0.0234,,7.,43.025,54.8808,44.74
6},{8.,0.0237,0.0304,0.0266,,8.,45.3197,58.1316,50.8652},{9.,
0.0242,0.0304,0.0258,,9.,46.2758,58.1316,49.3354},{10.,0.0249
,0.0309,0.0271,,10.,47.6144,59.0877,51.8213},{11.,0.0254,0.03
28,0.0272,,11.,48.5705,62.721,52.0125},{12.,0.0247,0.0336,0.0
284,,12.,47.2319,64.2507,54.3072},{13.,0.0269,0.0341,0.0299,,
13.,51.4388,65.2068,57.1755},{14.,0.0283,0.0333,0.0287,,14.,5
4.1159,63.6771,54.8808},{15.,0.0276,0.0355,0.0299,,15.,52.777
4,67.884,57.1755},{16.,0.0281,0.0355,0.0299,,16.,53.7335,67.8
84,57.1755},{17.,0.0297,0.0356,0.0316,,17.,56.7931,68.0752,60
.4263},{18.,0.0299,0.0361,0.0311,,18.,57.1755,69.0313,59.4702
},{19.,0.0298,0.0376,0.0323,,19.,56.9843,71.8996,61.7648},{20
.,0.0298,0.0374,0.0314,,20.,56.9843,71.5172,60.0438},{21.,0.0
305,0.0372,0.0336,,21.,58.3228,71.1347,64.2507},{22.,0.0304,0
.0385,0.0326,,22.,58.1316,73.6206,62.3385},{23.,0.0309,0.0385
,0.0334,,23.,59.0877,73.6206,63.8683},{24.,0.0311,0.0386,0.03
```

27.,,24.,,59.4702,73.8119,62.5297},{25.,,0.0323,0.038,0.0348,,25.,,61.7648,72.6645,66.5454},{26.,,0.0323,0.0391,0.0338,,26.,,61.7648,74.768,64.6332},{27.,,0.0326,0.0385,0.0328,,27.,,62.3385,73.6206,62.721},{28.,,0.0319,0.0398,0.0342,,28.,,61.,,76.1065,65.3981},{29.,,0.0319,0.0385,0.0343,,29.,,61.,,73.6206,65.5893},{30.,,0.033,0.041,0.0349,,30.,,63.1034,78.4012,66.7366},{31.,,0.0323,0.0392,0.0348,,31.,,61.7648,74.9592,66.5454},{32.,,0.0321,0.0409,0.0342,,32.,,61.3824,78.21,65.3981},{33.,,0.0337,0.0416,0.0348,,33.,,64.442,79.5485,66.5454},{34.,,0.0336,0.0414,0.035,,34.,,64.2507,79.1661,66.9278},{35.,,0.0328,0.0416,0.0345,,35.,,62.721,79.5485,65.9717},{36.,,0.0327,0.0408,0.0363,,36.,,62.5297,78.0188,69.4137},{37.,,0.0337,0.0414,0.0348,,37.,,64.442,79.1661,66.5454},{38.,,0.0326,0.0421,0.0365,,38.,,62.3385,80.5046,69.7962},{39.,,0.0326,0.041,0.0355,,39.,,62.3385,78.4012,67.884},{40.,,0.0337,0.041,0.0356,,40.,,64.442,78.4012,68.0752},{41.,,0.0343,0.041,0.035,,41.,,65.5893,78.4012,66.9278},{42.,,0.0342,0.0413,0.0352,,42.,,65.3981,78.9749,67.3103},{43.,,0.0352,0.0415,0.0344,,43.,,67.3103,79.3573,65.7805},{44.,,0.0326,0.0413,0.0356,,44.,,62.3385,78.9749,68.0752},{45.,,0.0342,0.0406,0.0355,,45.,,65.3981,77.6363,67.884},{46.,,0.0338,0.0413,0.0345,,46.,,64.6332,78.9749,65.9717},{47.,,0.0344,0.0409,0.0352,,47.,,65.7805,78.21,67.3103},{48.,,0.0349,0.042,0.0359,,48.,,66.7366,80.3134,68.6489},{49.,,0.0333,0.0413,0.0358,,49.,,63.6771,78.9749,68.4576},{50.,,0.0342,0.0424,0.0365,,50.,,65.3981,81.0783,69.7962},{51.,,0.0349,0.0421,0.0364,,51.,,66.7366,80.5046,69.605},{52.,,0.0349,0.0409,0.0356,,52.,,66.7366,78.21,68.0752},{53.,,0.0336,0.0416,0.0349,,53.,,64.2507,79.5485,66.7366},{54.,,0.0338,0.0424,0.0352,,54.,,64.6332,81.0783,67.3103},{55.,,0.0342,0.0424,0.0356,,55.,,65.3981,81.0783,68.0752},{56.,,0.0344,0.0421,0.0372,,56.,,65.7805,80.5046,71.1347},{57.,,0.0341,0.0424,0.0359,,57.,,65.2068,81.0783,68.6489},{58.,,0.035,0.042,0.0359,,58.,,66.9278,80.3134,68.6489},{59.,,0.0343,0.0424,0.0356,,59.,,65.5893,81.0783,68.0752}}

**Drop the label row (row 1) and the raw data columns (columns 1-5).**

sheet7=Drop[sheet7,1,5]

{{0.,,20.0784,31.9341,24.6677},{1.,,24.6677,35.1849,28.3009},{2.,,28.4921,40.5392,31.9341},{3.,,34.0376,44.3636,35.7586},{4.,,33.4639,45.8934,34.8025},{5.,,36.3323,51.8213,43.2163},{6.,,38.2445,48.7617,41.8777},{7.,,43.025,54.8808,44.746},{8.,,45.3197,58.1316,50.8652},{9.,,46.2758,58.1316,49.3354},{10.,,47.6144,59.0877,51.8213},{11.,,48.5705,62.721,52.0125},{12.,,47.2319,64.2507,54.3072},{13.,,51.4388,65.2068,57.1755},{14.,,54.1159,63.6771,54.8808},{15.,,52.7774,67.884,57.1755},{16.,,53.7335,67.884,57.1755},{17.,,56.7931,68.0752,60.4263},{18.,,57.1755,69.0313,59.0752}}

```
.4702},{19.,56.9843,71.8996,61.7648},{20.,56.9843,71.5172,60.0438},{21.,58.3228,71.1347,64.2507},{22.,58.1316,73.6206,62.3385},{23.,59.0877,73.6206,63.8683},{24.,59.4702,73.8119,62.5297},{25.,61.7648,72.6645,66.5454},{26.,61.7648,74.768,64.6332},{27.,62.3385,73.6206,62.721},{28.,61.,76.1065,65.3981},{29.,61.,73.6206,65.5893},{30.,63.1034,78.4012,66.7366},{31.,61.7648,74.9592,66.5454},{32.,61.3824,78.21,65.3981},{33.,64.442,79.5485,66.5454},{34.,64.2507,79.1661,66.9278},{35.,62.721,79.5485,65.9717},{36.,62.5297,78.0188,69.4137},{37.,64.442,79.1661,66.5454},{38.,62.3385,80.5046,69.7962},{39.,62.3385,78.4012,67.884},{40.,64.442,78.4012,68.0752},{41.,65.5893,78.4012,66.9278},{42.,65.3981,78.9749,67.3103},{43.,67.3103,79.3573,65.7805},{44.,62.3385,78.9749,68.0752},{45.,65.3981,77.6363,67.884},{46.,64.6332,78.9749,65.9717},{47.,65.7805,78.21,67.3103},{48.,66.7366,80.3134,68.6489},{49.,63.6771,78.9749,68.4576},{50.,65.3981,81.0783,69.7962},{51.,66.7366,80.5046,69.605},{52.,66.7366,78.21,68.0752},{53.,64.2507,79.5485,66.7366},{54.,64.6332,81.0783,67.3103},{55.,65.3981,81.0783,68.0752},{56.,65.7805,80.5046,71.1347},{57.,65.2068,81.0783,68.6489},{58.,66.9278,80.3134,68.6489},{59.,65.5893,81.0783,68.0752}}
```

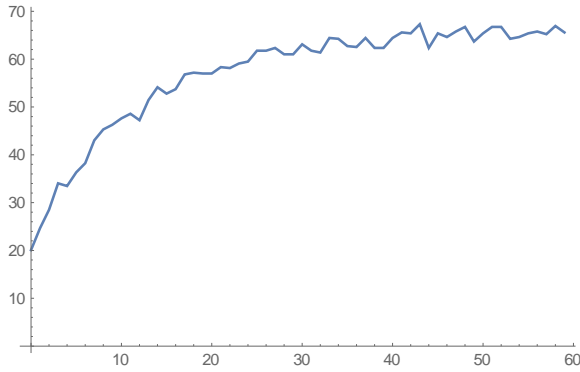
**Generate read1 as a paired list (time,value) by dropping the last two reads.**

```
read71=Drop[sheet7,None,-2]
```

```
{{0.,20.0784},{1.,24.6677},{2.,28.4921},{3.,34.0376},{4.,33.4639},{5.,36.3323},{6.,38.2445},{7.,43.025},{8.,45.3197},{9.,46.2758},{10.,47.6144},{11.,48.5705},{12.,47.2319},{13.,51.4388},{14.,54.1159},{15.,52.7774},{16.,53.7335},{17.,56.7931},{18.,57.1755},{19.,56.9843},{20.,56.9843},{21.,58.3228},{22.,58.1316},{23.,59.0877},{24.,59.4702},{25.,61.7648},{26.,61.7648},{27.,62.3385},{28.,61.},{29.,61.},{30.,63.1034},{31.,61.7648},{32.,61.3824},{33.,64.442},{34.,64.2507},{35.,62.721},{36.,62.5297},{37.,64.442},{38.,62.3385},{39.,62.3385},{40.,64.442},{41.,65.5893},{42.,65.3981},{43.,67.3103},{44.,62.3385},{45.,65.3981},{46.,64.6332},{47.,65.7805},{48.,66.7366},{49.,63.6771},{50.,65.3981},{51.,66.7366},{52.,66.7366},{53.,64.2507},{54.,64.6332},{55.,65.3981},{56.,65.7805},{57.,65.2068},{58.,66.9278},{59.,65.5893}}
```

**Plot the read.**

```
ListPlot[read71, Joined->True]
```



Fit an equation based on the read above and a guess for initial slope and y-intercept.

```
model71=NonlinearModelFit[read71,
b+a*Exp[-k*x], {k, {a, 15}, {b, 60}}, x]
```

```
FittedModel[ 65.8029 - 44.4024 e-0.0861859 x ]
```

Generate confidence intervals.

```
mp71[x_]=model71[{"MeanPredictionBands"}]
```

```
{ {65.8029 - 44.4024 E-0.0861859 x - 2.00247
```

$$\sqrt{0.0873907 + e^{-0.0861859 x} (-0.0446002 - 0.0543181 x) + e^{-0.172372 x} (0.430124 - 0.059254 x + 0.0153201 x^2)}$$

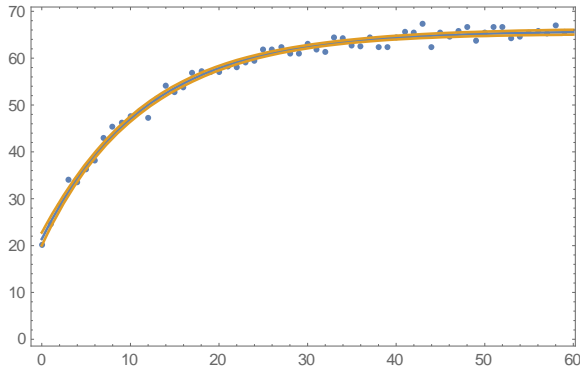
```
, 65.8029 - 44.4024 E-0.0861859 x + 2.00247
```

$$\sqrt{0.0873907 + e^{-0.0861859 x} (-0.0446002 - 0.0543181 x) + e^{-0.172372 x} (0.430124 - 0.059254 x + 0.0153201 x^2)}$$

```
}}]
```

Plot the real data and the overlaid fit with confidence intervals.

```
Show[ListPlot[read71], Plot[{model71[x], mp71[x]}, {x, 0, 60}], Frame->True]
```

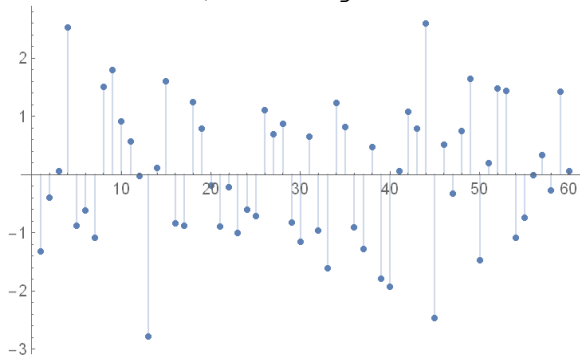


Calculate and plot the residuals.

```
model71["FitResiduals"]
```

```
{-1.32212,-0.399369,0.0612664,2.52068,-0.8842,-0.61328,-
1.08399,1.51041,1.79945,0.915548,0.566032,-0.0265348,-
2.78589,0.117537,1.59882,-0.836827,-
0.887209,1.24897,0.784283,-0.184118,-0.89712,-0.212688,-
1.00402,-0.598463,-0.72111,1.11018,0.685057,0.868711,-
0.827654,-1.15592,0.646376,-0.968468,-
1.60438,1.22263,0.818072,-0.90743,-1.27821,0.469279,-1.7853,-
1.92395,0.0522993,1.08294,0.784654,2.59866,-
2.46323,0.513657,-0.327075,0.750681,1.64296,-
1.47516,0.192113,1.48138,1.43616,-1.09122,-0.746832,-
0.0168594,0.333552,-0.269504,1.42454,0.0612436}
```

```
ListPlot[%,Filling->Axis]
```



```
model71["ParameterConfidenceIntervalTable"]
```

```
model71["ParameterTable"]
```

```
{
  {, Estimate, Standard Error, Confidence Interval},
  {k, 0.0861859, 0.00278756, {0.0806039,0.0917679}},
  {a, -44.4024, 0.655838, {-45.7157,-43.0891}},
  {b, 65.8029, 0.295619, {65.2109,66.3948}}
}
```

```
{, Estimate, Standard Error, t-Statistic, P-Value},  
{k, 0.0861859, 0.00278756, 30.918, 2.61646*10-37},  
{a, -44.4024, 0.655838, -67.7033, 3.71028*10-56},  
{b, 65.8029, 0.295619, 222.593, 1.74722*10-85}  
}
```

**Calculate and plot the derivative.**

```
v71=N[model71'[0]]
```

```
N[mp71'[0]]
```

```
3.82686
```

```
{{4.09456,3.55916}}
```

```
Plot[{model71'[x],mp71'[x]},{x,0,60}]
```

